VOL. 10 NO. 1 JULY 1965
PUBLISHED MONTHLY

Journal of

ELECTROANALYTICAL CHEMISTRY

International Journal Dealing with all Aspects
of Electroanalytical Chemistry,
Including Fundamental Electrochemistry

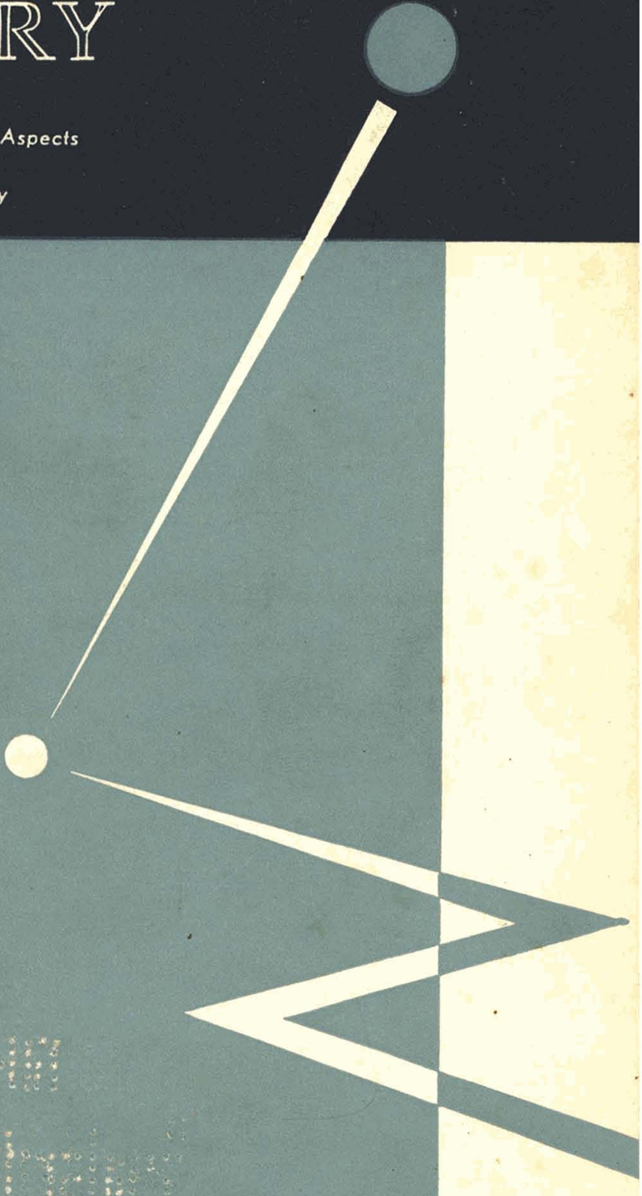

ELSEVIER

GENERAL INFORMATION

See also Suggestions and Instructions to Authors which will be sent free, on request to the Publishers.

Types of contributions

(a) Original research work not previously published in other periodicals.
(b) Reviews on recent developments in various fields.
(c) Short communications.
(d) Bibliographical notes and book reviews.

Languages

Papers will be published in English, French or German.

Submission of papers

Papers should be sent to one of the following Editors:

Professor J. O'M. Bockris, John Harrison Laboratory of Chemistry,
University of Pennsylvania, Philadelphia 4, Pa., U.S.A.
Dr. R. Parsons, Department of Chemistry,
The University, Bristol 8, England.
Professor C. N. Reilley, Department of Chemistry,
University of North Carolina, Chapel Hill, N.C., U.S.A.

Authors should preferably submit two copies in double-spaced typing on pages of uniform size. Legends for figures should be typed on a separate page. The figures should be in a form suitable for reproduction, drawn in Indian ink on drawing paper or tracing paper, with lettering etc. in thin pencil. The sheets of drawing or tracing paper should preferably be of the same dimensions as those on which the article is typed. Photographs should be submitted as clear black and white prints on glossy paper.

All references should be given at the end of the paper. They should be numbered and the numbers should appear in the text at the appropriate places.

A summary of 50 to 200 words should be included.

Reprints

Twenty-five reprints will be supplied free of charge. Additional reprints can be ordered at quoted prices. They must be ordered on order forms which are sent together with the proofs.

Publication

The *Journal of Electroanalytical Chemistry* appears monthly and has six issues per volume and two volumes per year, each of approx. 500 pages.

Subscription price (post free): £ 12.12.0 or $ 35.00 or Dfl. 126.00 per year; £ 6.6.0 or $ 17.50 or Dfl. 63.00 per volume.

Additional cost for copies by air mail available on request.

For advertising rates apply to the publishers.

Subscriptions

Subscriptions should be sent to:

ELSEVIER PUBLISHING COMPANY, P.O. Box 211, Amsterdam, The Netherlands.

SUMMARIES OF PAPERS PUBLISHED IN JOURNAL OF ELECTROANALYTICAL CHEMISTRY

Vol. 10, No. 1, July 1965

ELECTRODE KINETICS AT OPEN CIRCUIT AT THE STREAMING MERCURY ELECTRODE

I. THEORY

A general equation is derived for the potential, at open circuit, of an electrode of varying area at which a charge transfer process occurs. Application is made to the streaming mercury electrode for which there is continuous renewal of the double layer. The steady-state overvoltage is derived for mixed control by charge transfer and mass transfer for any value of the overvoltage. Simplified equations are given for small overvoltages (≤ 5 mV). Limiting cases are also analyzed. Application to electrode kinetics in media of low conductivity is considered, and two expected difficulties are indicated.

P. Delahay,
J. Electroanal. Chem., 10 (1965) 1–7

THE DETERMINATION OF THE HYDROGEN CONTENT OF A PALLADIUM–HYDROGEN ELECTRODE WITH THE AID OF THE LINEAR SWEEP VOLTAMMETRIC METHOD

The influence of disturbing factors on the apparent yield of hydrogen dissolved in a palladium micro-electrode was investigated using the method of voltammetric oxidation with varying potential. From an investigation of the partial processes which make up the anodic and cathodic processes the possible disturbing factors were established: electrochemical corrosion of the micro-electrode surface, the time interval between charging with hydrogen and the voltammetric oxidation and the stirring of the solution affect the anodic process, the presence of oxygen in the anolyte, the hydrogen content of the micro-electrode and the structure of the outer layer affect the cathodic process. The contribution of these factors to the disturbing of the apparent yield was tested experimentally and the possibility of removing these effects estimated. Under these conditions the voltammetric method allows the determination of the absolute hydrogen content of palladium between $3 \cdot 10^{-9}$ and $4 \cdot 10^{-6}$ moles with a maximum error of $\pm 5\%$.

R. V. Bucur,
J. Electroanal. Chem., 10 (1965) 8–18

II. THE POLAROGRAPHIC DIFFUSION COEFFICIENTS OF SOME SIMPLE CATIONS IN VARIOUS ELECTROLYTES, CALCULATED FOR INFINITE DILUTION AND UNDER POLAROGRAPHIC CONDITIONS

D. S. Turnham,
J. Electroanal. Chem., 10 (1965) 19–27

MODE OF INHIBITION OF POLAROGRAPHIC CURRENTS BY CYCLOHEXANONE

Cyclohexanone produces pronounced minima in the negative part of certain polarographic current–voltage curves; these minima are due to the formation of an insoluble film on the electrode surface. It was found that the reduction current at the bottom of the minimum is usually consistently identical with the current which flows under the same condition at some more positive fixed potential E_0, the value of which has been determined for each specific case. E_0 is found to occur in the middle part of the polarogram and is about 800 mV less negative than the potential of the bottom of the minimum. Even the effects of surface-active substances on the two currents seem to be identical. The cause of this decrease in the effective potential of the electrode is not known. The selectivity of the minimum-producing effect of cyclohexanone, which had hitherto been considered to be related to the half-wave potential of the reducible species, is explained by this relation in a simple manner.

K. Tsuji,
J. Electroanal. Chem., 10 (1965) 28–34

DIRECT DETERMINATION OF THE SURFACE EXCESS OF SPECIFICALLY ADSORBED IONS ON MERCURY

Gibbs' adsorption equation has been derived in the case of mixed solutions of strong electrolytes at constant molal ionic strength. Under these conditions, the specifically adsorbed surface excess of ionic species at the mercury electrode and the charge of the diffuse layer in presence of specific adsorption may be obtained. The main feature of the treatment consists in the fact that neither the differential equation of Poisson–Boltzman nor the integrated solution of Gouy–Chapman have to be introduced.

H. D. Hurwitz,
J. Electroanal. Chem., 10 (1965) 35–41

A POLAROGRAPHIC STUDY OF DIVALENT COBALT IN THE PRESENCE OF ELECTROLYTES OF NON-COMPLEXING BASES

A study has been made of the discharge of cobalt(II) ions at the dropping mercury electrode in the presence of non-complexing indifferent electrolytes. The influence of various factors such as concentration, surface-active agents and oxygen has been investigated. In the presence of oxygen a pre-wave is formed which develops its maximum height in the absence of all traces of carbon dioxide. The existence of this pre-wave is attributed to the formation at the electrode surface of a product of hydrolysis of the cobaltous ions owing to the liberation of hydroxyl ions on the reduction of the oxygen in solution. No such pre-wave is obtained in the absence of air. With hydrogen peroxide a catalytic wave is formed at a more positive potential than that corresponding to the normal reduction of this substance.

E. T. Verdier et G. Baptiste
J. Electroanal. Chem., 10 (1965) 42–50

THE POLAROGRAPHIC MEASUREMENT OF FORMATION CONSTANTS OF COPPER(II) COMPLEXES IN ORTHOPHOSPHATE MEDIUM

P. A. PELLA AND W. C. PURDY,
J. Electroanal. Chem., 10 (1965) 51–55

POLAROGRAPHIC MAXIMA AT THE DESORPTION POTENTIALS OF ORGANIC MOLECULES

Polarographic maxima belonging to neither the first nor the second kind are observed during the cathodic discharge of Cd^{2+} and Cu^{2+} on a dropping mercury electrode in the presence of camphor in the solution. Experimental data for the potential dependence of differential capacity as well as polarographic current at the same age of the life of the dropping mercury electrode are presented for various concentrations of camphor in solution. A theoretical correlation of the occurrence of such polarographic maxima with a slow and non-uniform adsorption of surface-active substances at their desorption potentials on the dropping mercury electrode, has been attempted.

S. SATHYANARAYANA,
J. Electroanal. Chem., 10 (1965) 56–67

THE DETERMINATION OF TRACES OF BISMUTH IN COBALT BY COLORIMETRY AFTER ELECTROLYTIC SEPARATION AND BY PULSE POLAROGRAPHY

Traces of bismuth (down to $3 \cdot 10^{-5}\%$) in cobalt were determined colorimetrically with dithizone after a prior separation of the bismuth onto a mercury cathode using controlled potential analysis and subsequent anodic stripping of the amalgam. The quantitative character of the method was controlled by pulse polarography. The conditions, (*i.e.*, cathode potential, electrolysis time, acidity, bismuth concentration) for electrodeposition of micro-quantities were investigated. Interferences from cobalt, mercury, tin(II), thallium(I), indium and lead are discussed. Analogous analyses of traces of bismuth in cobalt without preliminary separation (down to $6 \cdot 10^{-6}\%$) were performed with a pulse polarograph using the standard-addition method.

A. LAGROU AND F. VERBEEK,

J. Electroanal. Chem., 10 (1965) 68–75

VOLTAMMETRIC STUDIES OF Eu(III) IN FORMATE BUFFER
THE FORMAL POTENTIAL OF THE Eu(III)–Eu(II) SYSTEM

Polarographic and chronopotentiometric evidence for the formation of the Eu formate complexes, $Eu(HCOO)^{2+}$ and $Eu(HCOO)_2^+$, is given. Values for the corresponding step stability constants were estimated to be 20 and 120, respectively.

The effect of such formate complexes on the original determination of the formal potential of the Eu(III)–Eu(II) couple by McCoy (1963) is discussed. The conclusion is that McCoy's result is in error by approximately 70 mV and that the value of −0.35 V *vs.* N.H.E. is more realistic for the non-complexed system.

D. J. Macero, L. B. Anderson and P. Malachesky,
J. Electroanal. Chem., 10 (1965) 76–81

ANION EFFECTS ON THE REDUCTION OF In(III) IN ACIDIC SOLUTION

(Short Communication)

R. E. Visco,
J. Electroanal. Chem., 10 (1965) 82–84

JOURNAL OF ELECTROANALYTICAL CHEMISTRY

Vol. 10 (1965)

JOURNAL
of
ELECTROANALYTICAL CHEMISTRY

INTERNATIONAL JOURNAL DEALING WITH ALL
ASPECTS OF ELECTROANALYTICAL CHEMISTRY,
INCLUDING FUNDAMENTAL ELECTROCHEMISTRY

Vol. 10 1965

ELSEVIER PUBLISHING COMPANY
AMSTERDAM

PRINTED IN THE NETHERLANDS

ELECTRODE KINETICS AT OPEN CIRCUIT AT THE STREAMING MERCURY ELECTRODE

I. THEORY

PAUL DELAHAY*

Coates Chemical Laboratory, Louisiana State University, Baton Rouge, Louisiana 70803 (U.S.A.)

(Received March 16th, 1965)

Consider an electrode which exhibits the equilibrium potential E_e corresponding to the charge-transfer reaction $O+ne=R$ for given activities of O and R. If the area, A, of the electrolyte–electrode interface varies, the double-layer capacity, which is proportional to A, varies. There results a double-layer charging current (capacity current) which, at open circuit, must be entirely compensated by the faradaic current for the reaction $O+ne=R$. This reaction proceeds with an overvoltage, η, which can be measured with an instrument of very high input resistance (electrometer amplifier). The current–potential characteristic for the reaction $O+ne=R$ can thus be determined at open circuit by varying the capacity current density. Current densities as high as 0.02 A cm^{-2} are possible.

Until this work was completed, we knew of only two related investigations, (i) the measurement of double-layer capacities with a vibrating mercury–electrolyte interface (WATANABE[1]**) and (ii) oxygen analysis from the shift of the open-circuit potential of a dropping mercury electrode (LAITINEN, HIGUCHI AND CZUHA[2]). The earlier paper of ROSENBURG AND STEGEMAN[3] on the variation of potential of the streaming mercury electrode at open circuit should also be mentioned, but the interpretation is not correct and involves no consideration of electrode kinetics. After completion of this work we became aware of the work of SPEAR[4] on the potential variations of a mercury–electrolyte interface of varying area. This author used a funnel of suitable profile, which was independently studied in this laboratory by COLE[5], and examined the variations of potential as the level of the mercury–electrolyte interface varied. He considered the ideal polarized electrode and the case of an electrode with a faradaic process, namely the reduction of oxygen. The idea of compensation of the charging current by the faradaic current was clearly stated and examined by SPEAR.

The essential ideas involved in the present work were outlined in a preliminary communication[6], and an equation for the shift of potential for the streaming mercury electrode was reported***. Details on theory are given here, and experimental results are discussed in a subsequent paper[7]. Extension to the expanding mercury drop electrode is made elsewhere[8]. Work on the "funnel electrode", which was mentioned in

---

* Address after August 1965: Department of Chemistry, New York University, Washington Square, New York, N.Y., 10003.

** See previous references in this review.

*** It should be noted that the charging current for a streaming mercury electrode is caused by continuous removal of the double layer along with mercury. There is no variation of the electrode area.

the preliminary communication[6], was not completed because of difficulties caused by erratic electrode response. Likewise, studies on a vibrating mercury–electrolyte interface[9] were discontinued because of difficulties in the analysis of experimental results.

GENERAL EQUATION

The capacity current, i_{dl}, for an electrode of varying area, A, is obtained by differentiating, with respect to time t, the charge on the electrode $c(E-E_z)A$, where c is the double-layer integral capacity, E the potential (IUPAC-Stockholm convention), and E_z the point of zero charge. The capacity current is

$$(E-E_z)\,A\,\frac{\mathrm{d}c}{\mathrm{d}E}\,\frac{\mathrm{d}E}{\mathrm{d}t}+c\,A\,\frac{\mathrm{d}E}{\mathrm{d}t}+c(E-E_z)\,\frac{\mathrm{d}A}{\mathrm{d}t}$$

If this quantity is positive, a positive charge must be supplied to the electrode, and a net cathodic reaction must occur on the electrode at open circuit. Conversely, a net anodic reaction occurs at open circuit when the above quantity is negative.

We adopt for the faradaic current density, I_f, the polarographic convention according to which $I_f \gtrless 0$ for a cathodic or anodic process, respectively. Thus, one has in general at open circuit

$$(E-E_z)\,A\,\frac{\mathrm{d}c}{\mathrm{d}E}\,\frac{\mathrm{d}E}{\mathrm{d}t}+c\,A\,\frac{\mathrm{d}E}{\mathrm{d}t}+c(E-E_z)\,\frac{\mathrm{d}A}{\mathrm{d}t}-I_fA=0 \qquad (1)$$

The current density, I_f, is a function of E and of kinetic parameters for the electrode reaction, *e.g.*, the exchange-current density and the transfer coefficient. In principle, eqn. (1) can be solved for E as a function of time, and the shift of potential from its equilibrium value can be correlated to the kinetic parameters for the charge-transfer process.

CAPACITY CURRENT FOR THE STREAMING MERCURY ELECTRODE

We consider a streaming mercury electrode of the Heyrovsky type* which is characterized by a length, l, and a rate of flow of mercury, m. The radius, r of the mercury column in contact with the solution is supposed to be constant. The capacity current at constant potential can be computed immediately if one assumes that the mercury jet carries with it the double layer. This assumption is essentially valid, as shown by measurements of the charging current[4,7], and the capacity current is thus directly related to the rate of renewal of the mercury–solution interface.

At constant E

$$i_{dl}=c(E-E_z)\,\frac{2\,m}{r\delta} \qquad (2)$$

where δ is the density of mercury. The term, $2\,m/r\,\delta$, in eqn. (2) is the rate of renewal of the mercury–electrolyte interface, *i.e.*, the area $2\,\pi\,rl$ divided by the time required for an element of area to travel the length of the column. This time is l/v, v being the

---

* See ref. 10 for a review.

velocity of mercury ($v = m/\pi r^2 \delta$). For example, $i_{dl} \approx 3 \cdot 10^{-4}$ A for $E - E_z = 1$ V and the typical data: $c = 20$ μF cm^{-2}, $r = 0.005$ cm, $m = 1$ g sec^{-1}. The corresponding capacity current density is approximately 0.02 A cm^{-2} for $l = 0.5$ cm, *i.e.*, a relatively high value.

If no electrode reaction occurs, $i_{dl} = 0$, and $E = E_z$ according to eqn. (2). This corresponds to the well-known behavior of the streaming mercury electrode in the determination of E_z.

FARADAIC CURRENT FOR THE STREAMING MERCURY ELECTRODE

We consider a simple electrode process $O + n\,e = R$ involving soluble species and we consider mass transfer. The faradaic current density, I_f, is then

$$I_f = \frac{\exp\left[-\frac{\alpha n F}{RT}\eta\right] - \exp\left[\frac{(1-\alpha)nF}{RT}\eta\right]}{\frac{1}{I_a{}^0} + \frac{\exp\left[-\frac{\alpha n F}{RT}\eta\right]}{I_C{}^d} + \frac{\exp\left[\frac{(1-\alpha)nF}{RT}\eta\right]}{I_A{}^d}} \tag{3}$$

where η is the overvoltage; α, the transfer coefficient; $I_a{}^0$ the apparent (not corrected for double-layer effects) exchange-current density; $I_C{}^d$ and $I_A{}^d$ the cathodic and anodic diffusion-current densities, respectively; and F, R and T have their usual meaning. Then $I_f \gtrless 0$ for $\eta \lessgtr 0$, $I_C{}^d > 0$ and $I_A{}^d > 0$. Equation (3) is derived by combining the usual I *vs.* η characteristic with the following relationships

$$\frac{C_O}{C_O{}^0} = 1 - \frac{I_f}{I_C{}^d} \qquad \frac{C_R}{C_R{}^0} = 1 + \frac{I_f}{I_A{}^d} \tag{4}$$

where the C's are the concentrations at the electrode surface (no double-layer correction) and the C^0's are the bulk concentrations. Equations (4) follow directly from the Nernst model of the diffusion layer. They are not rigorous but will suffice for our purpose.

The current densities, $I_C{}^d$ and $I_A{}^d$, vary along the mercury column but are readily derived by assuming, as KORYTA[11] did, that semi-infinite linear diffusion is the sole mode of mass transfer and that the solution adjacent to the mercury column moves with the same velocity as mercury*.
Thus

$$I^d = \frac{nFD^{\frac{1}{2}}C^0}{\pi r \delta^{\frac{1}{2}}}\left(\frac{m}{l}\right)^{\frac{1}{2}} \tag{5}$$

where D is the diffusion coefficient of the substance being reduced or oxidized at the electrode. It is seen from eqn. (5) that I^d varies along the mercury column and is inversely proportional** to $l^{\frac{1}{2}}$. The faradaic current, i_f, is directly obtained by combination of eqns. (3) and (5) and subsequent integration.

---

* The earlier paper of RIUS, LLOPIS AND POLO[12] and the detailed studies of WEAVER AND PARRY[13] on velocity distribution and other topics may also be consulted. Reference is also made to SLOTTER's work[14].

** The diffusion current, which is obtained by integration of I^d from $l = 0$ to 1, is proportional to $l^{\frac{1}{2}}$. See KORYTA[11].

Equation (5) applies to a process with diffusion from solution toward the electrode. This equation can also be applied to the opposite case of diffusion from inside the mercury column toward the surface (anodic oxidation of amalgam). The approximation should be about the same as for eqn. (5). It was indeed assumed in the application of the equation for the flux for semi-infinite linear diffusion in the derivation of eqn. (5) that the diffusion-layer thickness is very small in comparison with the radius of the mercury column.

STEADY-STATE OVERVOLTAGE AT OPEN CIRCUIT

General case

By equating the capacity current of eqn. (2) to the faradaic current one obtains for the steady state*

$$\frac{2\,nFr\delta^{\frac{1}{2}}}{c}\left(\frac{l}{m}\right)^{\frac{1}{2}}\left[1-\frac{1}{\lambda}\ln\left(1+\lambda\right)\right]=G(\eta) \tag{6}$$

with

$$G(\eta)=(E-E_z)\,\frac{\dfrac{1}{C_O{}^0 D_O{}^{\frac{1}{2}}}+\dfrac{\exp\left(\dfrac{nF}{RT}\,\eta\right)}{C_R{}^0 D_R{}^{\frac{1}{2}}}}{1-\exp\left(\dfrac{nF}{RT}\,\eta\right)} \tag{7}$$

$$\lambda=\frac{\pi r\delta^{\frac{1}{2}}}{nF}\left\{\frac{\exp\left[-\dfrac{\alpha nF}{RT}\,\eta\right]}{C_O{}^0 D_O{}^{\frac{1}{2}}}+\frac{\exp\left[\dfrac{(1-\alpha)nF}{RT}\,\eta\right]}{C_R{}^0 D_R{}^{\frac{1}{2}}}\right\} I_a{}^0\left(\frac{l}{m}\right)^{\frac{1}{2}} \tag{8}$$

There, c is taken at the potential, E, corresponding to the particular value l/m at which the electrode operates. It is seen that $G(\eta)$ is proportional to $(l/m)^{\frac{1}{2}}$ and to the function $1-(1/\lambda)\ln(1+\lambda)$ (Fig. 1).

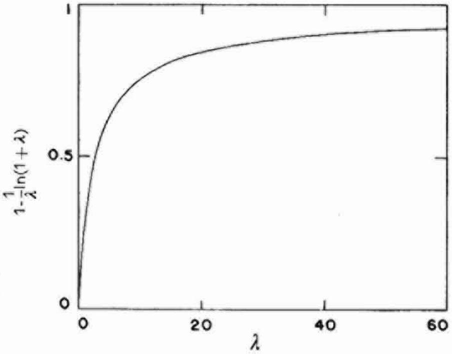

Fig. 1. Plot of the function in eqn. (6).

---

* The transient is too short to interfere in the measurements, as one can readily show by solving eqn. (1). The transient can easily be derived if one assumes, to simplify matters, that c is independent of E, that $|\eta| \leqslant 5$ mV and that the mercury column is established instantaneously. It is then found that the transient decays exponentially in a very short time ($\ll 1$ sec).

When $\lambda \to \infty$, $1-(1/\lambda)\ln(1+\lambda) \to 1$, and there is pure diffusion control. $G(\eta)$ is then proportional to $(l/m)^{\frac{1}{2}}$ according to

$$G(\eta) = \frac{2\, nFr\delta^{\frac{1}{2}}}{c}\left(\frac{l}{m}\right)^{\frac{1}{2}} \tag{9}$$

provided the integral capacity c is independent of potential in the interval being considered. When $\lambda \to 0$, $1-(1/\lambda)\ln(1+\lambda) \to \lambda/2$, and there is pure charge transfer control. Equation (6) then reduces to

$$\frac{E-E_z}{\exp\left[-\frac{\alpha nF}{RT}\eta\right]-\exp\left[\frac{(1-\alpha)nF}{RT}\eta\right]} = \frac{\pi r^2\delta}{c} I_a{}^0\left(\frac{l}{m}\right) \tag{10}$$

Small overvoltage

When $|\eta|$ does not exceed a few millivolts, eqn. (6) takes the form

$$-\frac{1}{\eta} = 2\,\frac{(nF)^2}{RT}\,\frac{1}{\frac{1}{C_O{}^0 D_O{}^{\frac{1}{2}}}+\frac{1}{C_R{}^0 D_R{}^{\frac{1}{2}}}}\,\frac{r\delta^{\frac{1}{2}}}{c(E-E_z)}\left(\frac{l}{m}\right)^{\frac{1}{2}}\left[1-\frac{1}{\lambda}\ln(1+\lambda)\right] \tag{11}$$

with

$$\lambda = \frac{\pi r\delta^{\frac{1}{2}}}{nF}\left(\frac{1}{C_O{}^0 D_O{}^{\frac{1}{2}}}+\frac{1}{C_R{}^0 D_R{}^{\frac{1}{2}}}\right)\left(\frac{l}{m}\right)^{\frac{1}{2}} I_a{}^0 \tag{12}$$

When $\lambda \to \infty$ (pure diffusion control), $1-(1/\lambda)\ln(1+\lambda) \to 1$ in eqn. (11), and $-1/\eta$ is proportional to $(l/m)^{\frac{1}{2}}$ provided c is constant. When $\lambda \to 0$ (pure charge transfer control), eqn. (11) takes the form

$$-\frac{1}{\eta} = \frac{nF}{RT}\,\frac{\pi r^2\delta}{c(E-E_z)} I_a{}^0\left(\frac{l}{m}\right) \tag{13}$$

i.e., $-1/\eta$ is proportional to l/m provided c is constant.

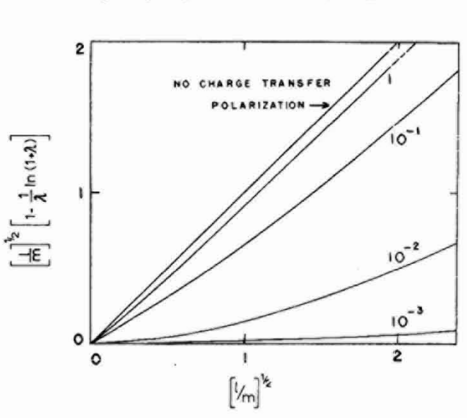

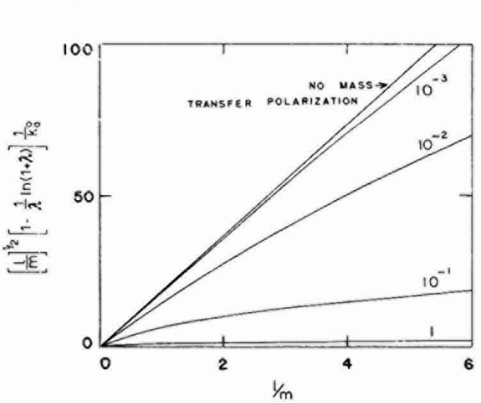

Fig. 2. Plot ($|\eta| \leqslant 5$ mV) showing increasing diffusion control as $k_a{}^0$ increases. Data: $C_O{}^0 = C_R{}^0$, $D_O = D_R = 10^{-5}$ cm^2 sec^{-1}, $r = 5 \cdot 10^{-3}$ cm.

Fig. 3. Plot ($|\eta| \leqslant 5$ mV) showing increasing charge transfer control as $k_a{}^0$ decreases. Same data as in Fig. 2.

Conditions under which pure diffusion control is approached can be determined from a plot of $(l/m)^{\frac{1}{2}}[1-(1/\lambda)\ln(1+\lambda)]$ against $(l/m)^{\frac{1}{2}}$ for usual values of l/m (Fig. 2). The apparent standard rate constant $k_a{}^0$ corresponding to each curve in Fig. 2 was related to $I_a{}^0$ by the following equation

$$I_a{}^0 = nFk_a{}^0(C_O{}^0)^{1-\alpha}(C_R{}^0)^{\alpha} \tag{14}$$

which applies to processes with simple kinetics. It is seen from Fig. 2 that diffusion control prevails almost entirely for $k_a{}^0 \geqslant 1$ cm sec^{-1}. Determination of $I_a{}^0$ for the conditions of Fig. 2 should be possible for $k_a{}^0 \leqslant 10^{-2}$ cm sec^{-1}. Potentialities are the same as in a relaxation method in which transients are observed in a time interval of the same order of magnitude as the time it takes an element of surface to travel the length of the mercury column. This time is of the order of a few milliseconds for usual conditions of operation.

Conditions under which pure charge-transfer control are approached can be determined from a plot of $(1/k_a{}^0)\,(l/m)^{\frac{1}{2}}[1-(1/\lambda)\ln(1+\lambda)]$ against l/m (Fig. 3). It is seen that mass transfer polarization becomes negligible for the conditions prevailing for Fig. 3 when $k_a{}^0 \leqslant 10^{-3}$ cm sec^{-1}. Equation (13) is then valid.

CONCLUSION

The potential of a streaming mercury electrode at open circuit, for the conditions discussed in this paper, can be correlated to the kinetics of the electrode process occurring at the electrode. Since measurements can be carried out at open circuit, application to the study of electrode kinetics in media of low conductivity is conceivable. However, two fundamental difficulties, at least, may hamper such an application: the complication arising from migration of reactant and/or product in a medium of low conductivity and interference by variations of potential along the mercury column. The first of these difficulties could be removed by the use of an equation for I^d[eqn. (5)] which includes the effect of migration*.

ACKNOWLEDGEMENT

This investigation was supported by the Office of Naval Research and by the National Science Foundation.

SUMMARY

A general equation is derived for the potential, at open circuit, of an electrode of varying area at which a charge transfer process occurs. Application is made to the streaming mercury electrode for which there is continuous renewal of the double layer. The steady-state overvoltage is derived for mixed control by charge transfer and mass transfer for any value of the overvoltage. Simplified equations are given for small overvoltages ($\leqslant 5$ mV). Limiting cases are also analyzed. Application to electrode kinetics in media of low conductivity is considered, and two expected difficulties are indicated.

---

* The rigorous derivation of such an equation is difficult, but the approximate approach followed for such a case, in polarography and chronopotentiometry, might be adopted.

REFERENCES

1 A. WATANABE, *J. Electrochem. Soc.*, 110 (1963) 72.
2 H. A. LAITINEN, T. HIGUCHI AND H. CZUHA, *J. Am. Chem. Soc.*, 70 (1948) 561.
3 J. E. ROSENBERG AND G. STEGEMAN, *J. Phys. Chem.*, 30 (1926) 1306.
4 C. D. SPEAR, *Transient Electrode Potentials of Mercury*, dissertation, University of Utah, 1960; microfilm Mic 60-3379, University Microfilms, Inc., Ann Arbor, Michigan.
5 D. COLE, unpublished investigation.
6 P. DELAHAY, *J. Phys. Chem.*, 68 (1964) 981.
7 V. S. SRINIVASAN, G. TORSI AND P. DELAHAY, *J. Electroanal. Chem.*, in press.
8 D. COLE, P. DELAHAY AND G. SUSBIELLES, *Collection Czech. Chem. Commun.*, submitted.
9 R. DE LEVIE, V. S. SRINIVASAN AND P. DELAHAY, unpublished investigation.
10 I. M. KOLTHOFF AND Y. OKINAKA, *Progress in Polarography*, Vol. 2, edited by P. ZUMAN, Interscience-Wiley, New York, 1962, pp. 367–372.
11 J. KORYTA, *Collection Czech. Chem. Commun.*, 19 (1954) 433.
12 A. RIUS, J. LLOPIS AND S. POLO, *Anales Real Soc. Espan. Fis. y Quim.*, 45B (1949) 1039.
13 J. R. WEAVER AND R. W. PARRY, *J. Am. Chem. Soc.*, 76 (1954) 6258; 78 (1956) 5542.
14 R. A. SLOTTER, *Kinetic Studies at the Streaming Mercury Electrode*, dissertation, University of Michigan, 1960; microfilm Mic 60-2058, University Microfilms, Inc., Ann Arbor, Michigan.

DIE BESTIMMUNG DES WASSERSTOFFGEHALTES DER PALLADIUM-WASSERSTOFFELEKTRODEN MIT HILFE DER VOLTAMETRISCHEN METHODE MIT LINEAR VERÄNDERLICHER SPANNUNG

ROMULUS V. BUCUR
Institut für Atomphysik, Sektion Cluj, Cluj (Rumänien)

(Eingegangen den 24. Februar 1965)

EINLEITUNG

In einer früheren Arbeit[1] wurde gezeigt, dass der relative Gehalt des im Palladium gelösten Wasserstoffs durch voltametrische Oxydation einer Palladium-Wasserstoffelektrode, mit linear veränderlicher Spannung, bestimmt werden kann. Zwischen der durch Elektrolyse bei konstantem Strom in das Palladium eingeführten, und der durch anodische voltametrische Oxydation zurückerhaltenen Wasserstoffmenge wurde ein linearer Zusammenhang gefunden. Die Rückgewinnungsausbeute* des Wasserstoffs in 2 N H_2SO_4 Lösung beträgt nur 84%. FRANKLIN UND FRANKLIN[2] haben mit einem ungefähr fünfmal grösseren Wasserstoffgehalt gearbeitet und dabei ebenfalls eine direkte Proportionalität zwischen der voltametrisch bzw. durch thermische Desorbtion bestimmten, im Palladium befindlichen Wasserstoffmenge festgestellt. In diesem Falle wurden aber keine Angaben in Bezug auf den Wert der Rückgewinnungsausbeute gegeben.

In der erwähnten Arbeit[1] wurde der kleine Wert der Rückgewinnungsausbeute ausschliesslich der Unwirksamkeit des anodischen Vorganges zugeschrieben. Eigentlich ist die in dieser Arbeit definierte Rückgewinnungsausbeute eine konventionelle Grösse, deren Änderung von der Veränderung sowohl der Wirksamkeit des anodischen wie auch derjenigen des kathodischen Prozesses verursacht sein kann, und infolgedessen auch übereinheitliche Werte annimmt. Aus diesem Grunde muss man das Verhältnis ϱ als eine *scheinbare Rückgewinnungsausbeute* betrachten.

Die Untersuchung der in jedem einzelnen Elektrodenprozess enthaltenen Teilprozesse kann uns auf die Art, wie letztere die scheinbare Rückgewinnungsausbeute beeinflussen können, einen Hinweis geben.

Der kathodische Prozess der Wasserstoffbeladung von Palladium besteht aus zwei nacheinanderfolgenden Teilprozessen:

die Durchtrittsreaktion mit Adsorbtion

$$H^+ + e \xrightarrow{Q_c^*} H\,(ads) \qquad (1)$$

---

* Diese wurde mit Hilfe des Verhältnisses zwischen der im anodischen, bzw. kathodischen Prozess verbrauchten Elektrizitätsmenge ausgerechnet, $\varrho = Q_a/Q_c$.

die Absorbtion der Wasserstoffatome aus der oberen Schicht des Metalls

$$\text{H (ads)} \longrightarrow \text{H (abs)} \qquad (2)$$

Wenn die Wirksamkeit der Absorbtion des Wasserstoffatoms aus der oberen Schicht nicht vollständig ist, wird ein Teil des Wasserstoffs durch Diffusion in der Diffusionsschicht der Lösung verlorengehen oder sich in Form von Molekülen, gemäss des folgenden Schemas, entweichen:

$$2\ \text{H (ads)} \longrightarrow \text{H}_2\ \text{(Gas)} \qquad (3)$$

und die beiden Prozesse (2) und (3) werden konkurrent.

Der anodische Oxydationsprozess des im Palladium gelösten atomaren Wasserstoffs besteht ebenfalls aus zwei nacheinanderfolgenden Teilprozessen:

die Übertragung des Wasserstoffatoms aus dem Inneren des Metallgitters in die obere Schicht

$$\text{H (abs)} \longrightarrow \text{H (ads)} \qquad (4)$$

und

die Desorbtion mit der Durchtrittsreaktion

$$\text{H (ads)} \xrightarrow{Q_a^*} \text{H}^+ + \text{e} \qquad (5)$$

Es kann gleichzeitig mit der Reaktion (5) auch eine Desorbtion mit Überführung der Wasserstoffmolekülen durch die Diffusionsschicht der Lösung stattfinden

$$2\ \text{H (ads)} \longrightarrow \text{H}_2\ \text{(dif)} \qquad (6)$$

Die beiden letzten Prozesse sind ebenfalls konkurrent; da die Geschwindigkeit der Durchtrittsreaktion viel grösser ist als die des Desorbtion–Diffusion-Prozesses, kann die Wirkung des letzteren vernachlässigt werden. Der Prozess (6) wird nur dann bestimmend wenn die Durchtrittsreaktionsgeschwindigkeit sich dem Werte Null nähert.

Mit Hilfe der in den Durchtrittsreaktionen (1) und (5) verbrauchten Elektrizitätsmengen, definiert man die *effektive Rückgewinnungsausbeute* des Wasserstoffs durch folgendes Verhältnis:

$$\varrho^* = \frac{Q_a^*}{Q_c^*} \qquad (7)$$

Diese Grösse ist ein direktes Mass der Wirksamkeit des Absorbtionprozesses (2) und nimmt bei einer totalen Absorbtion den maximalen Wert $\varrho^* = 1$ an.

Die Gegenwart von fremden Verbindungen, die in den kathodischen oder anodischen Prozessen reduziert oder oxydiert werden können, bringt die Erscheinung von sekundären Durchtrittsreaktionen mit sich, welche am Ende die verbrauchten Elektrizitätsmengen in den Durchtrittsreaktionen (1) und (5) verändern. Wenn man dieses in Betracht zieht, erhält man die scheinbare Rückgewinnungsausbeute aus folgendem Verhältnis:

$$\varrho = \frac{Q_a}{Q_c} = \frac{Q_a^* + \Sigma Q_i^a}{Q_c^* + \Sigma Q_i^c} \qquad (8)$$

wo die Summenglieder die in den sekundären Durchtrittsreaktionen verbrauchten Elektrizitätsmengen bedeuten.

Aus diesem Verhältnis folgt gleich, dass auch in dem Falle, in dem $\varrho^* = 1$ ($Q_a^* = Q_c^*$) ist, die scheinbare Ausbeute ϱ wegen der Differenz $\Delta = \Sigma Q_i^a - \Sigma Q_i^c$ einen von der Einheit verschiedenen Wert annehmen kann. Wenn $\Delta > 0$, ist die scheinbare Ausbeute grösser und wenn $\Delta < 0$, ist diese kleiner als die Einheit. Fehlt eine sekundäre Durchtrittsreaktion, so sind die Summenglieder $\Sigma Q_i^a = \Sigma Q_i^c = 0$ und die Werte der scheinbaren und der wahren Ausbeuten werden einander gleich. Bei einer totalen Absorbtion nimmt diese den Wert $\varrho = \varrho^* = 1$ an.

Die Bestimmung des Wasserstoffgehaltes von Palladium–Wasserstoff-Mikroelektroden mit Hilfe der voltametrischen Methode mit linear veränderlicher Spannung, benötigt die Kenntnis der wahren Ausbeute ϱ^*, welche im allgemeinen von der scheinbaren, experimentell bestimmbaren Ausbeute ϱ, verschieden ist. Wir nahmen uns vor, in dieser Arbeit die Wirkung einiger wichtigeren störenden Faktoren auf die Grösse ϱ zu untersuchen, und die Bedingungen zu bestimmen, unter welchen dieser Wert sich dem Werte von ϱ^* nähert.

APPARATUR

Das Schema der Versuchseinrichtung ist in Abb. 1 dargestellt. Diese ist prinzipiell dieselbe wie in der angeführten Arbeit[1] und enthält zwei unabhängige Kreisläufe: den Elektrolysenkreislauf bei konstantem Strom und den voltametrischen Kreislauf mit linear veränderlicher Spannung.

Der Elektrolysenkreislauf bei konstantem Strom wird bei der kathodischen Wasserstoffbeladung der geprüften Palladiumelektrode benützt. Diese besteht aus

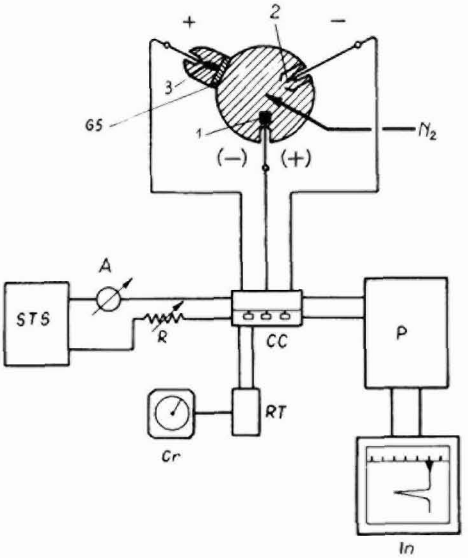

Abb. 1. Schema der elektrischen Einrichtung zur Untersuchung der voltametrischen Oxydation des in den (Pd–H)-Mikroelektroden gelösten Wasserstoffs.

einer stabilisierten Spannungsquelle von 300 V (STS), einem veränderlichen Widerstand dessen maximaler Wert 1.2 MΩ(R) ist und einem Instrument (A) zur Bestimmung des Elektrolysenstromes (I_e).

Die Aufladung der Palladiummikroelektrode mit Wasserstoff geschieht durch Schliessen des Elektrolysenkreislaufes mit Hilfe des Druckschalters (CC). Die Unterbrechung des Kreislaufes geschieht automatisch mit dem Zeitrelais (RT), dessen maximale Zeit 100 Sek. ist. Die Genauigkeit des Relais war ±4% für eine Sekunde und ±0.1% für eine Zeit mit der Grössenordnung von einigen zehn Sekunden. Dieses Relais betätigt auch den elektrischen Chronometer (Cr) auf dem die Elektrolysenzeit (t_e) ablesbar ist.

Der Voltameterkreislauf mit linear veränderlicher Spannung wird bei der Oxydation des im Palladium befindlichen Wasserstoffs benützt. Diese geschieht mit Hilfe eines Polarographs Heyrovsky Type LP 55 A (P), mit einem Registrierinstrument vorgesehen dessen Empfindlichkeit $2.5 \cdot 10^{-10}$ A/Skt (In) ist. Der voltametrische Kreislauf wird mit Hilfe desselben Druckschalters (CC) betätigt.

Die Elektrolysenzelle ist aus Glas, mit einer Wasserthermostatierungshülle versehen. Die Arbeitstemperatur wurde auf 25.0±0.1°C konstant gehalten.

In die Elektrolysenzelle sind drei Elektroden eingeführt: die untersuchte Palladiummikroelektrode (1) und zwei Hilfselektroden aus platiniertem Platin (2) und (3). Die Aktivierung der Elektrodenoberflächen wurde durch Bedeckung mit Metallschwarz nach einer in der Literatur[3] angegebenen Methode vorgenommen. Die Palladiummikroelektrode wurde aus einem $2 \cdot 10^{-3}$ cm dicken Palladiumblättchen (B.D.H.) mit einer geometrischen Fläche von etwa 8 mm² (Gewicht $1.9 \cdot 10^{-3}$ g) hergestellt. Diese funktioniert als Kathode im Elektrolysenkreislauf bei konstantem Strom und als Anode in dem voltametrischen Kreislauf. Die beiden Platinelektroden wurden aus Platinfaden mit $\phi = 0.2$ mm hergestellt und dienen als Anoden bzw. Kathoden in den entsprechenden Kreisläufen.

Der anodische Teil des Kreislaufes der Elektrolyse bei konstantem Strom ist vom Rest der Zelle mit einer Fritte G5 abgesondert die die Diffusion des Sauerstoffs zur Mikroelektrode (Pd–H) verhindert. Aus demselben Grunde wird durch die Lösung auf aktivem Kupfer[4] gereinigtes Stickstoff durchperlt. Die Bestimmungen wurden in 1 M H_2SO_4-, 0.05 M H_2SO_4- und 1 M H_3PO_4-Lösungen vorgenommen, welche durch Lösen der analytisch reinen Reagenzien in doppelt destilliertem Wasser hergestellt wurden.

ARBEITSMETHODE

Um den kathodischen und anodischen Prozess bei der voltametrischen Rückgewinnung des in den (Pd–H)-Mikroelektroden enthaltenen Wasserstoffs zu kontrollieren, registriert man zwei Arten von Strom–Zeit-Kurven:

(1) eine Strom–Zeit-Kurve für die mit Wasserstoff beladene Mikroelektrode (Kurve Nr. 1 aus Abb. 2)

(2) eine Strom–Zeit-Kurve für dieselbe, wasserstofflose Mikroelektrode (Kurve Nr. 2 aus Abb. 2)

Diese beiden Kurven überlagern sich auf dem Diagramm, wenn man denselben Nullpunkt für die Zeitskala nimmt. Auf diese Weise wird zwischen den Kurven (1) und (2) eine gut bestimmbare Fläche begrenzt, die die Elektrizitätsmenge Q_a darstellt, die für die Rückgewinnung des Wasserstoffs aus dem Palladium dient. Die Grösse der Fläche wurde durch graphische Integration mit einem polaren Planimeter bestimmt. Die Darstellung der Kurven (2) ist hauptsächlich in dem Falle wichtig, in dem der Wasserstoffgehalt der Mikroelektroden niedrig ist, d.h. wenn der Grundstrom relativ grosse Werte hat und die Begrenzung der Fläche nicht mehr willkürlich, durch Zeichnen einer unterbrochenen Linie (Abb. 2 (a)) geschehen kann. Im Falle eines erhöhten Wasserstoffgehaltes kann diese Begrenzung auch geometrisch durchgeführt werden, ohne Einführung grösserer Fehler. In unserem Falle wurden die Flächenbegrenzungen immer mit Überlagerung der beiden Strom–Zeit-Kurven gemacht.

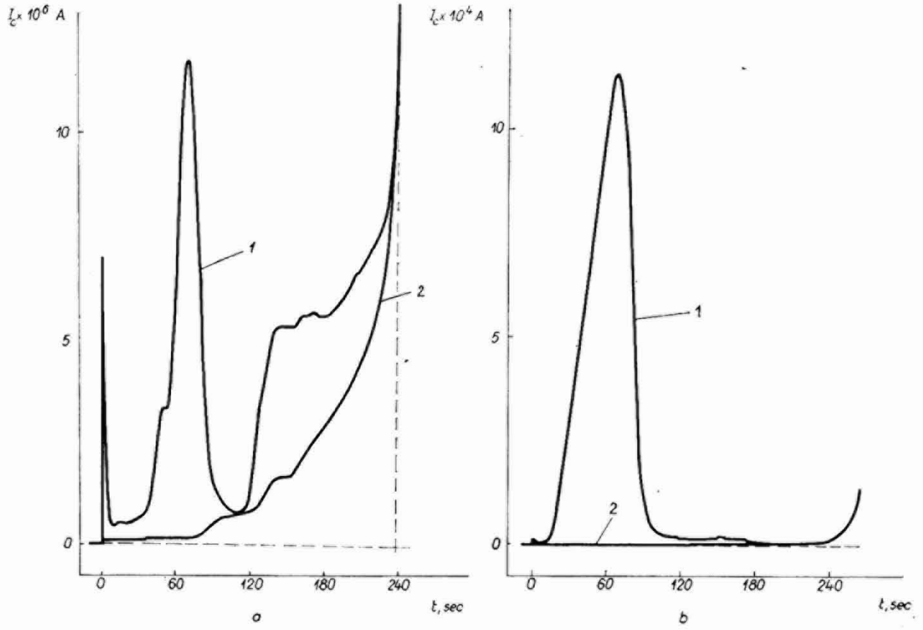

Abb. 2. Strom–Zeit-Kurven der voltametrischen Oxydation einer (Pd–H)-Mikroelektrode mit linear veränderlicher Spannung. (a) Kleiner Wasserstoffgehalt, $C_a = 1.36 \cdot 10^{-8}$ Mol H_2 (1 *M* H_2SO_4); (b) grosser Wasserstoffgehalt, $C_a = 190.5 \cdot 10^{-8}$ Mol H_2 (1 *M* H_2SO_4).

ERGEBNISSE UND DISKUSSION

In der vorliegenden Arbeit wurden einige wichtigere störende Faktoren untersucht, die zu einer Änderung der scheinbaren Ausbeute der Wasserstoffrückgewinnung führen können. Ein Teil dieser Faktoren beeinflusst die Wirksamkeit eines einzigen Elektrodenprozesses, ein anderer Teil die Wirksamkeit beider Prozesse. Um aber übereinstimmende Ergebnisse zu erhalten, ist es notwendig Arbeitsbedingungen zu verwirklichen, unter welchen der Effekt dieser störenden Faktoren in einem der Prozesse Null ist um die scheinbare Ausbeute in Abhängigkeit der Störungen die im anderen Elektrodenprozess erscheinen, zu bestimmen.

Der Einfluss der Störungen im anodischen Prozess

Um die Störungen die ausschliesslich im anodischen Prozess erscheinen überprüfen zu können, wurden diejenigen der kathodischen Wasserstoffbeladung der Mikroelektrode beseitigt. Dass heisst dass die Versuchbedingungen verwirklicht wurden in denen $\Sigma Q_i^c \cong 0$ und $Q_c \cong Q_c^*$, und zwar: totale Isolierung der Lösung vom Sauerstoff, Entfernung der Sauerstoffspuren mit Hilfe des gereinigtem Stickstoffs, Erhalten der Lösung in ungerührtem Zustand und Aktivierung der Oberfläche durch Bedeckung mit Palladiumschwarz. Unter diesen Bedingungen wurde der Einfluss der elektrochemischen Korrosion, der Mikroelektrodenoberfläche, des Zeitabstandes zwischen dem Kathoden- bzw. Anodenprozess, der Rührung der Lösung auf die scheinbare Rückgewinnungsausbeute in einer Versuchsreihe geprüft.

Elektrochemische Korrosion

Die anodische Oxydation des Palladiums in sauren Lösungen und bei grösseren Potentialen als 0.8 V gegen Normalwasserstoffelektrode, führt zur elektrochemischen Korrosion der Metalloberfläche[5-6]. Die Grösse dieser Wirkung muss vom Potential, von der Konzentration der Säuren und wahrscheinlich von der Natur der Anionen abhängen. Da die vollständige Extraktion des Wasserstoffs aus Palladium eine maximale Spannung von 1.7 V benötigt, wurde dieser Wert in allen Bestimmungen beibehalten, und der Effekt der Korrosion auf die Ausbeute ϱ in Abhängigkeit von der Konzentration und der Natur der Anionen verfolgt. Deshalb wurde die scheinbare Rückgewinnungsausbeute in 0.05 *M* H_2SO_4-, 1 *M* H_2SO_4- und 1 *M* H_3PO_4-Lösungen gemessen. Alle Bestimmungen wurden in ungerührter und mit gereinigtem Stickstoff (etwa 1 l/h) vom Sauerstoff befreiter Lösung vollzogen. Zwischen den Bestimmungen wurden die Lösungen magnetisch und mit Durchperlen von Stickstoff gerührt. Die Ergebnisse sind in Tabelle I für drei verschiedene Bereiche des Wasserstoffgehaltes der (Pd–H)-Mikroelektrode dargestellt.

Bei niedrigem Wasserstoffgehalt, in einer 0.05 *M* H_2SO_4-Lösung, sind die Ergebnisse nicht reproduzierbar und wurden deshalb in Tabelle I nicht eingetragen. Bei mittlerem und grossem Gehalt ist die Rückgewinnungsausbeute gut, das heisst die Mittelwerte sind 102% bzw. 99%. Bei mittlerem und kleinem Wasserstoffgehalt in 1 *M* H_2SO_4-Lösungen erhält man grosse Abweichungen (±4% bzw. ±9%), bei erhöhtem Wasserstoffgehalt ist der Rückgewinn gut. Man erhält endlich in 1 *M*

TABELLE I

0.05 M H_2SO_4			*1 M H_2SO_4*			*1 M H_3PO_4*		
$C_c \cdot 10^8$ (*Mol H_2*)	$C_a \cdot 10^8$ (*Mol H_2*)	ϱ (%)	$C_c \cdot 10^8$ (*Mol H_2*)	$C_a \cdot 10^8$ (*Mol H_2*)	ϱ (%)	$C_c \cdot 10^8$ (*Mol H_2*)	$C_a \cdot 10^8$ (*Mol H_2*)	ϱ (%)
—	—	—	0.243	0.223	92	0.236	0.248	105
—	—	—	0.596	0.653	110	0.501	0.505	101
—	—	—	0.964	0.962	102	0.788	0.753	96
5.31	5.45	103	5.31	5.90	111	5.21	5.45	105
10.64	10.65	100	10.37	11.15	108	10.65	10.66	100
—	—	—	15.71	16.16	103	15.69	15.87	101
124.3	126.0	101	124.3	127.2	102	124.3	126.8	102
248.7	246.8	99	248.7	251.1	101	248.7	252.5	102
373.0	361.7	97	373.0	364.1	98	373.0	359.8	97

Der Wasserstoffgehalt im Palladium und die Struktur der oberen Schicht

Wegen der kleinen Absorbtionsenergie des Wasserstoffs im Palladium, hat das Gas die Neigung zu einer spontanen Desorbtion aus dem Metall. Natürlich wächst die Geschwindigkeit des Desorbtionsprozesses mit dem Wasserstoffgehalt und kann bei grossen Werten durch Verminderung der Wirksamkeit des kathodischen Prozesses, die Rückgewinnungsausbeute empfindlich beeinflussen. In diesem Falle, ist von den beiden Prozessen (2) und (3) der Desorbtions–Diffusionsprozess übergreifend.

Um diese Wirkung zu überwachen, wurden Messungen der Elektrizitätsmenge Q_a^* bei hohen Wasserstoffgehalten ($2 \cdot 10^{-6}$ Mol –$6 \cdot 10^{-6}$ Mol) in ungerührtem, mit Hilfe von gereinigtem Stickstoff vom Sauerstoff befreiten 1 *M* H_3PO_4- und 0.05 *M* H_2SO_4-Lösungen vorgenommen. Die Ergebnisse sind in Abb. 3 sichtbar, wo

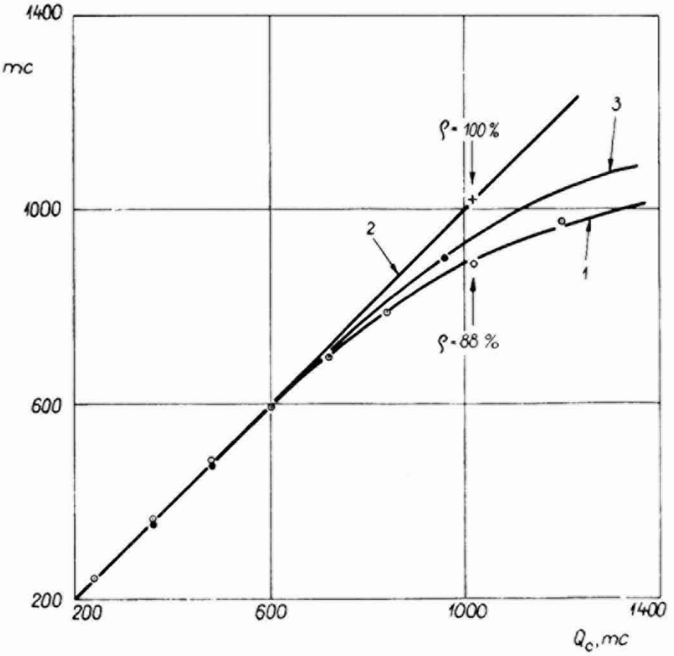

Abb. 3. Änderung der Elektrizitätsmenge Q_a^* in Abhängigkeit vom Wasserstoffgehalt. Temp. 25°C. (1) "Verbrauchte" Mikroelektrode in 1 *M* H_3PO_4; (2) reaktivierte Mikroelektrode in 1 *M* H_3PO_4; (3) "verbrauchte" Mikroelektrode in 0.05 *M* H_2SO_4.

auf der Abszisse die Elektrizitätsmenge Q_c aufgetragen wurde, welche für die Beladung der Mikroelektrode mit Wasserstoff verbraucht ist, auf der Ordinate wurde die Elektrizitätsmenge Q_a^* aufgetragen, welche für die Rückgewinnung des gelösten Wasserstoffs verbraucht ist. Kurve (1) entspricht einem kathodischen Beladungsstrom von $I_c = 2$ mA, für eine seit längerem mit Palladiumschwarz belegte Mikroelektrode, in 1 *M* H_3PO_4-Lösung. Es kann gleich beobachtet werden, dass angefangen von $Q_c \cong 600$ mC, die Rückgewinnungsausbeute zu sinken beginnt, umso mehr je höher der Wert Q_c ist. Gleichzeitig beobachtet man in der Kathoden-Prozessfolge eine sichtbare Entwicklung von Wasserstoff. Der auf Kurve (1) mit einem Kreis bezeichnete Wert entspricht einem viermal kleinerem Strom, $I_c = 0.5$ mA mit derselben Elektrode und bei gleichen Arbeitsbedingungen. Die scheinbare Rückgewinnungsausbeute bleibt praktisch bei demselben Wert $\varrho = 88\%$, wie im Falle eines hohen Stromes $I_c = 2$ mA.

Der mit einem Kreuz bezeichnete Wert auf der Gerade (2) wurde mit einem kathodischen Beladungsstrom von $I_c = 0.5$ mA unter denselben Bedingungen, aber auf der Mikroelektrode, die durch frische Belegung mit Palladiumschwarz reaktiviert wurden (3 Min zu 5 mA), erhalten. Gleichzeitig mit einer 1.8-maligen Vergrösserung der effektiven Oberfläche*, wurde auch eine gute Verbesserung der Rückgewinnungsausbeute, von $\varrho = 88\%$ zu $\varrho = 100\%$ festgestellt. Nachdem die Oberfläche dieser Elektrode in etwa acht Kathoden–Anoden-Prozessfolgen verwendet wurde, hat sich die Rückgewinnungsausbeute wieder vermindert und ihre Änderung in 0.05 *M* H_2SO_4-Lösung ist aus Kurve 3 sichtbar. Es wurde in H_2SO_4-Lösung gearbeitet, da in diesem Falle die Korrosion der Palladiumschwarzschicht und der Effekt der Strukturveränderung stärker ist.

Die durch Kurve 1 und 3 angegebene Art der Veränderung der Rückgewinnungsausbeute und hauptsächlich deren Unabhängigkeit von der Stromdichte (Kurve 2) zeigt, dass eigentlich der Desorbtions-Entwicklungsprozess der wahre Grund der Unwirksamkeit des kathodischen Beladungsprozesses bei hohen Wasserstoffgehalten ist. Die plötzliche Veränderung der Ausbeute durch Bedeckung mit Palladiumschwarz (Kurven 1 und 2) zeigt aber, dass die obere Schicht auch eine wichtige Rolle im Desorbtionsprozess spielt. Diese Rolle scheint die einer "energetischen Schranke" zu sein, deren Effekt manchmal sogar eine Hemmung der Desorbtion bei hohen Gehalten des in Palladium gelösten Wasserstoffs sein kann. Diese Hemmung begründet sich wahrscheinlich darauf dass der Wasserstoff viel stärker an die disperse Oberflächenschicht gebunden ist[8], und dieses vermindert die Geschwindigkeit des Desorbtionsprozesses. Dieses Problem wird in einer späteren Arbeit untersucht.

SCHLUSSFOLGERUNGEN

Die Rückgewinnungsausbeute des im Palladium gelösten Wasserstoffs ist von der elektrochemischen Korrosion der Mikroelektrodenoberfläche, vom Rührzustand der Lösung, von der Gegenwart des Sauerstoffs im Anolit, von der Konzentration des Wasserstoffs in der Mikroelektrode und der Struktur der auf der Oberfläche befindlichen aktiven Palladiumschwarzschicht beeinflusst. Alle diese Störungsfaktoren können bewältigt werden und unter passenden Umständen können die entsprechenden Effekte aufgehoben werden. Auf diese Weise kann die voltametrische Oxydationsmethode mit linear veränderlicher Spannung zur Bestimmung des absoluten, im Palladium gelösten Wasserstoffgehaltes zwischen den Werten von $3 \cdot 10^{-9}$ Mol und $4 \cdot 10^{-6}$ Mol, mit einer maximalen Abweichung von $\pm 5\%$ benützt werden.

---

* Diese Oberfläche wurde durch kontrollierte Oxydation der Mikroelektrodenoberfläche voltametrisch bestimmt, der ein Beladen mit Wasserstoff und dann die Rückgewinnung des gelösten Wasserstoffs folgt.

solution was placed in a thermostatic bath at 25° ± 0.1° and deoxygenated with oxygen-free nitrogen saturated with water vapour at 25°. The solution was then polarographed over a suitable range, the polarogram of applied voltage against maximum throw of the galvanometer (instantaneous current at end of drop life) was drawn and the diffusion current obtained by the usual method of determining wave heights. The applied potential was then set at the half-wave potentials and the drop time determined. Ten drops of mercury were collected, dried and weighed to determine rate of mercury flow.

This procedure was repeated for the same reducible ion of the same concentration but with different strengths of supporting electrolyte. Several electrolytes were used for each ion investigated.

Calculations

The diffusion coefficients were then calculated using

(1) the value of x determined by the slope of current - time curve over the last 2 sec of drop life[4];

(2) the value of A determined in a similar manner[4];

(3) with $A = 23.5$.

Calculations of the diffusion coefficient were made with these two values of A for the following reasons.

(i) Although instantaneous current is measured, the drops are not first drops but are the subsequent drops as used in normal polarographic work and as such the theoretical values of $A = 39$ for the instantaneous current equation[6] does not necessarily hold.

(ii) The values of A for non-first drops were found experimentally[4] to approximate to the value of 23.5—the value theoretically found by MATSUDA[3] when allowing for capillary cut-off. The possible exceptions are copper and indium when A approaches 39.

(iii) The average value of x in eqn. (1) was found[3] to be 0.199 and this represents a value of A considerably lower than 39.

The values of diffusion coefficient at zero concentration of supporting electrolyte were obtained by extrapolating the graph of diffusion current against electrolyte concentration to zero electrolyte concentration.

Since the viscosity of the solution affects the diffusion coefficient[7], viscosities of all solutions used were calculated using the equation,

$$\eta_s = \eta_o \left(1 + \tfrac{5}{2}\phi\right) \tag{4}$$

where η_s = calculated solution viscosity,

η_o = viscosity of solvent (water),

ϕ = total volume of particles which was determined from ionic and molecular radii, the apparent degree of ionization being obtained from conductivity data.

Although this equation is strictly valid only for idealized non-electrolytes, it was felt that little error would occur in its use which was primarily to extrapolate the diffusion coefficients to zero supporting electrolyte concentration. The Jones–Dole equation for electrolytes was not applied since the constants for some of the electrolytes used could not be found in the literature. Experimental values were not contemplated, since the change in viscosity over the concentration range used is so small, and it was thought that the determinations would not be of sufficient accuracy.

Errors and limitations

The reducible-ion concentration was accurately known; *m*, the mercury flow rate and *t*, the drop time were reproducible within ± 0.0027 mg/sec and ± 0.02 sec, respectively. The diffusion current could be read to $\pm 0.02\ \mu$A. For the average values used this gives a diffusion coefficient, $\pm 0.12 \times 10^{-6}\,\text{cm}^2\text{sec}^{-1}$ (*ca.* 1.7%).

Results

Tables 1–3 give the values of the diffusion coefficient calculated using the three values given above.

TABLE 1

DIFFUSION COEFFICIENTS CALCULATED USING EXPERIMENTAL VALUES OF x IN EQN. (1)

Electrolyte (mM)	*Pb*	*Cd*	*Cu*	*Zn*	*Ni*	*In*
x	0.197	0.170	0.206	0.205		
$Al(NO_3)_3$		$> D_o$				
0	9.970		6.652	9.666		
8	9.840		6.733	9.296		
24			5.133	8.655		
32	9.045					
40			6.690	8.622		
56	9.045		6.692	7.290		
72			6.370	6.422		
80	8.661					
100	8.789		6.692	6.666		
x	0.207	0.186	0.206	0.205		0.20
$Sr(NO_3)_2$		$> D_o$				
0	9.567		6.589	8.387		4.139
8			6.789	8.109		4.026
16	9.389					4.082
24			6.964	7.478		4.234
32	9.066					
40			6.920	7.478		3.913
56	8.747		6.237	6.815		3.711
72			6.703	6.746		3.486
80	8.586					
100	8.651		5.952	6.697		2.462
x	0.206	0.186	0.206	0.205	0.20	0.20
KNO_3		$> D_o$				
0	10.48		7.040	8.327	7.863	4.370
8			7.323	9.781	8.222	4.875
16	10.35					4.880
24			6.966	8.695	7.551	4.412
32	10.20					
40			6.922	7.489	7.132	4.412
48	9.732					
56			6.878	7.860	7.079	4.133
64	9.462					
72			7.010	8.433	6.463	4.296
80	9.356					
100	10.35		7.143	7.767	6.594	4.362

TABLE 2A

DIFFUSION COEFFICIENTS FROM EQN. (2) WHEN A IS EXPERIMENTAL VALUE

Electrolyte	*Experimental A*					
(mM)	*Pb*	*Cd*	*Cu*	*Zn*	*Ni*	*In*
$Al(NO_3)_3$	21.71	15.0	31.3	32.0		
0	9.019	7.795	6.629	7.268		
8	8.925	7.607	6.707	8.309		
24		7.130	5.287	7.261		
32	8.259					
40		7.040	6.685	7.306		
56	8.259	6.763	6.707	7.334		
72		6.352	6.465	7.499		
80	7.949					
100	8.131	6.379	6.707			
$Sr(NO_3)_2$	17.09	15.9	32.9	32.0		39.8
0	9.626	7.527	5.932	7.223		3.708
8		7.476	6.102	7.100		3.596
16	9.454					3.652
24		7.148	6.234	6.654		3.727
32	9.030					
40		7.287	6.214	6.654		3.469
56	8.920	7.148	5.665	6.137		3.231
72		6.727	6.038	6.079		3.196
80	8.677					
100	8.656	6.741	5.438	6.036		
KNO_3	24.90	15.0	30.8	32.0		37.5
0	9.859	7.767	7.044	7.327		3.951
8		8.180	7.327	8.387	7.186	4.360
16	9.849					4.365
24		7.784	7.008	7.796	6.676	4.021
32	9.715					
40		7.673	6.958	6.674	6.327	4.021
48	9.356					
56		7.724	6.902	6.975	6.391	3.779
64	9.097					
72		7.724	7.078	7.397	5.781	3.895
80	8.988					3.993
100	9.849	7.254	7.174	6.899	5.900	
HNO_3	25.8	19.0	32.6	32	16.3	36.4
0	8.748	7.306	5.395	8.117		3.445
8		7.443	4.647	7.939	7.930	3.535
16	8.726					3.352
24		7.164	5.299	7.730	7.812	3.679
32	8.687					
40		7.303	5.433	7.573		3.577
56		7.343	5.433	7.102	5.953	3.145
72		7.164	5.706	6.078	5.289	
80	8.452					
100	8.452	6.866	5.866	5.176		
KCl	25.7	30.1		32	24.3	22.1
0	9.355	6.895		8.381		4.758
8		7.169		7.977	7.326	5.087
16	9.780					4.866
24		6.792		7.282	6.633	4.780
32						

Table 2a (Continued)

Electrolyte (mM)	*Experimental A* *Pb*	*Cd*	*Cu*	*Zn*	*Ni*	*In*
40	9.357	6.882		7.092	6.417	4.907
56		6.963		7.092	5.747	4.345
72		6.963		7.177	5.955	4.617
80	9.070					4.420
100	8.996	6.793		6.406	5.955	
KCNS				32	15.1	
0				7.398		
8				8.138	7.793	
24				7.158	7.222	
40				7.131	6.831	
56				6.912	6.690	
72				6.912	6.436	

Cadmium diffusion coefficients using experimental values of x were generally greater in value than that calculated by the Nernst equation at infinite dilution, and hence were not recorded. Nickel in aluminium nitrate and strontium nitrate electrolytes and indium in aluminium nitrate gave extremely low results, probably due to hydrolysis.

TABLE 3

AVERAGE VALUES OF DIFFUSION COEFFICIENT CALCULATED: (1) FROM EQN. (1); (2) FROM EQN. (2), WITH A = 23.5; (3) FROM EQN. (2) WITH A = EXPERIMENTAL VALUE

Electrolyte		$D \cdot 10^6 (cm^2\ sec^{-1})$					
		Pb	*Cd*	*Cu*	*Zn*	*Ni*	*In*
		D_o					
		9.35	*7.21*	*7.46*	*7.05*	*7.21*	*5.15*
$Al(NO_3)_3$	(1)	9.31	7.38	6.81	7.60		
	(2)	8.98	6.94	7.19	8.40		
	(3)	8.90	7.20	6.70	7.18		
$Sr(NO_3)_2$	(1)	9.27	7.38	7.07	7.20		4.53
	(2)	9.02	7.20	6.90	7.42		4.59
	(3)	9.27	7.48	6.32	6.88		4.13
KNO_3	(1)	10.25	7.57	7.07	8.00	7.47	4.41
	(2)	9.90	7.23	7.40	7.88	6.97	4.41
	(3)	9.80	7.83	7.10	7.35	6.83	4.04
HNO_3	(1)	9.77	7.50	5.64			3.90
	(2)	9.07	7.30	5.48	8.91	7.70	3.90
	(3)	8.78	7.22	5.10	8.10	8.20	3.58
KCl	(1)	10.38	7.81		8.00	6.90	4.92
	(2)	9.35	7.38		7.65	6.96	4.92
	(3)	9.60	7.25		7.17	6.89	4.92
KCN_3	(1)				8.13	7.42	
	(2)				7.70	7.14	
	(3)				7.29	7.61	

MODE OF INHIBITION OF POLAROGRAPHIC CURRENTS BY CYCLOHEXANONE*

KEIICHI TSUJI

Rikagaku-kenkyusho, Institute of Physical and Chemical Research, Komagome, Bunkyo-ku, Tokyo (Japan)

(Received January 25th, 1965)

INTRODUCTION

Cyclohexanone and its C-alkyl derivatives have been known to affect the polarograms of certain reducible substances in acid media, producing a pronounced current minimum in the negative potential region[1]. Later, this effect was attributed to the formation of an insoluble film by the action of the ketone on the mercury cathode[2]. According to ARAI's electrolytic[3] and KALVODA's oscillopolarographic[4] studies, such a surface film most likely consists of cyclohexylmercury(I); this conclusion is supported by the results of a.c. and d.c. voltammetric study by the present author[5]. The mechanism of current inhibition by this film, however, has remained unsolved.

One important feature of this kind of inhibitory action is its peculiar selectivity[1]. This selectivity was at first considered to be related to the half-wave potentials, rather than oxidation states, complexed states and charges of the reducible species. Only those species whose half-wave potentials are found in the potential region more negative than -0.5 V *vs.* S.C.E. were affected (in normal mineral acids). More precisely, the index, γ, which was introduced before[1] as the ratio $\Delta i_{\min}/\Delta i_{\lim}$, is near zero for species with more negative half-wave potentials and is near unity for those with less negative half-wave potentials. Here, $\Delta i_{\min}$ and $\Delta i_{\lim}$ denote current changes at the bottom of the minimum and at the current plateau, respectively, both being induced by a small change of concentration of reducible substances.

Though characteristic, this relation does not form a suitable basis for the discussion of inhibition mechanism, because the half-wave potential is not necessarily a parameter directly related to electrode reactions. An explicit relation would be established instead if we could justify a speculative assumption that $i_{\min}$, the current flowing at the bottom of the minimum (after correction for blank current), is at all times simply equal to i_0, which is the current at a hypothetical potential E_0 given for each case.

This hypothetical relation is explained on curve b, Fig. 1a. Here E_0 was chosen so that i_0 is equal to $i_{\min}$. When both currents are subjected to change by any available means which does not affect the essential polarographic conditions of the original

---

* This paper constitutes the third part of the series of investigations on the effect of cyclohexanone on polarographic currents; it follows previous papers on this subject[1,2].

system, the current at this potential E_0 should necessarily follow the course identical with that of i_{min} if the above assumption is valid. Also, the plot of i_0 *vs.* i_{min} should be on a straight 45° line. The present work was carried out to prove this validity and thereby to make the foundation for the discussion of the inhibition mechanism.

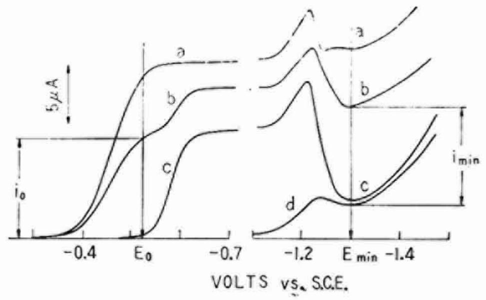

Fig. 1a. Polarograms of Tl(I), Cd(II) and their mixture in 1 N H_2SO_4 containing $5 \cdot 10^{-3}$ M cyclohexanone. (a), $2 \cdot 10^{-3}$ M Tl_2SO_4; (b), 1.2×10^{-3} M $CdSO_4$ + 0.8×10^{-3} M Tl_2SO_4; (c), $2 \cdot 10^{-3}$ M $CdSO_4$; (d), blank.

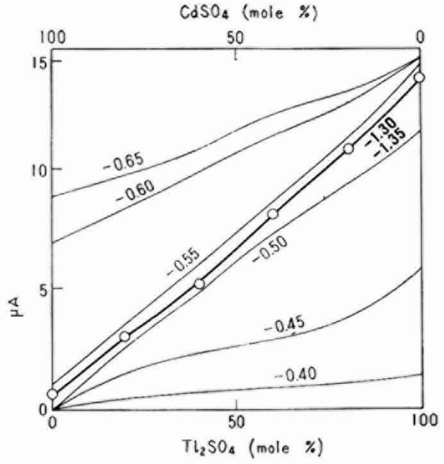

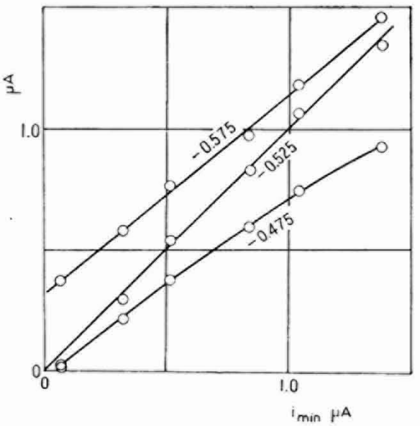

Fig. 1b. Current–molar ratio curves for Cd(II)–Tl(I) system.

Fig. 1c. Relationship of currents at −0.575, 0.525 and −0.475 V to i_{min} (at −1.35 V).

EXPERIMENTAL

A Yanagimoto recording polarograph PA 102 was utilized for current and potential measurements. A conventional H-type cell with agar bridge or a cell designed to prevent the test solution from being contaminated by chloride ion (both with saturated calomel external electrode) was used. Capillary characteristics were: $m = 1.046$, $t = 3.67$ in deaerated 0.1 N HCl with open circuit. Cyclohexanone was purified through its bisulfite compound. Other chemicals were of reagent-grade. Experiments were usually carried out at 25°.

In the first experiment, mixtures of thallium(I) sulfate and cadmium(II) sulfate in varying proportions were polarographed in 1 N H_2SO_4 containing $5 \cdot 10^{-3}$ M cyclohexanone (Fig. 1a). The total metal sulfate content was maintained at $2 \cdot 10^{-3}$ mole/l. In this medium, half-wave potentials of these sulfates were −0.46 and −0.57 V, respectively, and the index, γ, is slightly less than 1 for thallium(I) and nearly zero for cadmium(II). The bottom of the current minimum produced by cyclohexanone was found at −1.30 V. When cadmium(II) was increased and thallium(I) decreased, the current at −1.30 V, *i.e.*, i_{min}, decreased. Polarographic currents were measured at small potential intervals for each mixture, and were plotted against molar proportions of the two species. The resultant curves are shown in Fig. 1b. It is easily seen that the curve for the current at −1.30 V (i_{min}) and also that at −1.35 V agree with the curve at −0.525 V. The potential, E_0, for this system is therefore −0.525 V. In addition,

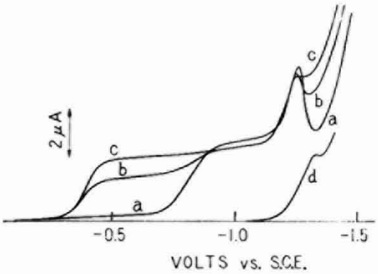

Fig. 2a. Polarograms of Ti(IV) and the effect of the addition of citric acid, in 0.1 N HCl containing $5 \cdot 10^{-3}$ M cyclohexanone. $2 \cdot 10^{-3}$ M $TiCl_4$ with (a), 0; (b), $2 \cdot 10^{-2}$ M; (c), 8.5×10^{-2} M citric acid added. (d), blank without citric acid.

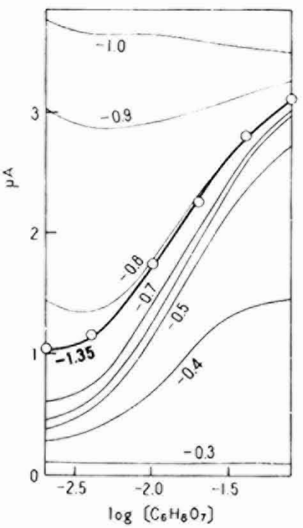

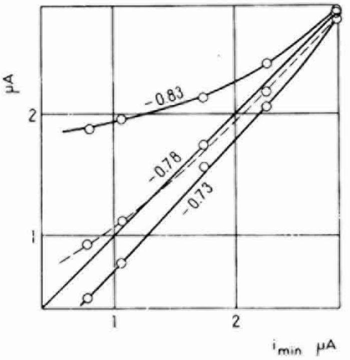

Fig. 2b. Current–log (citric acid) curves for Ti(IV)–citric acid system. Concns. in moles/l.

Fig. 2c. Relationship of currents at −0.73, 0.78 and −0.83 V to i_{min} (at −1.35 V).

the curve at −1.25 V was found to agree with that at −0.575 V. The relation of the current at −0.525 V to i_{min} and also those of currents at potentials −0.475 and −0.575 V are graphically shown in Fig. 1c. The agreement of the curve at −0.525 V with the theoretical 45° straight line is apparent.

An analogous experiment with thallium(I) chloride and indium(III) chloride in 1 *N* HCl containing $5 \cdot 10^{-3}$ *M* cyclohexanone gave similar results. The curves for the currents at −1.30, −1.35 and −1.40 V were superimposed one above another becoming a single curve which agreed with the curve at −0.525 V, and the curve for −1.25 V agreed with the curve at −0.550 V.

Another method of changing the current is by the addition of complexing agents to the solution of a certain reducible species; this was done with titanium(IV) chloride and citric acid in 0.1 *N* HCl containing $5 \cdot 10^{-3}$ *M* cyclohexanone. On the addition of citric acid, a new wave due to the reduction of the complex ($E_{\frac{1}{2}} = -0.39$ V) developed at the expense of the original wave ($E_{\frac{1}{2}} = -0.85$ V). The current i_{min} also increased as shown in Fig. 2a. By a procedure similar to that used before, current curves were drawn with the logarithm of citric acid concentration as abscissa (Fig. 2b). It is evident that i_{min} (at −1.35 V) corresponds approximately to the curve at −0.78 V, deviating slightly to less negative potentials at lower citric acid concentrations. The relation of the current at −0.78 V to i_{min} is shown graphically in Fig. 2c. The curve deviates slightly from the theoretical 45° straight line. Currents at −0.73 and −0.83 V are also shown in the same figure.

One more example of this kind is the reduction of tin(IV) chloride in 1 *N* $HClO_4$ containing $5 \cdot 10^{-3}$ *M* cyclohexanone and 0.001% Triton X-100*, in which current change was effected by the addition of lithium chloride. In this case, the potential chosen so that the current at this potential was equal to i_{min} (at −1.31 V) did not remain constant but shifted towards more positive potentials, linearly with the logarithm of chloride concentration up to 1.0 *M*. At higher chloride concentrations, a constant value of −0.57 V was found. Temperature dependence of wave height and the current–time curve during one drop life were examined, and it was shown that the ill-developed wave at lower chloride concentrations has a significant kinetic character.

In the following cases, the deformation and negative shift of the reduction waves by the addition of surface-active substances were utilized to test the validity of the aforementioned assumption. The addition of Triton X-100 to a $2 \cdot 10^{-3}$ *M* solution of tin(IV) chloride in 1 *N* HCl containing $5 \cdot 10^{-3}$ *M* cyclohexanone causes a decrease of the height and a slight negative shift of the wave ($E_{\frac{1}{2}} = -0.45$ V, with 0.0025% Triton X-100). E_{min} was found at −1.27 V, and i_{min} also decreased along with the addition of Triton X-100. By a procedure similar to that already described, it was found that the i_{min}–log [Triton] curve was confined to a narrow range between the current curves at −0.500 and −0.475 V.

As the last example, $2 \cdot 10^{-3}$ *M* cystine solution in 0.1 *N* HCl containing $5 \cdot 10^{-3}$ *M* cyclohexanone was used. On the addition of a small amount of thymol, the half-wave potential of the wave shifted in a negative direction from about −0.4 V, and the current minimum was simultaneously produced (Fig. 3a).

According to KOLTHOFF AND BARNUM[6] this shift is due to the formation of an adsorbed film of thymol which inhibits the reduction of cystine. By plotting the current

---

* The addition of Triton X-100 improved the development of the first wave of Sn(IV).

against logarithm of thymol concentration, the curves shown in Fig. 3b were obtained. The current curve at E_{min} (-1.45 V) lay between those at -0.60 and -0.65 V. The relations of the currents at -0.54, 0.64 and -0.74 V to i_{min} are shown in Fig. 3c.

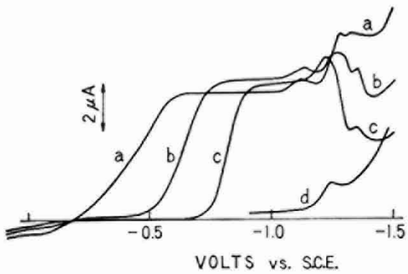

Fig. 3a. Polarograms of $2 \cdot 10^{-3}$ *M* cystine in 0.1 *N* HCl containing $5 \cdot 10^{-3}$ *M* cyclohexanone with (a), 0; (b) $1 \cdot 10^{-4}$ *M*; (c), $1 \cdot 10^{-3}$ *M* thymol added; (d), blank curve.

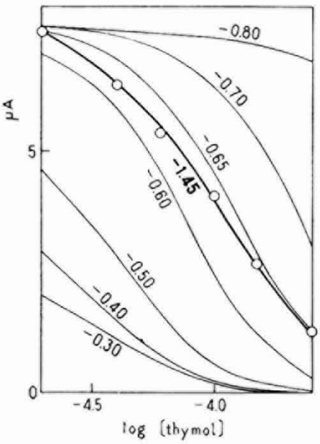

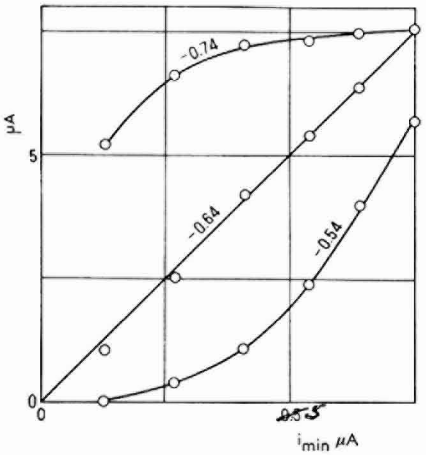

Fig. 3b. Current–log (thymol) curves for cystine–thymol system. Concns. in moles/l.

Fig. 3c. Relationship of polarographic currents at -0.54, 0.64 and -0.74 V to i_{min} (at -1.45 V.)

DISCUSSION

It is known that the current–time curve during one drop life, at the potential at which the inhibition by cyclohexanone occurs, is much distorted and irregular, due to the time-dependent formation of the surface film and to the capacity phenomena[1]. On the other hand, polarographic measurement of the current yields only an average current. Strictly speaking, the comparison of such a current measured polarographically, with the average current at another potential where the current–time curve is approximately normal, may, therefore, introduce some error in the determination of E_0. However, in view of the reasonable agreement found between two currents i_0 and i_{min} in the above experiments, the approximation adopted in current measurements is considered to be adequate. Except for the case of the Sn(IV)–Cl^- system, E_0 was found to be a fixed potential for each system, and can be used to predict i_{min} and hence the presence of the current minimum. The failure of this principle in the Sn(IV)–Cl^- system may be due to the kinetic character of the wave at lower chloride concentrations and to the possible difference between reaction kinetics at E_{min} and E_0. The effect of tin on the shape of the current minimum, which seems to catalyze the reduction of hydrogen ion, should also be considered.

In the above experiments, the current at the bottom of the minimum was chosen for comparison with the currents at other potentials, but this is rather an arbitrary choice taken for the sake of convenience. In fact, as in the Tl(I)–Cd(II) system, a potential slightly more negative than E_{min} invariably corresponded to a potential less negative than E_0. This was also deduced from the results of KALOUSEK's polarography which will appear in another paper.

It is rather surprising that the current change at E_0 is usually faithfully reproduced at E_{min} despite the large voltage difference and the variety of current-controlling factors included in the experiments. Although it may seem strange, we conclude that a mercury cathode, polarized at E_{min} and covered with the surface film, behaves exactly like a naked electrode polarized at E_0 in regard to electrode phenomena including the effect of surface-active substances.

The difference between E_0 and E_{min}, which may be regarded as the measure of the decrease of effective potential of the electrode, amounts to about 800 mV. That E_0 is usually found to be a constant potential for a system, independent of the flow of the current, excludes the possibility that a simple resistive component alone creates the potential difference. At the present stage, it is only suggested that probable non-linear current–voltage characteristics of the system comprising mercury cathode, organometallic layer and aqueous phase may be responsible for this phenomenon.

Now that the correspondence between i_{min} and i_0 is established, the selectivity of the effect of cyclohexanone already noted can be explained in a simple manner. As soon as the dropping electrode is polarized to a sufficiently negative potential (about -1.2 V in normal mineral acids), the surface film is formed at an early stage of the drop growth and the electrode behaves as if its applied potential was suddenly brought back to E_0. For easily reducible substances, this means no significant current change, because E_0 is included in the current plateau. For others, however, no current or only a fraction of the limiting current flows at E_0, and the current drops to a minimum with the formation of the surface film.

CONCLUSION

The assumption, that the current which flows at the bottom of polarographic minimum caused by cyclohexanone is identical with the current which flows at a hypothetical fixed potential E_0 given for each system, was experimentally justified in five out of six cases. It leads to a supposition that the electrode phenomena (including the effect of surface-active substances) at the film-covered surface may be very similar to those which occur at the naked surface polarized at E_0. A potential difference of about 800 mV was found between E_0 and E_{min}, and this corresponds to the decrease of effective potential due to the covering of the surface by the film. The selectivity of the minimum-producing effect of cyclohexanone in regard to reducible species can be explained in a simple manner by this relation.

ACKNOWLEDGEMENTS

The author thanks Dr. H. IKEDA and Dr. R. TAMAMUSHI of this institute who provided various facilities for this work. Assistance by Miss A. ERIGUCHI is deeply appreciated.

SUMMARY

Cyclohexanone produces pronounced minima in the negative part of certain polarographic current–voltage curves; these minima are due to the formation of an insoluble film on the electrode surface. It was found that the reduction current at the bottom of the minimum is usually consistently identical with the current which flows under the same condition at some more positive fixed potential E_0, the value of which has been determined for each specific case. E_0 is found to occur in the middle part of the polarogram and is about 800 mV less negative than the potential of the bottom of the minimum. Even the effects of surface-active substances on the two currents seem to be identical. The cause of this decrease in the effective potential of the electrode is not known. The selectivity of the minimum-producing effect of cyclohexanone, which had hitherto been considered to be related to the half-wave potential of the reducible species, is explained by this relation in a simple manner.

REFERENCES

1 K. TSUJI, *Sci. Papers Inst. Phys. Chem. Res.*, 56 (1962) 167.
2 K. TSUJI, *Rev. Polarog. (Kyoto)*, 11 (1964) 233.
3 T. ARAI, *Bull. Chem. Soc. Japan*, 32 (1959) 184.
4 R. KALVODA, *Chem. Zvesti*, 16 (1962) 330.
5 K. TSUJI, unpublished results.
6 I. M. KOLTHOFF AND C. BARNUM, *J. Am. Chem. Soc.*, 63 (1941) 520.

JOURNAL OF ELECTROANALYTICAL CHEMISTRY

DIRECT DETERMINATION OF THE SURFACE EXCESS OF SPECIFICALLY ADSORBED IONS ON MERCURY

HENRI D. HURWITZ*
The Electrochemistry Laboratory, University of Pennsylvania, Philadelphia (U.S.A.)
(Received February 15th, 1965)

It is well known that at a mercury electrode, the relative surface excess of an adsorbed species, as well as the density of charge on the metal, may be obtained from the Gibbs–Duhem relation extended to the case of the ideal polarised electrode. FRUMKIN AND IOFA[1] and later GRAHAME[2] and PARSONS AND DEVANATHAN[3] have shown how this relation can be used for the determination of the relative surface excess of an ionic species. However, it is impossible by means of thermodynamic arguments only, to determine the extent to which the so called "specific adsorption" contributes to the overall excess and to the charge density. In particular, this limitation appears if one attempts to recover the adsorption isotherm of specifically adsorbed ionic components from double-layer capacity measurements or from electrocapillary curves. Such attempts are based, in fact, on the choice of a particular diffuse-layer model. Thus, in the case of the commonly-treated system, namely a symmetrical electrolyte, it has become customary to make use of the Gouy–Chapman relations[2,4] although the theoretical limitations of this model have often been emphasized[5,6].

The purpose of the following approach is to show how a very general physical assumption regarding the structure of the diffuse layer, together with a careful thermodynamic analysis, removes the need to use Gouy–Chapman potentials, and thus may overcome the difficulties quoted above in the matter of obtaining the adsorption isotherms.

We consider a system of mixed electrolytes $\Sigma_{n-1}^{p} AB_n$ $(n=1,2 \ldots p)$ where A is the common ion and where $B_1, B_2 \ldots B_p$ are the hetero ions. We assume, also, that all electrolytes are symmetrical and univalent; this implies the following relation for the ionic charges,

$$-z_A = z_{B_1} = z_{B_2} \ldots = z_{B_p} \;; \qquad |z_{B_n}| = 1 \;; \tag{1}$$

Furthermore, the special condition of constant molal ionic strength, J, is applied to all systems investigated. Hence one has in terms of the ionic molalities m_A, $m_{B_1} \ldots m_{B_p}$:

$$J = \tfrac{1}{2}(m_A + \sum_n m_{B_n}) = m_A. \tag{2}$$

By using Gibbs' adsorption equation, the change of surface tension, σ, at constant temperature may be written

$$(\mathrm{d}\sigma)_T = -\Gamma_{A,0}\mathrm{d}\mu_A - \sum_n \Gamma_{B_{n,0}}\mathrm{d}\mu_{B_n} - q_M\mathrm{d}\psi \;, \tag{3}$$

---

* On leave of absence from the Free University of Brussels, Belgium.

where $\psi = \varphi_I - \varphi_{II}$ defines the electrical potential difference between the electrode and the bulk of the solution (Fig. 1), μ is the chemical potential in the bulk of the solution

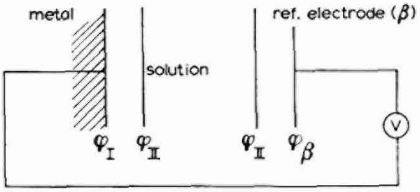

Fig. 1. The reference-electrode circuit.

and where q_M, the surface charge density at the electrode, is related to the electroneutrality condition in the following way,

$$q_M = -\left(\frac{\partial\sigma}{\partial\psi}\right)_{T,\mu} = -\Gamma_{A,0}z_A F - \sum_n \Gamma_{B_n,0} z_{B_n} F \tag{4}$$

The relative surface excess, $\Gamma_{X,0}$, is, as usual, given in terms of the absolute surface excess, Γ_X, of any component X and of the solvent Γ_0. Those absolute surface excesses are defined for a Gibbs' plane corresponding to the impermeable boundary for charge components. Thus by definition

$$\Gamma_{X,0} = \Gamma_X - \Gamma_0 \frac{m_X}{m_0}. \tag{5}$$

If a reference electrode β, reversible to the ionic component A, is used for the determination of the potential difference, the change of the measured potential, E, may be expressed, as illustrated in Fig. 1, by

$$\mathrm{d}E = \mathrm{d}(\varphi_I - \varphi_{II}) + \mathrm{d}(\varphi_{II} - \varphi_\beta) = \mathrm{d}\psi - \frac{\mathrm{d}\mu_A}{z_A F} \tag{6}$$

To proceed further σ is differentiated with respect to the molality m_{B_i} (of any hetero ion B_i) by maintaining constant T, E, J and the molalities of all hetero ions with the exception of B_1 and of course B_i (the latter condition is indicated in the next relation by m_B'). The resulting equation, which can be readily deduced from eqn. (3), is

$$\frac{1}{RT}\left(\frac{\partial\sigma}{\partial \ln m_{B_i}}\right)_{\substack{T,E,J\\ m_B'}} = -\Gamma_{A,0}\left(\frac{\partial \ln \gamma_A m_A}{\partial \ln m_{B_i}}\right)_{\substack{T,E,J\\ m_B'}} - \sum_n \Gamma_{B_n,0}\left(\frac{\partial \ln \gamma_{B_n} m_{B_n}}{\partial \ln m_{B_i}}\right)_{\substack{T,E,J\\ m_B'}} - \frac{q_M}{RT}\left(\frac{\partial\psi}{\partial \ln m_{B_i}}\right)_{\substack{T,E,J\\ m_B'}}, \tag{7}$$

where γ_A, γ_{B_n} are the molal ionic activity coefficients. Under the condition of constant ionic strength (2) and taking into account the reversibility of the reference electrode β for A as given in eqn. (6), eqn. (7) reduces to

$$\frac{1}{RT}\left(\frac{\partial \sigma}{\partial \ln m_{B_i}}\right)_{\substack{T,E,J\\ m'_B}} = -\Gamma_{B_i,0} + \frac{m_{B_i}}{m_{B_1}}\Gamma_{B_1,0} - \Gamma_{A,0}\left(\frac{\partial \ln \gamma_A}{\partial \ln m_{B_i}}\right)_{\substack{T,E,J\\ m'_B}} - \sum_n \Gamma_{B_n,0}\left(\frac{\partial \ln \gamma_{B_n}}{\partial \ln m_{B_i}}\right)_{\substack{T,E,J\\ m'_B}} - \frac{q_M}{z_A F}\left(\frac{\partial \ln \gamma_A}{\partial \ln m_{B_i}}\right)_{\substack{T,E,J\\ m'_B}}. \tag{8}$$

In order to evaluate the contribution of the differentials of the ionic molal activity coefficients in eqn. (8) it would be particularly appropriate to express these quantities in terms of the mean molal activity coefficients $\gamma_{AB_n} = (\gamma_A \gamma_{B_n})^{\frac{1}{2}}$. This can be done by using eqn. (4) in eqn. (8). Then the latter equation reduces to

$$\frac{1}{RT}\left(\frac{\partial \sigma}{\partial \ln m_{B_i}}\right)_{\substack{T,E,J\\ m'_B}} = -\Gamma_{B_i,0} + \frac{m_{B_i}}{m_{B_1}}\Gamma_{B_1,0} - 2\sum_n \Gamma_{B_n,0}\left(\frac{\partial \ln \gamma_{AB_n}}{\partial \ln m_{B_i}}\right)_{\substack{T,E,J\\ m'_B}} \tag{9}$$

It is apparent upon examining eqn. (9) that, in the case of a binary mixture of strong electrolytes ($AB_1 + AB_2$), the differentials in the right-hand term may be correctly estimated by introducing Harned's rule[7] according to which $\ln \gamma_{AB_n}$ can be expressed as a linear function of the partial molality of AB_n. Since the Harned coefficients, α, are generally small ($\alpha \leqslant 0.1$)

$$\begin{aligned} \left(\frac{\partial \ln \gamma_{AB_2}}{\partial \ln m_{B_2}}\right)_{T,E,J} &= m_{B_2}\alpha_{1,2} < 0.1 \\ -\left(\frac{\partial \ln \gamma_{AB_1}}{\partial \ln m_{B_2}}\right)_{T,E,J} &= m_{B_2}\alpha_{2,1} < 0.1\,. \end{aligned} \tag{10}$$

By extending these inequalities to the more general multicomponent system considered above, it becomes permissible to neglect the differentials in the right-hand side of eqn. (9). Therefore this equation is approximately given by

$$\left(\frac{\partial \sigma}{\partial \ln m_{B_i}}\right)_{\substack{T,E,J\\ m'_B}} = -\Gamma_{B_i,0} + \frac{m_{B_i}}{m_{B_1}}\Gamma_{B_1,0} = -\Gamma_{B_i} + \frac{m_{B_i}}{m_{B_1}}\Gamma_{B_1}\,. \tag{11}$$

Let us now assume that B_1 is non-specifically adsorbed and that Γ_{B_i} consists of two parts: the first part, $\Gamma_{B_i}{}^D$, corresponding to the adsorption in the diffuse part of the double layer and the second, $\Gamma_{B_i}{}^A$, representing the contribution to the surface excess of the amount specifically adsorbed in the inner layer. Hence

$$\Gamma_{B_i} = \Gamma^D_{B_i} + \Gamma^A_{B_i} \tag{12}$$

and

$$\Gamma_{B_1} = \Gamma^D_{B_1}. \tag{13}$$

At this point it seems necessary to make a very general statement about the ion distributions in the diffuse layer. Considering a model of long-range Coulombic interactions and small *specific* short-range effects of the diffuse-layer ions among each other and with the electrode, it is possible to introduce the relation

$$\frac{\Gamma^{D}_{B_i}}{\Gamma_{B_1}} = \frac{m_{B_i}}{m_{B_1}} \tag{14}$$

which, after substitution into eqn. (11), and on account of eqn. (12), leads to

$$\frac{1}{RT}\left(\frac{\partial \sigma}{\partial \ln m_{B_i}}\right)_{\substack{T,E,J\\ m'_B}} = -\Gamma^{A}_{B_i}. \tag{15*}$$

The latter expression yields the absolute surface excess (at the impermeable boundary for charge components) corresponding to the amount of species B_i specifically adsorbed.

It will be noted that eqns. (11) and (15) do not depend any longer on the position of Gibbs' reference surface. This point can also be readily inferred from the following argument. Let the Gibbs' surface be shifted through some distance perpendicular to the electrode. Then, a quantity of B_1 and B_i has to be added to or substracted from the total surface excess in order to maintain the solution phase uniform as far as the surface. The amount of B_1 and B_i so transferred must be in the same ratio as the molalities m_{B_1} and m_{B_i} in the bulk of the solution. But, although this transfer affects separately the values of $\Gamma_{B_1}{}^{D}$ and of $\Gamma_{B_i}{}^{D}$ as shown in eqns. (12) and (13), neither the difference $[(m_{B_i}/m_{B_1})\Gamma_{B_1} - \Gamma_{B_i}]$ in eqn. (11) nor the specifically adsorbed excess $\Gamma_{B_i}{}^{A}$ in eqn. (15) are altered.

Another feature of the present derivation is that it leads to $\Gamma_{B_i}{}^{A}$ by adopting eqn. (14), a straightforward expression for the model of the diffuse layer. In connection with this assumption, it may be of some interest to propose a more refined picture which accounts for some specific behaviour of B_1 and B_i in the diffuse layer. Such effects were studied in a previous publication[8] and should correspond to the model of double layer presented roughly in Fig. 2. The distance between the electrode and the

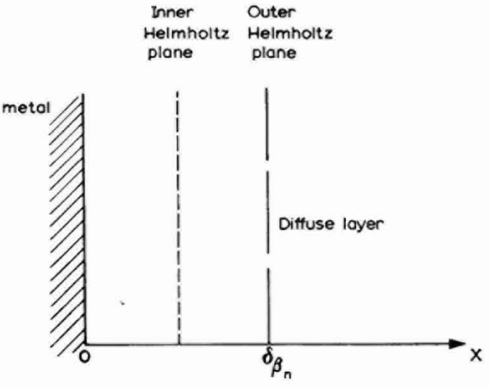

Fig. 2. The simplified model of the electrochemical double layer.

---

* A recent communication of Dr. R. PARSONS indicates that a relation of the type (15) has been used for the determination of the adsorption isotherm of specifically adsorbed chloride ions on mercury. The author became aware of Dr. PARSONS work after the present paper had been written.

outer Helmholtz plane (*i.e.*, the plane defined by the centres of fully hydrated ions at their closest approach of the electrode) may be different for the components B_n and shall therefore be designated by the parameter δ_{B_n}. Equation (14) should now be rewritten in the following way:

$$\frac{\Gamma^D_{B_i}}{\Gamma_{B_1}} = K\,\frac{m_{B_i}}{m_{B_1}} \tag{16}$$

where K is a function of different factors like the ionic specific volume, the polarisability of the medium, the self-atmosphere effects in the diffuse layer[8] and the distances of closest approach δ_{B_n} as stated above. Since eqn. (11) does not depend any more on the position of the Gibbs' reference plane, we shall choose arbitrarily this plane to be the plane defined by the electrode surface[9].

Hence, in dilute solutions, K can be shown[8] to be given by the general relation

$$K \doteq \frac{\dfrac{d}{1000}\left\{\displaystyle\int_{\delta_{B_i}}^{\infty}\left[\exp.\left(-\frac{\omega_{B_i}}{kT}\right)-1\right]\mathrm{d}x-\delta_{B_i}\right\}}{\dfrac{d}{1000}\left\{\displaystyle\int_{\delta_{B_1}}^{\infty}\left[\exp.\left(-\frac{\omega_{B_1}}{kT}\right)-1\right]\mathrm{d}x-\delta_{B_1}\right\}}, \tag{17}$$

where ω_{B_n} is the potential of mean force referring to the ions B_n in the diffuse layer and d is the bulk density of the solution. By substituting eqns. (12) and (17) into eqn. (11) one gets

$$\frac{1}{RT}\left(\frac{\partial\sigma}{\partial\ln m_{B_i}}\right)_{\substack{T,E,J\\ m'_B}} = -\Gamma^A_{B_i} - \frac{m_{B_i}d}{1000}\left\{\int_{\delta_{B_i}}^{\infty}\left[\exp.\left(-\frac{\omega_{B_i}}{kT}\right)-1\right]\mathrm{d}x \right.$$
$$\left. - \int_{\delta_{B_1}}^{\infty}\left[\exp.\left(-\frac{\omega_{B_1}}{kT}\right)-1\right]\mathrm{d}x - [\delta_{B_i}-\delta_{B_1}]\right\}, \tag{18}$$

or by supposing $\delta_{B_1} \simeq \delta_{B_i} = \delta$,

$$\frac{1}{RT}\left(\frac{\partial\sigma}{\partial\ln m_{B_i}}\right)_{\substack{T,E,J\\ m'_B}} = -\Gamma^A_{B_i} - \frac{m_{B_i}d}{1000}\left\{\int_{\delta}^{\infty}\left[\exp.\left(-\frac{\omega_{B_i}}{kT}\right) - \exp.\left(-\frac{\omega_{B_1}}{kT}\right)\right]\mathrm{d}x\right\}. \tag{19}$$

On the basis of this refined model, it is clear that the validity of eqn. (15) depends on two conditions: $\delta_{B_1} = \delta_{B_i}$ and $\omega_{B_1} = \omega_{B_i}$. If the restriction of these conditions is to be avoided, the more general relations, eqn. (18) or eqn. (19), have to be used. The correction resulting from the use of eqn. (19) may be estimated with the calculations presented in ref. 8, but the effects so included are small and may be generally ignored in the case of strong specific adsorption. This would be particularly true for the case of a super-equivalent adsorption of $B_2 \ldots B_n$. Then, the charge of the inner Helmholtz plane, $q_{\text{i.h.p.}}$, and the charge of the metal, q_M, are of opposite sign and $|q_{\text{i.h.p.}}| > |q_M|$. Under these conditions the diffuse layer is mainly constituted by the common ion A.

Despite the use of the simplifications $\delta_{B_1} = \delta_{B_i}$ and $\omega_{B_1} = \omega_{B_i}$, the treatment suggested here does provide important information on the structure of the diffuse layer *in the presence of specific adsorption*. For instance, combining eqns. (4) and (15), the density of charge $q_M{}^D$ induced by the diffuse layer on the electrode is obtained, thus

$$\left(\frac{\partial\sigma}{\partial E}\right)_{T,\mu} + \frac{F}{RT}\sum_{n\neq 1} z_{B_n}\left(\frac{\partial\sigma}{\partial \ln m_{B_i}}\right)_{\substack{T,E,J\\ m'_B}} = z_A F\Gamma_A^A - q_M^D \simeq -q_M^D \qquad (20)^*$$

where the specific adsorption of A and B_1 is assumed negligible. The values of $\Gamma_{A,0}{}^D$ and of $\Gamma_{B_i,0}{}^D$ may also be deduced separately from eqns. (15) and (20) and from the relative surface excess, $\Gamma_{B_i,0}$, calculated by Grahame's method[2] at the same potential E.

Equations (11) and (15) can be applied without any difficulty to the values of the interfacial tension, σ, measured in solutions of mixed electrolytes at the mercury electrode. In the case of the binary systems NaF–NaX or KF–KX ($X = \mathrm{Cl}^-, \mathrm{Br}^-, \mathrm{I}^-$), investigated at constant molal ionic strength, the treatment would lead to the specifically adsorbed surface excess of Cl^-, Br^-, I^-, provided that the specific adsorption of F^- is considered negligible, which seems a reasonable assumption. Likewise, the determination of $\Gamma_{\mathrm{Cs}^+}{}^A$ for Cs^+ from mixtures of the type LiCl–CsCl is possible if the specific adsorption of Li^+ is assumed to be weak.

The treatment provides, on the other hand, a direct experimental method for investigating the diffuse part of the electrochemical double layer in presence of specific adsorption. As has been pointed out in eqn. (20), the charge density $q_M{}^D$ may be obtained at any potential where $X = \mathrm{Cl}^-, \mathrm{Br}^-, \mathrm{I}^-$, is specifically adsorbed. However, such experimental systems as LiF–LiX or NaF–NaX have to be used in order to fulfil the requirement that $A(=\mathrm{Li}^+ \text{ or } \mathrm{Na}^+)$ and $B_1(=\mathrm{F}^-)$ are mainly adsorbed in the diffuse layer.

Furthermore, it is worth emphasizing that neither the Debye–Hückel approximation for the potential of mean force $\omega_{B_n}{}^{5,6}$ nor the integrated form of the Poisson–Boltzman relation have to be introduced in the present treatment, and that the specifically adsorbed surface excess obtained, appears to be independent of the location of Gibbs' reference surface.

ACKNOWLEDGEMENT

This work arose from valuable discussions with Professor L. GIERST, of the Free University of Brussels, Belgium, to whom the author expresses his gratitude. The author also wishes to thank Prof. J. O'M. BOCKRIS for helpful discussions.

SUMMARY

Gibbs' adsorption equation has been derived in the case of mixed solutions of strong electrolytes at constant molal ionic strength. Under these conditions, the specifically adsorbed surface excess of ionic species at the mercury electrode and the charge of the diffuse layer in presence of specific adsorption may be obtained. The main feature of the treatment consists in the fact that neither the differential equation of Poisson–Boltzman nor the integrated solution of Gouy–Chapman have to be introduced.

---

* In obtaining eqn. (20) from eqn. (4) it has been assumed that $[\partial \ln \gamma_A/(\partial E)]_{T\mu} = 0$

REFERENCES

1 A. N. FRUMKIN AND Z. IOFA, *Zh. Fiz. Khim.*, 13 (1939) 931.
2 D. C. GRAHAME, *Chem. Rev.*, 41 (1947) 441.
3 R. PARSONS AND M. A. V. DEVANATHAN, *Trans. Faraday Soc.*, 49 (1953) 404.
4 R. PARSONS, *Modern Aspects of Electrochemistry*, edited by J. O'M. BOCKRIS, Butterworths, London, 1954.
5 F. H. STILLINGER AND J. G. KIRKWOOD, *J. Chem. Phys.*, 33 (1960) 1282.
6 R. H. FOWLER AND E. A. GUGGENHEIM, *Statistical Thermodynamics*, Cambridge University Press, 1956, ch. 9.
7 H. H. HARNED AND B. B. OWEN, *The Physical Chemistry of Electrolytic Solutions*, Rheinhold Publishing Corp., New York, 1963, ch. 14.
8 H. D. HURWITZ, A. SANFELD AND A. STEINCHEN-SANFELD, *Electrochim. Acta*, 9 (1964) 929.
9 D. C. GRAHAME AND R. PARSONS, *J. Am. Chem. Soc.*, 88 (1961) 1291.

ETUDE POLAROGRAPHIQUE DU COBALT BIVALENT EN PRESENCE D'ELECTROLYTES DE BASE NON COMPLEXANTS

E. T. VERDIER ET Mlle G. BAPTISTE
Laboratoire de Chimie Générale 2, Faculté des Sciences, Montpellier (France)

(Reçu novembre 23me, 1965)

INTRODUCTION

Malgré le grand nombre d'ouvrages traitant de la polarographie du cobalt, certains aspects du problème s'étant révélés encore imparfaitement connus[1], il nous a paru intéressant de reprendre l'étude polarographique des ions bivalent du cobalt en nous limitant, en premier lieu, au comportement de ces ions en milieu aqueux et en présence uniquement d'électrolytes de base dont les anions, nitrate et perchlorate, ne sont pas susceptibles de former des complexes, même instables, avec le cobalt.

APPAREILLAGE ET REACTIFS

Toutes les mesures ont été faites à l'aide d'un appareil enregistreur M.E.C.I. type LX. La sensibilité de l'appareil était telle qu'une substance réductible de concentration $5 \cdot 10^{-5}\ M$ donnait tout juste un palier; la limite inférieure de concentration des solutions dont les courbes courant–tension ont pu être effectivement étudiées était donc de l'ordre de $10^{-4}\ M$.

L'électrode de référence utilisée était une électrode au calomel KCl saturé. Elle plongeait dans un compartiment contenant la solution étudiée mais séparé du compartiment cathodique par une membrane de cellophane[2,3], ou par une paroi de verre fritté dans les cas où le contact du cellophane avec la solution étudiée donne lieu à des modifications des courbes courant–tension et de ce fait le rend inutilisable.

Normalement, les solutions électrolysées étaient soigneusement débarrassées de leur oxygène par un barbotage préalable d'azote R. Tous les produits utilisés étaient des composés "pur pour analyse", dont la pureté adéquate a été vérifiée polarographiquement dans chaque cas. Les mesures ont été faites à 25.0° et le capillaire utilisé au cours de ce travail avait les caractéristiques suivantes: temps de goutte 3.0 sec; débit de mercure, dans l'eau, sous une pression de 60 cm de mercure, 0.0037 g/sec.

DONNEES EXPERIMENTALES

Solutions aqueuses de perchlorate de sodium

Les courbes obtenues présentent toutes des maxima très accentués lesquels ont été éliminés par filtration[4,5]. Cette technique présente l'avantage sur l'utilisation d'autres substances tensio-actives mieux définies, de ne pas entraîner de déplacement de la courbe courant–tension.

Les résultats obtenus montrent que le potentiel de demi-palier $E_{\frac{1}{2}}$ varie entre -1.1 V pour des solutions $5 \cdot 10^{-4}$ *M* en cobalt et 0.1 *M* en $NaClO_4$ et -1.3 V pour des solutions $2 \cdot 10^{-2}$ *M* en cobalt et 5 *M* en $NaClO_4$. Le courant limite dépend de la racine carrée de la hauteur du réservoir de mercure sauf dans le cas des solutions 5 *M* où la réaction n'est pas contrôlée par la diffusion. Les valeurs de $n\alpha$ calculées à partir de la pente de la droite $E = f\,(\log i/i_d - i)$ varient entre 0.3 et 0.6 et sont très inférieures à la valeur théorique pour une réaction réversible de deux électrons (E est le potentiel de l'électrode pour un courant i et i_d le courant limite.) Il faut noter que les valeurs de $n\alpha$ pour les fortes concentrations de perchlorate ont été calculées pour la première partie de la courbe et non pour la région où elle présente un palier incliné.

Solutions aqueuses de nitrate de potassium

L'ion nitrate a également un pouvoir complexant faible. Par contre il n'est pas possible de l'utiliser dans un domaine de concentration aussi étendu que l'ion perchlorate car, à des concentrations molaires il présente déjà un début de palier vers -1.5 V dû à sa réduction. Aux plus fortes concentrations, le palier des ions cobalt est donc complétement masqué.

Le potentiel de demi-palier $E_{\frac{1}{2}}$ varie entre -1.2 V et -1.3 V pour des solutions $5 \cdot 10^{-4}$–$2 \cdot 10^{-3}$ *M* en cobalt et 10^{-1} *M* en KNO_3. Il est donc plus négatif pour ces solutions que pour des solutions de perchlorate. Ceci serait peut-être lié à une plus forte adsorption à l'interphase solution–mercure des ions cobalt hydratés en présence d'ions perchlorate qu'en présence d'ions nitrate, les maxima sur les courbes courant–tension étant plus prononcés dans le premier cas que dans le deuxième.

Influence des substances tensio-actives

Pour une méme concentration de cobalt, la hauteur du courant-limite est approximativement constante pour toutes les substances citées ci-dessous, mais $E_{\frac{1}{2}}$ varie entre -1.1 V pour la gélatine et -1.5 V pour certaines concentrations de Triton X-100.

Gélatine. Cette substance donne, aux concentrations utilisées, des courbes dont l'allure est assez proche d'une courbe pour une réaction réversible. La valeur de $n\alpha$ (0.8) est plus élevée que dans les autres cas, mais reste néanmoins inférieure à la valeur théorique. En présence d'ions nitrate, l'addition de gélatine rend le potentiel de demi-palier nettement plus positif (Fig. 1).

Triton X-100. En l'absence d'air, le Triton X-100 déplace le potentiel de demi-palier vers des valeurs d'autant plus négatives que sa concentration augmente. Etant donné l'écart de -0.4 V entre les potentiels de demi-palier en présence de gélatine et de Triton X-100, l'utilisation de ces composés pourrait présenter un intérêt analytique et assurer une meilleure séparation avec d'autres éléments également réductibles dans ce domaine de potentiel.

Substances tensio-actives ioniques. Les substances cationiques (bromure de dodécyl trimethyl ammonium) produisent un effet analogue au Triton X-100, non ionique, c'est-à-dire, un déplacement du potentiel de demi-palier vers des valeurs plus négatives, alors que les composés anioniques (laurate de sodium) ont un effet moins prononcé.

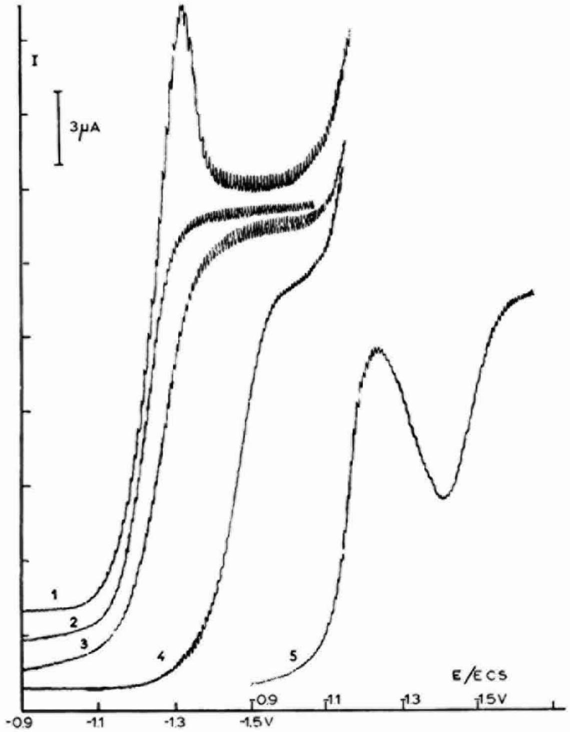

Fig. 1. Influence des substances tensio-actives sur la décharge du cobalt. Solution de base: Co^{2+}, $2 \cdot 10^{-3}$ *M*; KNO_3, 0.1 *M*; (1), en l'absence d'air; (2), +0.006% gélatine en l'absence d'air; (3), filtrée plusieurs fois en l'absence d'air; (4), +0.005% Triton X-100 en l'absence d'air; (5), Même solution que 4 mais en équilibre avec l'air.

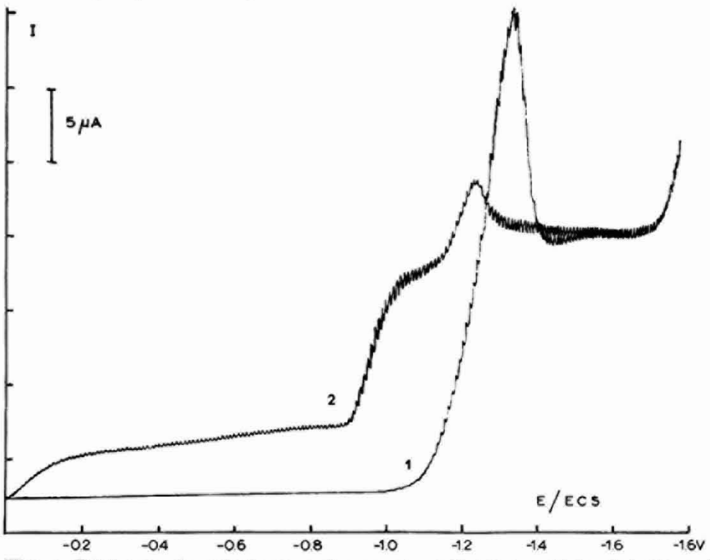

Fig. 2. Décharge du cobalt en présence et en l'absence d'air. Solution: Co^{2+}, $2 \cdot 10^{-3}$ *M*; KNO_3, 0.1 *M*; (1), après barbotage d'azote; (2), en présence d'air mais en l'absence de CO_2.

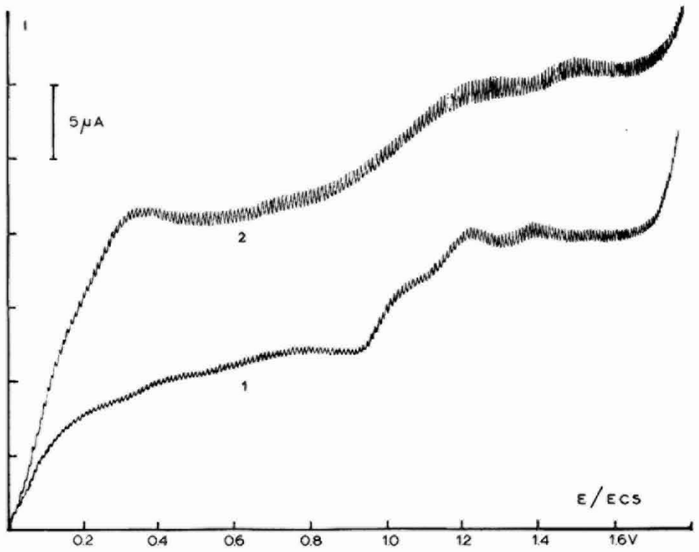

Fig. 3. Influence de la concentration d'oxygène sur la décharge du cobalt. Solution: Co^{2+}, $2 \cdot 10^{-3}$ M; KNO_3 0.1 M; (1), oxygène barboté 10 sec; (2), oxygène barboté 50 sec.

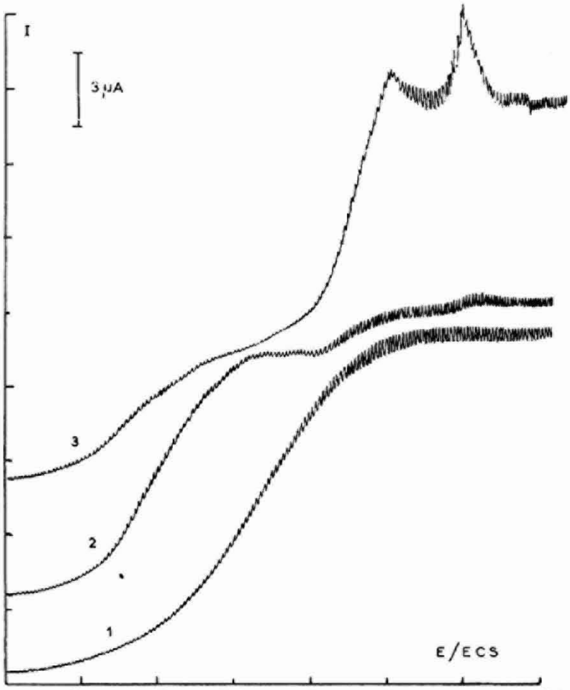

Fig. 4. Influence de l'eau oxygénée sur la décharge du cobalt. Solution de base: 0.1 M KNO_3; (1), H_2O_2, 10^{-3} M; (2) H_2O_2, 10^{-3} M; Co^{2+}, 10^{-3} M; (3), H_2O_2, 10^{-3} M; Co^{2+}, $2 \cdot 10^{-3}$ M.

Décharge du cobalt en présence d'oxygène

Dans une des premières études sur le comportement du cobalt à l'électrode à gouttes de mercure, BRDICKA[6] mentionne l'existence dans bien des cas ("many cases") d'un petit palier précédant le palier normal dû à la décharge des ions cobalt à partir d'une solution de chlorure cobalteux. Ce genre de palier s'étant produit de façon assez inattendue et peu reproductible au cours d'une étude préliminaire[1] les conditions expérimentales ont été variées afin de permettre d'établir exactement les facteurs influençant la formation de ce palier.

Influence de l'air. Il est important de noter en premier lieu, que ce palier n'est jamais formé en présence d'anions non complexants si l'on prend la précaution de débarrasser soigneusement la solution à électrolyser de toute trace d'oxygène. La Fig. 2 montre le genre de courbes obtenues en l'absence et en présence d'oxygène. A des concentrations d'oxygène plus élevées que celle d'une solution en équilibre avec l'air, la courbe courant–tension du cobalt est sensiblement modifiée (Fig. 3).

On note l'existence d'un nouveau palier entre -0.3 et -0.4 V qui augmente avec la concentration d'oxygène, l'apparition du palier de l'eau oxygénée, la diminution du pré-palier et l'existence d'un petit maximum vers -1.4 à -1.5 V qui se transforme en petit palier pour des concentrations plus élevées d'oxygène.

A des concentrations d'oxygène réalisées en barbotant ce gaz à travers la solution pendant 10–50 sec les deux paliers à -1.0 V disparaissent complètement et sont remplacés par une vague étirée typique de la réduction de l'eau oxygénée. Signalons enfin qu'il suffit d'un simple barbotage d'azote pour que l'on retrouve de nouveau le palier ordinaire du cobalt. (Fig. 2, courbe 1)

Influence de l'eau oxygénée. Le palier de l'eau oxygénée pouvant être totalement absent pour un certain rapport des concentrations $[Co^{2+}]/[H_2O_2]$, (Fig. 2) une série de courbes a été enregistrée pour différentes concentrations de ces deux composés en présence d'un électrolyte de base 0.1 M KNO_3. Les courbes dans la Fig. 4; font ressortir l'existence d'un palier étiré, entre -0.3 et -0.8 V, situé à un potentiel plus positif que celui de la réduction de l'eau oxygénée et dont la hauteur est un peu moins grande que celle du palier correspondant à la réduction de l'eau oxygénée en solution. Ce palier diminue avec la concentration du cobalt pour une concentration donnée d'eau oxygénée.

Influence du gaz carbonique, du glycérol et de l'alcool éthylique. En plus de l'oxygène dont la présence est essentielle pour la formation du pré-palier du cobalt, il a été rapidement mis en évidence que ceci n'était pas le seul facteur intervenant. Une séries de mesures effectuées à différents pH en absence de gaz carbonique montre, comme le confirme l'étude récente de DAHMS[7], que le pH joue un rôle secondaire, le palier étant formé dans tout le domaine de pH que l'on peut étudier avec les solutions en question (pH 4–8). Ce n'est cependant qu'après un barbotage prolongé d'air, soigneusement débarrassé de gaz carbonique que le pré-palier atteint son développement maximum. Des courbes obtenues avec des solutions $2 \cdot 10^{-3}$ M en Co^{2+}, 0.1 M en KNO_3, et 0.1 M en $NaHCO_3$ ne donnent pas de premier palier, d'où l'on peut conclure que ce sont les ions bicarbonates plutôt que le gaz carbonique qui interviennent dans cette réaction.

Il a été mentionné que, dans certains cas l'utilisation d'une membrane de cellophane pour séparer les compartiments cathodique et anodique entraînait une modification des courbes courant–tension du cobalt. En effet, il suffit d'agiter une solution de cobalt 10^{-3} M et 0.1 M en KNO_3 avec du cellophane pour que le premier palier se développe comme en l'absence de gaz carbonique. Il semble que cet effet puisse être rattaché à la présence dans le cellophane de glycérol, impureté généralement associée à ces membranes, car ce composé additionné à une solution de cobalt-nitrate de potassium produit exactement le même effet (Fig. 5). Des mesures de pH montrent que le glycérol modifie le pH de la solution d'une manière analogue à un barbotage prolongé d'air purifié ou d'azote. L'effet du glycérol serait donc lié à la diminution de la solubilité du gaz carbonique dans des solutions aqueuses[8]. L'éthanol favorise également, et probablement pour la même raison[8], la formation du premier palier. Pour ces dernières courbes, $n\alpha$ peut atteindre la valeur élevée de 1.5.

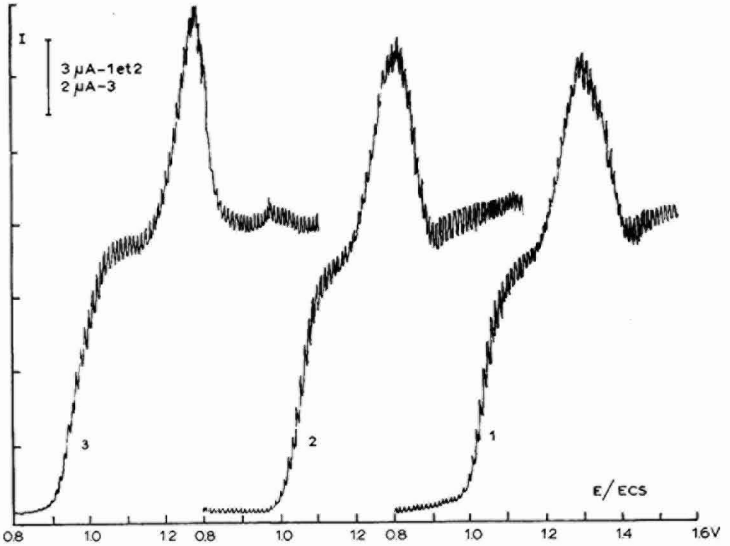

Fig. 5. Influence du glycérol et de l'éthanol sur la décharge du cobalt. Solution de base: 0.1 M KNO_3; (1), Co^{2+}, $2 \cdot 10^{-3}$ M; solution saturée d'air sans CO_2; (2), Co^{2+}, $2 \cdot 10^{-3}$ M; glycérol, 4%; (3), Co^{2+}, $2 \cdot 10^{-3}$ M; éthanol, 4%.

La hauteur de ce premier palier ne dépend pas rigoureusement de la racine carrée de la hauteur du réservoir de mercure. Le phénomène contrôlant la réaction à l'électrode ne serait donc pas uniquement un phénomène de diffusion. Il ne s'agit pas non plus d'une réaction purement cinétique car le courant-limite ne reste pas constant comme l'exigerait une telle réaction.

Influence de substances tensio-actives en présence d'air. Il a été signalé, dans la première partie, que le Triton X-100 déplaçait les courbes du cobalt vers des valeurs plus négatives. En présence d'oxygène, les courbes présentent un maximum ayant une forme inhabituelle. (Fig. 1, courbe 5). Ce maximum disparait complètement après un barbotage d'azote.

KOLTHOFF ET OKINAKA[9] ont montré qu'à une électrode rotative à gouttes de mercure, la déscription du Triton X-100 se fait, pour des concentrations voisines de

0.05%, à -1.6 V. Ceci correspondrait au potentiel de formation du palier du cobalt en présence de cette substance tensio-active. Le rôle de l'oxygène reste cependant à expliquer et ceci ne pourra se faire qu'à partir d'une étude des courbes courant–temps pour des gouttes individuelles.

DISCUSSION DES RESULTATS

En présence d'ions non complexants la décharge du cobalt se fait à partir d'ions hydratés[10], le potentiel de demi-palier variant avec la concentration de l'électrolyte de base, la nature de l'anion associé à celui-ci et la présence de substances tensio-actives. La hauteur du palier correspond à la réduction d'un ion bivalent à l'état de métal[10].

Par contre, en présence d'oxygène le phénomène est plus complexe. En premier lieu, l'absence totale de palier dû à l'eau oxygénée pour des solutions en équilibre avec l'air et contenant du cobalt 10^{-3} M et du KNO_3 0.1 M, montre que l'eau oxygénée doit réagir immédiatement lors de sa formation à l'électrode avec les ions bivalents du cobalt pour former du cobalt trivalent, lequel doit être aussitôt précipité (le produit de solubilité $[Co^{3+}]$ $[OH^-]^3 = 3.2 \cdot 10^{-43}$ [11]. Le calcul montre qu'à pH 7 l'équilibre énergétique est déjà nettement déplacé dans le sens d'une oxydation du cobalt. Or, au voisinage de l'électrode, le pH est sans doute plus élevé que dans la solution même, à la suite de la libération d'ions OH^- provenant de la réduction de l'oxygène.

Lorsque la concentration de l'eau oxygénée est voisine de celle du cobalt en solution, un phénomène nouveau apparaît, la réduction de l'eau oxygénée à un potentiel moins négatif que sa valeur habituelle. Il s'agirait donc d'une réduction catalysée de l'eau oxygénée semblable à celle produite en présence de composés de fer[12–15].

A des concentrations encore plus fortes d'oxygène ou d'eau oxygénée, les ions OH^- libérés à l'électrode entraînent une diminution du palier du cobalt qui peut aller jusqu'à sa suppression totale. Le dernier maximum ou palier sur la courbe à -1.4 V doit correspondre à la réduction des ions cobalteux en milieu alcalin mentionné par Laitinen et Kivalo[16]. Il reste à expliquer la nature du premier palier du cobalt bivalent. Brdicka[6] a postulé l'existence d'un composé formé par hydrolyse de l'ion cobalteux. Les travaux de Gayer et Woontner[17] ont montré, qu'il y avait formation, en solution de chlorure cobalteux, d'ions $Co(OH)^+$ et ils ont donné pour la constante $a_{CoOH^+} \cdot a_{H^+}/a_{Co^{2+}}$ la valeur moyenne de 6.3×10^{-13} pour des solutions entre 0.01 et 0.1 M. Utilisant cette valeur, ainsi que les autres constantes donnees par Gayer et Garrett[18], il est possible de montrer que la concentration en $Co(OH)^+$ dans une solution de sel cobalteux doit passer par un maximum pour un pH voisin de 7, mais ceci n'explique pas le fait que le palier se développe uniquement en présence d'oxygène, et de toute façon la concentration du $Co(OH)^+$ en solution est si petite que la décharge du cobalt pourrait difficilement se faire à partir de ce composé.

On peut trouver cependant, une explication qualitative du phénomène si l'on accepte l'hypothèse de Brdicka selon laquelle le cobalt se décharge plus facilement à partir du produit d'hydrolyse de l'ion hydraté, $Co(H_2O)_x{}^{2+}$, vraisemblablement $CoOH(H_2O)_{x-1}{}^+$, qu'à partir de l'ion hydraté lui-même.

A des potentiels situés sur la courbe courant–tension, avant la décharge du cobalt, le nombre de ces ions à l'électrode est beaucoup plus grand que celui des ions

OH^- libérés par la réduction de l'oxygène. La concentration des ions OH^- à la surface dépend, à ce potentiel, de la diffusion des molécules d'oxygène à travers la couche de diffusion, alors que dans le cas du cobalt, la concentration est uniforme dans toute la solution et pour une solution $2 \cdot 10^{-3}$ *M* en équilibre avec l'air, la concentration du cobalt doit être de l'ordre de huit fois celle de l'oxygène. Il y aurait donc, compte tenu du rapport des concentrations $[Co^{2+}]/[OH^-]$ à la surface de l'électrode, formation de $CoOH^+$, et possibilité de décharge de Co^{2+} à partir de ce composé avec la formation du premier palier. Lorsqu'on atteint ensuite des potentiels pour lesquels la décharge des ions $Co(H_2O)_x{}^{2+}$ commence, il se produit alors au voisinage immédiat de l'électrode un appauvrissement en ions cobalt. Le rapport $[Co^{2+}]/[OH^-]$ à la surface de l'électrode devient, pour les solutions ci-dessus, de l'ordre de 4 à 1. Dans ces conditions c'est $Co(OH)_2$ qui aura tendance à se former entraînant une diminution dans la hauteur du palier. Si la concentration des ions cobalt est suffisante, il n'y aura plus assez d'ions OH^- à l'interphase pour réagir avec ceux-ci et la décharge se fera à nouveau à partir des ions hydratés.

Il a été montré[16,19,21] que la décharge des ions cobalteux à partir d'une solution d'ions cobaltiques se fait à un potentiel 0.2 V plus positif que la décharge de ces ions à partir d'une solution d'ions cobalteux. Cet effet semble être lié à la libération à la surface de l'électrode d'ions hydroxyle avec la formation d'une couche d'hydroxyde cobalteux, parfois même visible au microscope. Ceci entraîne des anomalies plus ou moins reproductibles sur les courbes courant–tension. Il est permis de se demander si ce palier ne correspondrait pas au premier palier du cobalt décrit dans ce travail.

Quant à l'influence du gaz carbonique sur le développement du palier elle est difficilement explicable pour le moment. On sait[22] que le carbonate de cobalt est peu soluble. Cependant aux concentrations utilisées, et étant donné la faible teneur en CO_2 d'une solution en équilibre avec l'air, il est peu probable que ce soit là l'effet important. Il faudrait plutôt envisager la formation d'un complexe des produits d'hydrolyse du cobalt avec les ions bicarbonate. Malheureusement peu d'études ont été faites sur ce sujet, aussi sera-t-il nécessaire d'effectuer d'autres travaux avant de pouvoir rendre compte de ce phénomène. C'est cependant là qu'il faut chercher la raison pour laquelle ce premier palier du cobalt semble parfois avoir échappé à l'attention des chercheurs[7].

SUMMARY

A study has been made of the discharge of cobalt(II) ions at the dropping mercury electrode in the presence of non-complexing indifferent electrolytes. The influence of various factors such as concentration, surface-active agents and oxygen has been investigated. In the presence of oxygen a pre-wave is formed which develops its maximum height in the absence of all traces of carbon dioxide. The existence of this pre-wave is attributed to the formation at the electrode surface of a product of hydrolysis of the cobaltous ions owing to the liberation of hydroxyl ions on the reduction of the oxygen in solution. No such pre-wave is obtained in the absence of air. With hydrogen peroxide a catalytic wave is formed at a more positive potential than that corresponding to the normal reduction of this substance.

BIBLIOGRAPHIE

1 G. BAPTISTE, Diplôme d'Etudes Supérieures, Faculté des Sciences, Montpellier, 1964.
2 L. SERAK, *Collection Czech. Chem. Commun.*, 18 (1953) 439.
3 O. GAWRON, *Anal. Chem.*, 22 (1950) 614.
4 E. T. VERDIER, *Collection Czech. Chem. Commun.*, 11 (1939) 216.
5 L. MEITES, *Polarographic Techniques*, Interscience Publishers, New York, 1955, p. 315.
6 R. BRDICKA, *Collection Czech. Chem. Commun.*, 3 (1931) 396.
7 H. DAHMS, *J. Electroanal. Chem.*, 8 (1964) 5.
8 A. SEIBEL, *Solubility of Inorganic and Metal Organic Compounds*, Vol. 1, Van Nostrand Co. Inc., New York, 3rd ed., 1952, p. 232.
9 I. M. KOLTHOFF ET Y. O. OKINAKA, *J. Am. Chem. Soc.*, 81 (1959) 2298.
10 E. T. VERDIER ET F. ROUELLE, *Compt. Rend.*, 259 (1964) 1856.
11 S. I. SOBOL, *Zh. Obshch. Khim.*, 23 (1953) 906; *Stability Constants of Metal-ion Complexes*, Part II, *Inorganic Ligands*, p. 12. J. BJERRUM, G. SCHWARZENBACH ET L. G. SILLEN, *Chem. Soc. London, Spec. Publ.* 1958.
12 R. BRDICKA ET C. TROPP, *Biochem. Z.*, 289 (1937) 301.
13 R. BRDICKA ET K. WIESNER, *Collection Czech. Chem. Commun.*, 12 (1947) 39.
14 E. P. PARRY, PH. D. Thesis, Minesota, 1950.
15 Z. POSPISIL, *Collection Czech. Chem. Commun.*, 18 (1953) 337.
16 H. A. LAITINEN ET P. KIVALO, *J. Am. Chem. Soc.*, 75 (1953) 2199.
17 K. H. GAYER ET L. WOONTNER, *J. Am. Chem. Soc.*, 74 (1952) 1436.
18 K. H. GAYER ET A. B. GARRET, *J. Am. Chem. Soc.*, 72 (1950) 3921.
19 A. A. VLCEK, *Z. Physik. Chem. (Leipzig) Sonderheft*, (1958) 143.
20 H. A. LAITINEN, A. J. FRANK ET P. KIVALO, *J. Am. Chem. Soc.*, 75 (1953) 2865.
21 A. S. TRIFONOV ET ST. KOBARELOVA, *Bulgar. Akad. Nauk. Izv. Khim. Inst.*, 6 (1959) 229; 7 (1960) 133. (*C. A.* 54 (1960) 5294; 55 (1961) 175.
22 P. PASCAL, *Nouveau Traité de Chimie Minérale*, Tome XVII, Masson et Cie., Paris, 1964, p. 450.

THE POLAROGRAPHIC MEASUREMENT OF FORMATION CONSTANTS OF COPPER(II) COMPLEXES IN ORTHOPHOSPHATE MEDIUM

PETER A. PELLA AND WILLIAM C. PURDY
Department of Chemistry, University of Maryland, College Park, Md. (U.S.A.)

(Received August 26th, 1964)

INTRODUCTION

In biological systems, metal cations are known to function as coenzymes and as catalysts. Studies of Cu(II)-binding substances such as salicylaldoxime, ethyl xanthate, and ferrocyanide showed inhibition of oxidase activity by 50%[1]. Copper(II) was partly removed from proteins by the action of trypsin or chymotrypsin. KNOBLOCK AND PURDY[2] have measured instability constants of Cu(II) complexes with radiation-protective drugs and demonstrated a correlation between the instability constant and radiation prophylaxis.

Copper(II) is present in human blood serum loosely bound to albumin and tightly bound to the alpha$_2$-globulin and ceruloplasmin[3]. Human blood serum contains about 114 μg of Cu(II) per 100 ml. It is known that albumin functions as a transport mechanism for Cu in the blood. The function of ceruloplasmin is unknown. It does possess polyphenol oxidase activity and is suggested to play a part in the oxidation of serotonin and epinephrine. D-Penicillamine was found to be effective in treatment of Wilson's disease. In this disease, hypercupremia or increase of ceruloplasmin was observed[4]. D-Penicillamine acts by removing the Cu(II) from ceruloplasmin by complexation.

It has been suggested that antithyroid drugs may have their mechanism of action through complex formation with Cu(II). It was reported that Cu(II) formed a 1:3 complex with thyroxine and could enter into a redox system with it. FRIEDEN AND FLITMAN[5] have shown that Cu(II) is reduced in the presence of thyroxine. GEMMILL[6,7] demonstrated an increased rate of oxidation of ascorbic acid oxidase, a Cu-containing enzyme, in the presence of thyroxine. A free-radical mechanism was postulated for this reaction. FRIEDEN[8] found that ascorbic acid oxidase was inhibited by free Cu(II) and postulated that the action of thyroxine on ascorbic acid oxidase may be through the removal of Cu(II).

There is some speculation as to the mechanism of salicylates in explaining their antipyretic action. According to SCHUBERT[9], a test for infection in the body is to note the rise in Cu(II) level. Experimental evidence shows that Cu(II) itself does have antipyretic action and the function of the salicylates is to transport small amounts of Cu(II) to an intracellular site. It is stated that salicylate agents transport copper in a complex form to the cellular site and then the complex dissociates, leaving the Cu(II) at the site. SCHUBERT tested derivatives of salicylic acid and found that only those substances which could form complexes with Cu were effective in reducing fever.

In the present paper, the polarographic method has been applied to measure the apparent formation constants of complexes of Cu(II). Among the metal-binding agents used were amino acids, vitamin B_6 compounds, and antipyretic drugs. The supporting electrolyte was an orthophosphate buffer of pH 7.4. This medium was chosen as it is one of the major buffering systems of the blood.

EXPERIMENTAL

Acetylsalicylic acid and S-acetylsalicylic acid (thioaspirin) were synthesized and purified for use. Aspirin was synthesized by the procedure of ADAMS AND JOHNSON[10]. Thioaspirin was synthesized in a similar manner except that thiosalicylic acid was used as a starting material and the product was recrystallized from benzene.

Reagent-grade chemicals were used in the preparation of the orthophosphate buffer used as the supporting electrolyte. The pH of this buffer was 7.4 and the ionic strength was 0.2 M. The directions for the preparation of the buffer are described elsewhere[11].

Penicillin G and coenzyme A were obtained from Drs. HENERY-LOGAN and VEITCH, respectively, of the University of Maryland. 1-Aminocyclopentane-carboxylic acid was synthesized and purified by Mr. VARGHESE of the University of Maryland. The vitamin B_6 compounds and the amino acids were obtained from Nutritional Biochemicals Corp., Cleveland, Ohio, and Eastman Kodak Co., Rochester, N.Y. A sample of 99.7% pure thiosalicylic acid was obtained from Evans Chemetics, Inc., New York.

All polarographic measurements were made with a Sargent Model XV Polarograph. A Lingane H-cell fitted with a saturated calomel reference electrode and a 3% agar-saturated potassium chloride plug was employed. The solution of the Cu in the supporting electrolyte was placed in the sample compartment of the H-cell and flushed with nitrogen gas for 15 min. During the course of the polarogram, a nitrogen atmosphere was maintained above the sample solution. The nitrogen used was deoxygenated by passage through two solutions of chromous sulfate and one of supporting electrolyte before entrance into the H-cell. All polarograms were obtained on a sample thermostatted at $25 \pm 0.2°$.

Reversibility of the electrode reactions was tested by determining the slopes of the log $(i_d - i)/i$ *vs.* E plots. Data for these plots were obtained by manual operation of the polarograph. Applied voltages were calibrated with a Leeds and Northrup Model 8687 Potentiometer.

The calculation of the apparent formation constant from polarographic data has been described elsewhere[2,12,13].

RESULTS AND DISCUSSION

It was found that penicillin G decomposed rapidly in the presence of Cu(II). Yellowing of the solution was indicative of this decomposition. A wave suitable for study was not obtained until decomposition was virtually complete. The formation constant obtained was 2.1×10^{14} as compared to 1.4×10^{15} for Cu(II)–D-penicillamine.

A formation constant for a Cu(II)–coenzyme A complex could not be obtained although a shift in the Cu half-wave potential was observed. The shift obtained for a metal: coenzyme A ratio of 1:2 was 150 mV. However, at increased concentrations of coenzyme A, interfering anodic waves completely masked the Cu(II)-complex wave.

The Cu(II)–histidine complex was 400 times stronger than the Cu(II)–glycine complex in orthophosphate buffer. 1-Aminocyclopentanecarboxylic acid formed a complex with Cu(II) of about the same strength as the glycine and leucine complexes. The DL-methionine complex was found to be similar in strength to the amino-acid complexes studied except for the histidine complex. Hippuric acid and niacin showed no tendency to complex.

Among the vitamin B_6 compounds, pyridoxal exhibited the greatest binding strength, an unexpected result. Examination of the structures would lead one to expect that pyridoxamine would form the strongest complex. However, polarographic results show that pyridoxal shifted the Cu(II) half-wave potential to a greater extent than did pyridoxamine or pyridoxine.

Copper(II) forms a weak complex with acetylsalicylic acid. However, thiosalicylic acid and S-acetylsalicylic acid exhibited considerable binding strength for Cu(II) in this buffer. The experimental results are collected in Table 1.

TABLE 1

THE CALCULATED FORMATION CONSTANTS OF Cu(II) COMPLEXES

Concn. Cu(II) $\cdot 10^4$ *M*	*Complexing agent*	*n*	*p*	$K_{formation}$
5.05	Acetylsalicylic acid	1	1	10^3
5.70	Penicillin G (penicillamine)	1	2	2.2×10^{14}
5.70	Thiosalicylic acid	1	3	2.9×10^{12}
5.05	S-Acetylsalicylic acid	1	3	2.2×10^{11}
5.05	Pyridoxine-HCl	1	1	5.9×10^3
5.05	Niacin	–	–	no complex
5.05	Pyridoxamine-2HCl	1	1	7.1×10^4
5.05	Pyridoxal-HCl	1	2	5.0×10^8
5.05	1-Aminocyclopentanecarboxylic acid	2	2	1.0×10^9
5.05	Glycine	2	2	1.0×10^9
5.05	D,L-Leucine	2	2	6.3×10^8
5.05	Coenzyme A	1	–	complex
5.00	L(+)-Histidine-HCl	2	2	1.0×10^{13}
5.00	Hippuric acid	1	–	no complex
5.00	D,L-Methionine	2	2	1.8×10^9

n is the number of electrons in the reduction of the complex ion.
p is the number of moles of ligand reacting with one mole of Cu(II).

The results of this study show that the number of electrons involved in the reduction of Cu(II) complexes in a neutral phosphate buffer is not always one. The Cu(II)–amino acid complexes all exhibited waves which correspond to two-electron reductions. The other complexes listed in the table exhibited one-electron reduction waves. The amino acid which did not complex with Cu(II), hippuric acid, had no effect on the one-electron reduction wave of Cu(II). Various other complexes of Cu(II) were also studied in the phosphate buffer at a pH of 7.4 to ascertain the number of electrons involved in the reductions. Copper(II)–penicillamine and Cu(II)–

ethylenediamine exhibited one-electron reduction waves whereas Cu(II)–EDTA exhibited a two-electron reduction. There appears to be no correlation between size and binding strength of the ligands and the number of electrons involved in the reduction of the Cu(II) complex.

In studies carried out by KNOBLOCK AND PURDY[2], one-electron reductions of Cu(II) complexes in neutral and basic phosphate buffers were reported regardless of the complexing agent used. These investigators, however, did not study any Cu(II)–amino acid complexes. CHRISTIAN AND PURDY[12] suggested that the reduction product of Cu(II) in neutral or basic phosphate buffer is a stable or insoluble Cu(I)–phosphate species. An attempt to isolate this species by bulk electrolysis experiments failed because of the precipitation of Cu(II) phosphate above pH 6.0. In order to determine if a Cu(I) species could be stabilized in a bulk solution of orthophosphate buffer, freshly prepared cuprous chloride was added to a solution of the phosphate buffer. It was found that the added cuprous chloride disproportionated rapidly to Cu(II) and metallic Cu. A polarogram was run on this solution and one wave corresponding to a one-electron reduction was obtained.

These results indicate that a Cu(I) species is not stable in the buffer, yet a Cu(I) species is postulated as the reduction product of Cu(II) in neutral phosphate buffer. It must be emphasized that a reduction product present at the electrode surface may or may not be stable in the bulk of the solution. Other polarographic data indicated that there was no adsorption occurring at the electrode surface.

These studies suggest that the structure of the complex being reduced at the mercury surface may play a part in determining the nature of the reduction product, that is, whether the reduction stops at a Cu(I)–phosphate species or proceeds to the metal amalgam.

ACKNOWLEDGEMENT

The authors are indebted to the Office of the Surgeon General of the U.S. Army for partial support of this work under contract No. DA-49-193-MD-2593.

CONCLUSIONS

The apparent formation constants for a number of Cu(II) complexes with amino acids, vitamins, and antipyretics have been determined by the polarographic method. The supporting electrolyte used in this study was an orthophosphate buffer of pH 7.4. It has been shown that the amino-acid complexes of Cu(II) were reduced to the metal amalgam whereas Cu(II) with the B_6 vitamins and the antipyretics was reduced to a stable Cu(I) species. A possible explanation was presented to account for the observed behavior.

REFERENCES

1 E. COHEN AND L. ELVEHJEM, *J. Biol. Chem.*, 107 (1934) 97.
2 E. C. KNOBLOCK AND W. C. PURDY, *J. Electroanal. Chem.*, 2 (1961) 493.
3 G. S. SHIELDS, *Metal-Binding in Medicine*, edited by M. J. SEVEN AND L. A. JOHNSON, J. B. Lippincott Co., Philadelphia, Pa., 1960, pp. 259–262.
4 I. H. SCHEINBERG AND A. G. MORELL, *J. Clin. Invest.*, 36 (1957) 1193.

5 E. FRIEDEN AND R. FLITMAN, *Arch. Biochem. Biophys.*, 64 (1956) 513.
6 C. L. GEMMILL, *J. Biol. Chem.*, 192 (1951) 749.
7 C. L. GEMMILL, *Am. J. Physiol.*, 167 (1951) 349.
8 E. FRIEDEN, *Biochim. Biophys. Acta*, 9 (1952) 696.
9 J. SCHUBERT, *Chimia (Aarau)*, 11 (1957) 113.
10 R. ADAMS AND J. R. JOHNSON, *Laboratory Experiments in Organic Chemistry*, The Macmillan Co., New York, 4th ed., 1949, p. 451.
11 G. D. CHRISTIAN AND W. C. PURDY, *J. Electroanal. Chem.*, 3 (1962) 363.
12 G. D. CHRISTIAN AND W. C. PURDY, *ibid.*, 5 (1963) 85.
13 I. M. KOLTHOFF AND J. J. LINGANE, *Polarography*, Interscience Publishers, New York, 2nd ed., 1952, p. 241.

POLAROGRAPHIC MAXIMA AT THE DESORPTION POTENTIALS OF ORGANIC MOLECULES

S. SATHYANARAYANA
Department of Chemistry, Indian Institute of Technology, Bombay-76 (India)

(Received December 30th, 1964)

INTRODUCTION

At present, two kinds of maxima are well-known in d.c. polarography. Maxima of the first kind arise because of a gradient in interfacial tension along the surface of the growing mercury drop due to asymmetry of the electric field around the dropping mercury electrode. Maxima of the second kind are due to tangential motions of the surface of the mercury drop under the action of a sufficiently large head of the mercury column giving rise to a non-radial growth of the dropping mercury electrode (D.M.E.). The quantitative treatments of these two kinds of maxima have been worked out and subjected to experimental verification[1,2].

There are instances quoted in the literature when maxima pertaining to neither of these two kinds are observed experimentally, particularly at the potentials of desorption of electro-inactive organic surfactants at the D.M.E.[3-5].*

The subject was reviewed by FRUMKIN *et al.*[3] who also gave the probable theoretical bases for the occurrence of polarographic maxima at the desorption potentials of organic molecules. However, experimental data obtained in support of the theory were inconclusive.

In the course of our study on adsorption, and inhibition of electrochemical reactions, definite experimental evidence has been obtained showing the occurrence of polarographic maxima at the desorption potentials of camphor; they are easily reproducible. The present paper deals with the results obtained and a further development of the theory to explain most of the observed phenomena.

EXPERIMENTAL

General

The inhibition of the rate of cathodic discharge of Cd^{2+} and Cu^{2+} by adsorption of camphor was studied by d.c. polarographic current as well as differential capacity measurements at the dropping mercury electrode.

It is well-known that current–time curves at a dropping mercury electrode are quite complex in the presence of adsorbed, although electro-inactive, organic molecules and ions[7-9]. The measurement of average currents, which would carry little physical significance under these conditions, was discarded in favour of measurement

---

* Maxima due to catalytic hydrogen currents in d.c. polarography[6] are to be distinguished from maxima at desorption potentials, and are not considered in this paper.

of instantaneous currents at the end of the drop life. In order to achieve complete correspondence between these currents and the adsorption of camphor from the solution, differential capacities were also measured at the end of the drop life, using the *same* dropping mercury electrode, and the *same* drop time. Although the adsorption of camphor is known[8] to be a slow process, since identical moments of drop life have been used in the present work for the measurement of adsorption (differential capacity) as well as reaction rate (d.c. polarographic current), a quantitative correlation of the two phenomena is possible.

Polarographic measurements

The polarising circuit was designed to have as low a resistance as possible ($\sim$800 Ω with galvanometer and shunt at highest sensitivity; much less than this value at other sensitivities). The polarisation of the dropping mercury electrode was thus always constant within 0.2 mV for each drop. Relatively long drop times were chosen, in the range 8–10 sec, for two reasons: (i) with such a large drop time the flow-rate of mercury is small enough to prevent the occurrence of any polarographic maxima of the second kind; (ii) the measurement of current at the end of the drop life (and corresponding measurement of differential capacity) can be carried out manually with a sufficient accuracy. A critically damped galvanometer with a period of 4 sec and sensitivity of 1.75×10^{-9} A/mm was used to measure accurately the currents at the end of the drop life ($\sim$9 sec).

Capacity measurements

The differential capacities were measured by the bridge method, which is essentially the same as that of GRAHAME[10], in which, as pointed out later by DAMASKIN[11], there is a significant advantage in using the polarising source of e.m.f., not across the cell, but across a diagonal of the bridge. The test signal for the bridge was of 400-c/sec frequency and 5-mV amplitude. Necessary shielding and grounding were provided to minimise parasitic capacitances.

With such a bridge technique, the accuracy of capacity measurements at a D.M.E. depends essentially on the accuracy of the measurement of the time of balance which is used for calculating the area. Since it was desired in the present work to measure differential capacities at the end of drop life, the state of balance was adjusted to be at the moment of drop detachment, and the corresponding drop time was automatically measured by an electronic mechanical relay[12] connected to the output of the preamplifier of the oscilloscopic null detector. The drop-time measurements were precise to 0.01 sec. A precision decade capacity box (Leeds and Northrup Catalogue No. 1091) was used in the variable arm of the bridge. The precision of capacity measurement was about 0.5% except at the desorption potentials where it was about 2%. The mass rate of flow of mercury through the capillary was known, and the drop times determined as above, and the area of the mercury drop at the moment of detachment could then be calculated assuming a spherical shape for the electrode.

In order to achieve internal consistency, the capillary, the height of mercury column, and the cell used were the same for capacity and polarographic studies. The solution for capacity measurements was the same as the supporting electrolyte for polarographic studies so as to obtain ideal polarisability of the dropping mercury electrode in the former case. Since the activities of the reducible ions (Cd^{2+} and Cu^{2+})

used in the polarographic studies were about 1 mM in each case, the specific adsorption of these ions may not be significant enough to alter the structure of the double layer when these ions are present in the solution.

Chemicals

Care was taken to prevent contamination of chemicals by surface-active impurities. Twice-distilled water with the second distillation over alkaline permanganate in an all-glass assembly was used throughout. The inorganic salts used (sodium sulphate, copper sulphate and cadmium sulphate) were recrystallised from A.R. grade salts and ignited in air below the temperatures of decomposition. Sulphuric acid of A.R. grade was distilled under reduced pressure. Mercury, purified by prolonged aeration under hot dilute nitric acid was distilled under vacuum. For de-aerating the solution, hydrogen from an all-glass electrolysis unit was used; it was passed over heated platinum black (catalyst), then successively through alkaline plumbite solution and silica gel, and finally bubbled through the solution under study for 2 h. The supporting electrolyte used in all the experiments was 0.5 M Na_2SO_4 and 0.001 M H_2SO_4; the latter is necessary to suppress the hydrolysis of the copper and cadmium salts in the otherwise neutral solution.

Camphor was sublimed slowly to get clear white needles. A small quantity was dissolved in 50% aqueous methanol before use. Methanol was purified by distillation in an all-glass assembly.

Cell

The cell was of all-glass construction with suitable inlets through ungreased ground-glass joints for the D.M.E. reference electrode, and addition of surfactant. The reference electrode used for measuring the potential of the dropping mercury electrode was of mercury–mercurous sulphate type in contact with a solution of 0.5 M Na_2SO_4 and 0.001 M H_2SO_4. The reference-electrode bridge filled with the same solution (thus avoiding liquid junction potentials) was connected to the cell through a closed, ungreased stopcock, which terminated in a Luggin capillary close to the D.M.E. A large platinum cylinder surrounding the dropping mercury electrode was used as the auxiliary electrode.

Procedure

The addition of various quantities of camphor to the test solution was accomplished so that before, and between successive additions of the camphor solution, access of air to the test solution was completely avoided. To a known volume of the de-aerated solution in the cell, the camphor solution was added dropwise through a fine capillary tip. This capillary was fused to a reservoir containing the solution of camphor and attached to the cell by an ungreased ground-glass joint. The dropwise addition of camphor was effected by compressing the air space above the camphor solution in the reservoir with a flexible polyethylene cap so that drops were formed and detached slowly from the vertical tip. After the addition of the desired number of drops of camphor solution, hydrogen was bubbled through the solution for one minute to effect mixing. The same schedule of stirring by hydrogen was used for both polarographic and capacity measurements. Then the measurements of current or the differential capacity at the end of the drop life were carried out manually at 1–5 mV intervals when there was a sharp change, and at wider intervals of potentials otherwise. The potential measurements were carried out correct to ±0.5 mV using a Cambridge Vernier potentiometer.

The capillary characteristics were: $m = 1.4$ mg/sec and $t = 9.6$ sec, with a 30 cm head of mercury at the null point of mercury in the solution; the cross section of the capillary bore at the tip was circular and of 90 μ internal diameter.

RESULTS AND DISCUSSION

The polarographic current–potential curves for the discharge of Cd^{2+} and Cu^{2+} are shown in Figs. 1 and 2 for various concentrations of camphor in the solu-

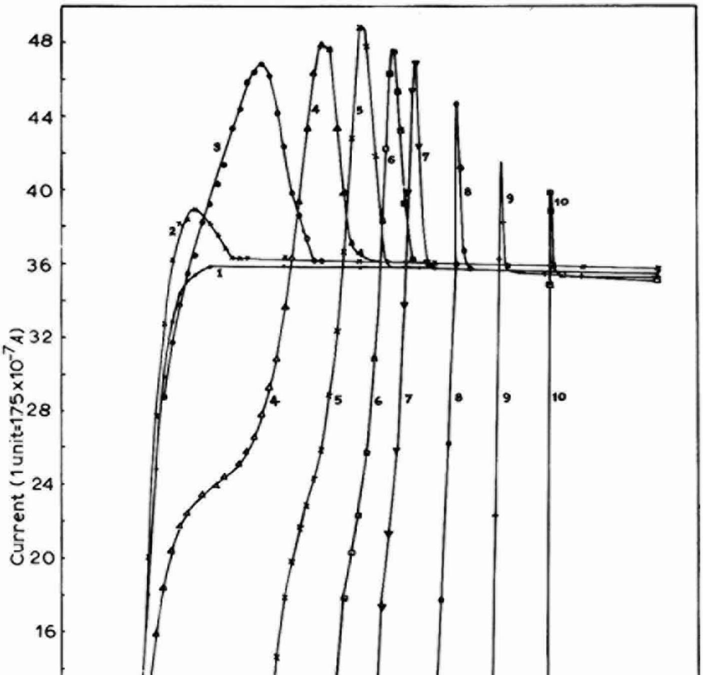

Fig. 1. Effect of varying concn. (x) of camphor on the polarographic reduction of Cd^{2+} ion from a soln. of 0.5 M Na_2SO_4 and 0.001 M H_2SO_4. x:— (1), 0; (2), 6; (3), 9; (4), 12; (5), 15; (6), 18; (7), 21; (8), 30; (9), 45; (10), 75 · 10^{-5} M.

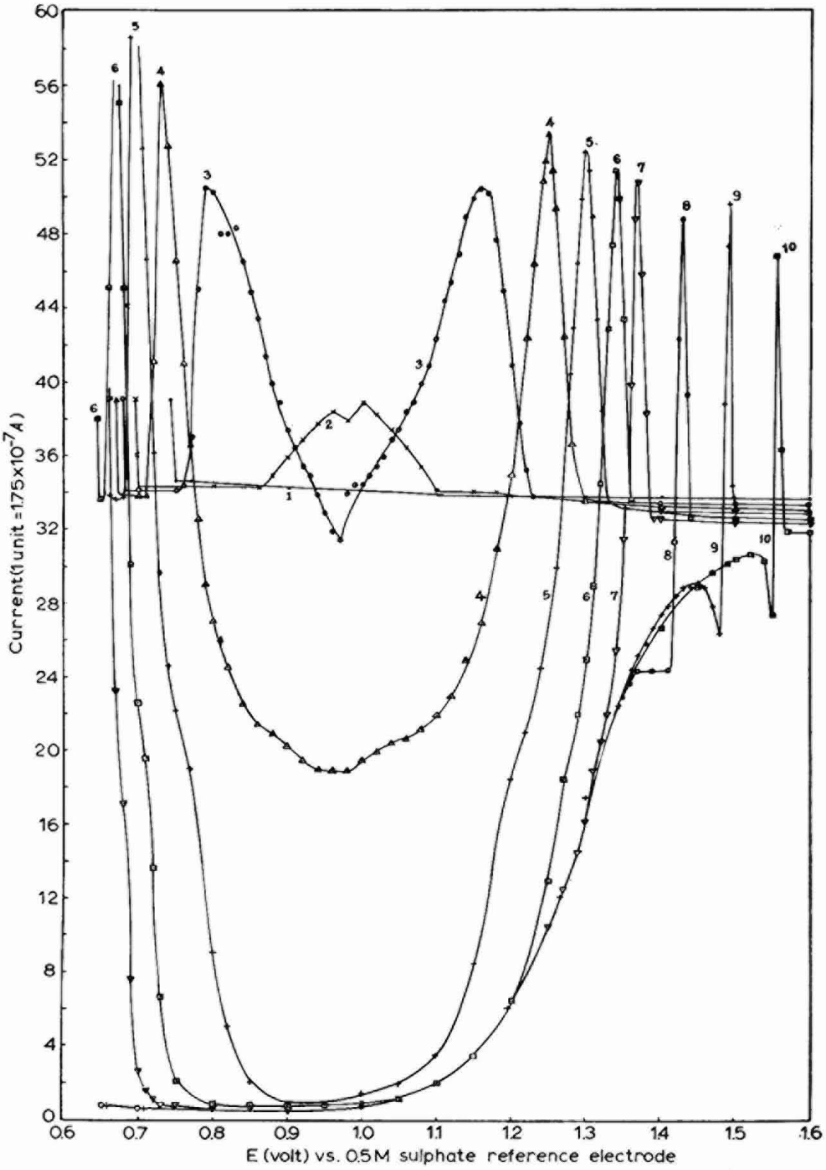

Fig. 2. Effect of varying concn. (x) of camphor on the polarographic reduction of Cu^{2+} ion from a soln. of 0.5 M Na_2SO_4 and 0.001 M H_2SO_4. x: — (1), 0; (2), 6; (3), 9; (4), 12; (5), 15; (6), 18; (7), 21; (8), 30; (9), 45; (10), 75 · 10^{-5} M.

tion. The corresponding differential capacity–potential curves are shown in Fig. 4.

The polarographic curves for Cd^{2+}/Cd reaction show (Fig. 1) the expected inhibition of the electrode reaction in the region of adsorption of camphor, but unusual and well-defined maxima at its desorption potentials (the latter correspond to the potentials at which there is a sharp change in the differential capacity). It is to be noted that for each concentration of camphor in the solution the current maximum occurs at the corresponding desorption potential.

The generality of this phenomenon is particularly evident from the polarographic curves for the Cu^{2+}/Cu reaction in the presence of camphor in the solution (Fig. 2). Apart from the maxima of the first kind which are associated with the reduction of Cu^{2+} at large positive potentials, there are *two more* maxima on each curve (up to curve 6) corresponding to the two desorption potentials of camphor. For clarity in this regard, a typical curve 4 from Fig. 2 has been shown separately in Fig. 3 together with the corresponding differential capacity curve (curve 4 in Fig. 4) for the same solution without Cu^{2+}. The initial large currents are due to maxima of the first kind. With a negative shift in the potential, the current decreases until the limiting diffusion current is reached at a potential of -0.685 V (*vs.* 0.5 M sulphate reference electrode), corresponding to the cessation of maxima of the first kind, apparently on

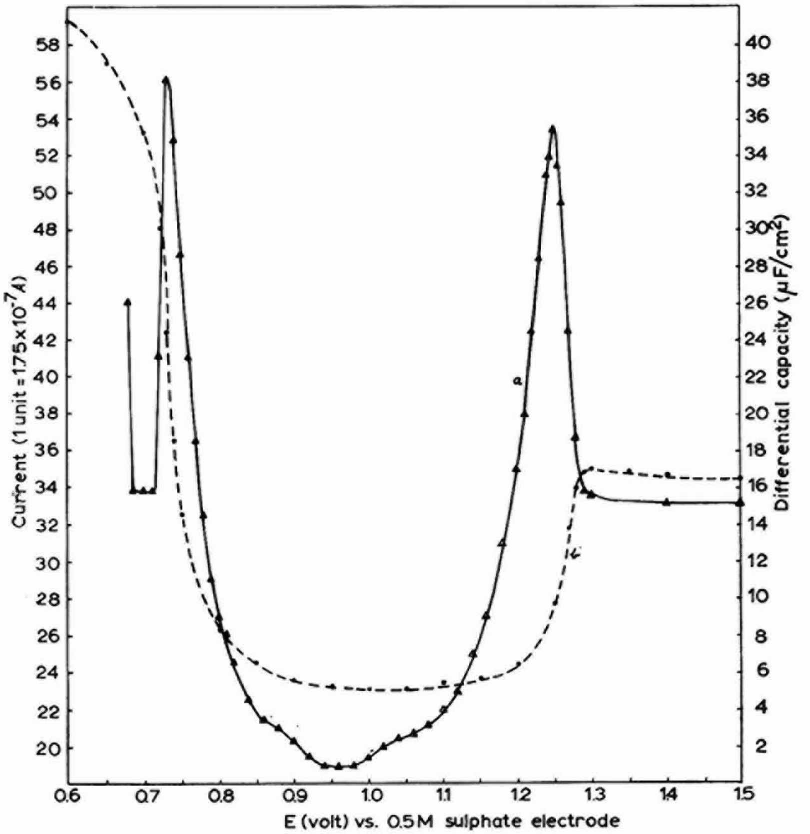

Fig. 3. (a), Full line, polarographic current–potential curve for the reduction of Cu^{2+} from a soln. of 0.5 M Na_2SO_4, 0.001 M H_2SO_4, and $12 \cdot 10^{-5}$ M camphor; (b), dashed line, differential capacity–potential curve at the D.M.E. in a soln. of 0.5 M Na_2SO_4, 0.001 M H_2SO_4 and $12 \cdot 10^{-5}$ M camphor.

adsorption of traces of camphor. Thereafter, as the sharp desorption potential of camphor on the positive branch (of the electrocapillary curve) is reached, a sharp current maximum is observed which at more negative potentials merges with the inhibited region of polarographic currents, far less than the normal value of the limiting diffusion current in this region. Finally, at the desorption potential on the negative branch (of the electrocapillary curve), the second current maximum develops, merging in the end with the limiting diffusion current slightly decreased in magnitude probably because of a decrease in the diffusion coefficient of Cu^{2+} in the presence of camphor.

With the increasing addition of camphor to the solution (Fig. 2), the maxima of the first kind and the adjacent maxima at the positive potential of desorption of camphor, approach each other (curves 2–6 of Fig. 2) until, at camphor concentrations corresponding to curves 7–10 of Fig. 2, either these first two maxima merge with each other, or the curves show inhibition at even large positive potentials. For this reason, and also because the potential span of the current maxima at either of the desorption potentials is just a few millivolts (less than 5 mV for larger concentrations of camphor), a careful recording of the polarographic curves is required to observe these maxima. The use of a large period galvanometer (measurement of average current during drop life) or recording polarographs (continuous scanning of the entire potential range in 10–15 min) may not show up these maxima at all, or may show them only to a small extent. The polarographic curves for the reduction of Cd^{2+} from an ammoniacal solution in the presence of camphor, studied by STROMBERG AND ZAGAINOVA[13] do not show any current maxima obviously because of the use of 0.01% gelatin in the solution. The polarographic reduction of *p*-nitrobenzoic acid in the presence of camphor, studied by KASTENING AND HOLLECK[14], and the polarographic reduction of the EDTA complex of Cu(II) in the presence of camphor studied by LAITINEN AND SUBCASKY[15], show only a small, spiky maximum at the desorption potential of camphor.

Regarding the curves of differential capacity in solutions containing camphor (Fig. 4), it is significant that the normally observed capacity peaks at the desorption potentials are conspicuously absent. Such a behaviour is characteristic of differential capacities measured at high frequencies for many other organic surfactants[16]. From considerations of the kinetic picture of the electrical double layer with adsorbed organic molecules, it is known that the height of the capacity peaks decreases with increasing a.c. frequency due to the inertia of the large, oriented organic molecules to move in-phase with the applied alternating voltage. However, the unusual feature of the capacity curves for camphor is that, even at as low a frequency as 400 c/sec, the capacity peaks are insignificant. The "tensammetric" curves for solutions containing camphor given by JEHRING[17] also show similar behaviour but the differential capacity curves obtained in the present work, directly by the bridge method with a relatively slow D.M.E., are more accurate[18].

The absence of the peaks on the capacity curves for solutions containing camphor and measured at the relatively low frequency of 400 c/sec, leads us to the conclusion that the adsorption–desorption step for camphor at the mercury/solution interface is a much slower process than for other organic molecules such as aliphatic alcohols for which there are prominent peaks on the capacity curves at such frequencies. This result for camphor is in agreement with the conclusions obtained by other methods[8].

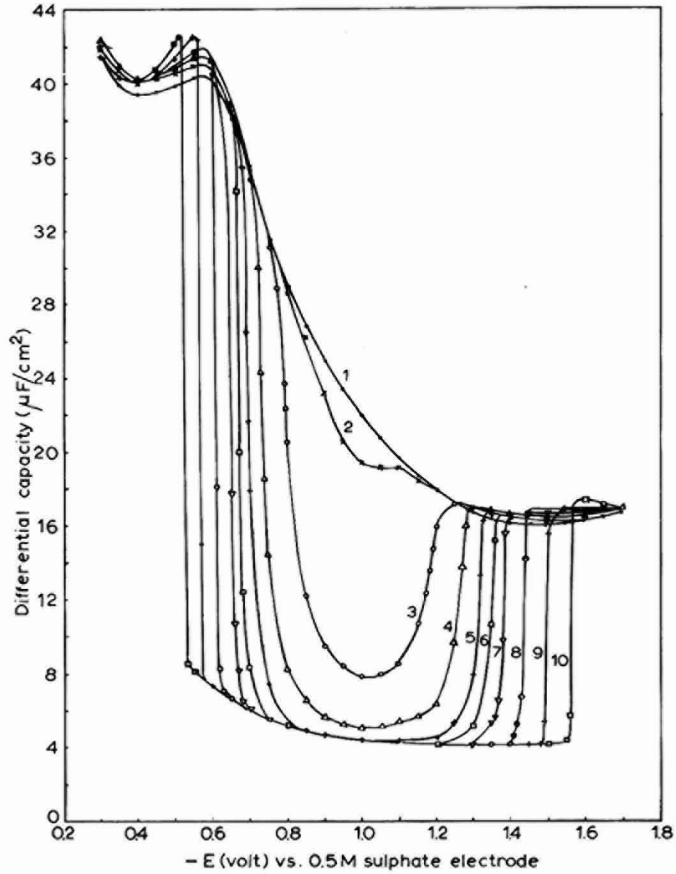

Fig. 4. Effect of varying concn. (x) of camphor on the differential capacity–potential curve at the D.M.E. in a soln. of 0.5 M Na_2SO_4 and 0.001 M H_2SO_4; a.c. frequency, 400 c/sec. x:— (1), 0; (2), 6; (3), 9; (4), 12; (5), 15; (6), 18; (7), 21; (8), 30; (9), 45; (10), $75 \cdot 10^{-5}$ M.

In addition to the slowness of the adsorption process itself, there is also a potential-dependent diffusion-controlled component for the adsorption of camphor. This is seen from the dependence of the differential capacity per unit area on the height of the mercury column at two potentials—one near the desorption region (−1.35 V *vs.* the reference electrode) and another near the region of maximum adsorption (Fig. 5). There is no control of the adsorption process by mass transfer at the D.M.E. in the region of maximum adsorption of camphor, but a significant mass transfer control near the potential of desorption. It thus follows from capacity measurements that the adsorption–desorption process of camphor is especially slow at the desorption potentials at the D.M.E.

The correlation of the adsorption of camphor at the D.M.E. and the occurrence of the polarographic maxima at the desorption potentials of camphor may now be discussed from a semi-quantitative standpoint as follows.

It has been shown[19] that in the absence of polarographic maxima of the second kind, there may occur at the desorption potentials of organic molecules under certain conditions, a gradient in the concentration of the surfactant $(\partial c/\partial x)$ along the surface of the growing mercury drop. The consequent difference in interfacial tension between the "neck" and the bottom of the mercury drop will lead to a tangential motion of the mercury surface characterised by a velocity V where*

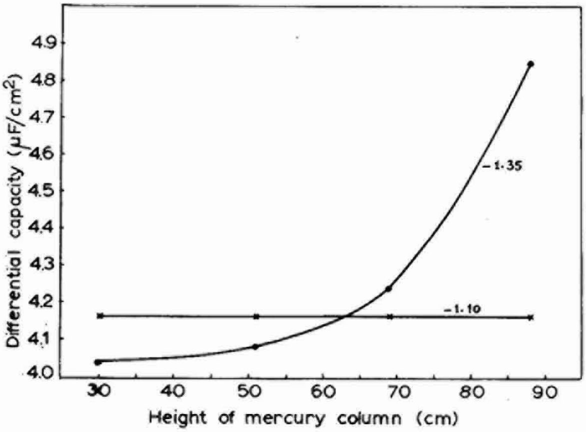

Fig. 5. Effect of the height of the mercury column on the differential capacity of the D.M.E. in a soln. of 0.5 M Na_2SO_4, 0.001 M H_2SO_4 and $30 \cdot 10^{-5}$ M camphor. The potentials of the D.M.E. are shown on each curve, in V *vs.* 0.5 M sulphate electrode.

$$V \simeq \frac{A_0 \Gamma_e c^{-1} \left(\frac{\partial c}{\partial x}\right) a}{2u+3u'+\gamma_a+\gamma_q} \tag{1}$$

Where A_0 is a constant at a given temperature, Γ_e and c are the average values of the equilibrium surface excess and concentration, respectively, of the surfactant at the D.M.E. at a given potential, a is the radius of the mercury drop (the X-axis being taken in the direction of change in the concentration of the surfactant on the electrode surface), u and u' are the viscosities of mercury and the solution, respectively, γ_a and γ_q are inhibition coefficients (inhibiting the tangential motion) due to adsorbed molecules and double-layer charges, respectively.

Since the concentration, c, of the surfactant is related to Γ_e by an adsorption isotherm, c is also a function of the electrode potential E. Thus,

$$\left(\frac{\partial c}{\partial x}\right)_\mu = \left(\frac{\partial c}{\partial E}\right)_\mu \left(\frac{\partial E}{\partial x}\right)_\mu$$

where μ is the composition of the solution. The gradient in potential along the surface of the drop, $(\partial E/\partial x)_\mu$, will arise for the same reasons as those producing polarographic

---

* The notation of eqn. (1) in this paper is slightly different from that used in eqn. (7) of ref. 3.

maxima of the first kind *viz.* asymmetry of the electric field around the D.M.E. when the surface charge density is different from zero. It is well-known[1], also, that $\gamma_a \propto \Gamma_e^2/c$ and $\gamma_q \propto q^2$. From the Frumkin relation $q = q_0(1-\theta) + q_1\theta$ where q_0 and q_1 are charge densities on the metal for uncovered ($\theta = 0$) and fully covered ($\theta = 1$) surface and $\theta = \Gamma_e/\Gamma_{\max}$, where $\Gamma_{\max}$ is the maximum value of Γ_e it follows that, to a first approximation, $\mathrm{d}\Gamma_e \propto (-|\mathrm{d}q|)$ over a small potential range. Considering, therefore, only the narrow regions of desorption potentials (about 50-mV wide), the denominator of eqn. (1) may be considered constant to a first approximation because, as Γ_e decreases, q will increase more or less proportionately. The desorption potentials are also necessarily away from the potentials of zero charge and therefore the magnitude $(\partial E/\partial x)_\mu$ will be constant in this region. Under these conditions eqn. (1) reduces to

$$V \simeq A_1 \Gamma_e c^{-1} \left(\frac{\partial c}{\partial E}\right)_\mu \tag{2}$$

where A_1 is a constant for a given solution at the desorption potentials.

Since the equilibrium value Γ_e is usually not reached at the D.M.E., the actual value of the surface excess Γ_t at time t of the life of the drop (t is the drop time in the present work) is to be correlated with V in eqn. (2). This is possible if it is assumed for simplicity that Henry's law isotherm is valid for the adsorption of camphor. It is also known[21] that the use of Langmuir's isotherm in place of the linear isotherm gives qualitatively similar rates of adsorption. The conclusion that may be drawn with the above assumption may, therefore, be expected to be qualitatively valid.

For adsorption obeying the isotherm $\Gamma_e = Kc$ and controlled by semi-infinite linear diffusion (K is the adsorption constant for camphor in the present case) it has been shown[20] that

$$\Gamma_t = \Gamma_e \left(1 - \exp \frac{Dt}{K^2} \operatorname{erfc} \sqrt{\frac{Dt}{K}}\right) \tag{3}$$

where D is the diffusion coefficient of the surfactant. From eqns. (2), (3) and the equation for the isotherm, it follows that if K is independent of the potential in the narrow regions of desorption,

$$V \simeq A_1 \left(\frac{\Gamma_e}{\Gamma_t}\right) \left(\frac{\partial \Gamma_t}{\partial E}\right)_\mu \tag{4}$$

For a high-frequency capacity curve it is known that[16]

$$C = C_0(1-\theta) + C_1\theta$$

where, in the present work, C_0, C_1 and C are the differential capacities of the electrode corresponding to the coverage being 0, 1 and θ, respectively, and measured at the end of time t after the formation of a drop.

In a narrow potential range such as the desorption potentials, C_0 and C_1 do not change much, and therefore from the equations for C and θ,

$$\left(\frac{\partial \Gamma_t}{\partial E}\right)_\mu \propto \left(\frac{\partial C}{\partial E}\right)_\mu$$

at the desorption potentials.

Hence, it follows that

$$V \simeq A_2 \left(\frac{\Gamma_e}{\Gamma_t}\right) \left(\frac{\partial C}{\partial E}\right)_\mu \tag{5}$$

where A_2 is a constant.

Since $(\partial \Gamma_t/\partial E)_\mu$ in the general eqn. (4), or $(\partial C/\partial E)_\mu$ in eqn. (5) for substances giving insignificant capacity peaks (even at low frequencies), acquires quite large values at the desorption potentials (sharp change in the capacity curves), the *possibility* exists for a large V and therefore polarographic maxima at these potentials of desorption. However, the fact that such maxima are not observed for all organic substances but clearly evident for camphor, is to be explained by the effect of the term (Γ_e/Γ_t) in eqn. (5). If the adsorption process is fast enough, adsorption equilibrium is attained well within the drop life and the function $(\Gamma_e/\Gamma_t) \rightarrow 1$ and V tends to some finite value which may not be large enough. However, if the adsorption process is very slow, the function $(\Gamma_e/\Gamma_t) \gg 1$ and V may attain very large values at the desorption potentials causing polarographic maxima at these potentials. It has been inferred above from measurements of differential capacity that the adsorption of camphor from solution on a D.M.E. is particularly slow at the desorption potentials. Hence, at these potentials, one should expect polarographic maxima, irrespective of the nature of the ion undergoing charge transfer at the electrode. Thus, the reversible potential for the discharge of Cd^{2+} being close to the null point of mercury in the solution, the above type of polarographic maxima occurs only at the negative potential of desorption of camphor. On the other hand, the discharge of Cu^{2+}, which starts at potentials decidedly positive to the potential of zero charge of mercury in the solution, must show *two* such maxima, (in addition to the usual maxima of the first kind) corresponding to positive and negative potentials of desorption of camphor, on either side of the null point; this is confirmed by experiment.

It may therefore be concluded that well-defined polarographic maxima occur at the desorption potentials of organic molecules in the solution if the rate of attainment of adsorption equilibrium is sufficiently small at these potentials. The gradient in concentration of the surfactant at the electrode surface causing tangential movements of the mercury drop, arises as a result of the asymmetry of the electric field around the D.M.E. and a relatively slow adsorption of the organic substance with sharp potentials of desorption. The effect is not specific to the nature of the reducible ion.

ACKNOWLEDGEMENTS

The author is indebted to Prof. HIRA LAL for his keen interest in the work and to T. V. PADMA for valuable assistance during the course of the work.

SUMMARY

Polarographic maxima belonging to neither the first nor the second kind are observed during the cathodic discharge of Cd^{2+} and Cu^{2+} on a dropping mercury electrode in the presence of camphor in the solution. Experimental data for the potential dependence of differential capacity as well as polarographic current at the same age of the life of the dropping mercury electrode are presented for various concentrations of camphor in solution. A theoretical correlation of the occurrence of such polarographic maxima with a slow and non-uniform adsorption of surface-active substances at their desorption potentials on the dropping mercury electrode, has been attempted.

REFERENCES

1 V. G. LEVICH, *Physicochemical Hydrodynamics*, Prentice-Hall, New York, 1962, p. 561.
2 M. VON STACKELBERG AND R. DOPPELFELD, *Advances in Polarography*, Vol. I, edited by I. S. LONGMUIR, Pergamon Press, London, 1960, p. 68.
3 A. N. FRUMKIN, S. SATHYANARAYANA AND N. V. NIKOLAEVA-FEDOROVICH, *Izv. Akad. Nauk SSSR*, (1962) 1977; (refs. to earlier work also given in this paper).
4 W. WERONSKII, *Trans. Faraday Soc.*, 58 (1962) 2217.
5 V. F. IVANOV AND Z. A. IOFA, *Zh. Fiz. Khim.*, 34 (1960) 2517.
6 S. G. MAIRANOVSKII, *J. Electroanal. Chem.*, 6 (1963) 77.
7 J. KUTA AND I. SMOLER, *Progress in Polarography*, Vol. I, edited by P. ZUMAN AND I. M. KOLTHOFF, Interscience Publishers Inc., New York, 1962, p. 43.
8 R. W. SCHMID AND C. N. REILLEY, *J. Am. Chem. Soc.*, 80 (1958) 2087.
9 A. N. FRUMKIN, O. A. PETRII AND N. V. NIKOLAEVA-FEDOROVICH, *Dokl. Akad. Nauk SSSR*, 136 (1961) 1158.
10 D. C. GRAHAME, *J. Am. Chem. Soc.*, 68 (1946) 301.
11 B. B. DAMASKIN, *Zh. Fiz. Khim.*, 32 (1958) 2199.
12 S. SATHYANARAYANA, *Indian J. Chem.*, 2 (1964) 474.
13 A. G. STROMBERG AND L. S. ZAGAINOVA, *Zh. Fiz. Khim.*, 31 (1957) 1043.
14 B. KASTENING AND L. HOLLECK, *Z. Elektrochem.*, 64 (1960) 823.
15 H. A. LAITINEN AND W. J. SUBCASKY, *J. Am. Chem. Soc.*, 80 (1958) 2623.
16 A. N. FRUMKIN AND B. B. DAMASKIN, *Dokl. Akad. Nauk SSSR*, 129 (1959) 862.
17 H. JEHRING, *Z. Physik. Chem. (Leipzig).*, 226 (1964) 59.
18 A. N. FRUMKIN AND B. B. DAMASKIN, *J. Electroanal. Chem.*, 3 (1962) 36.
19 Ref. 3., p. 1981, eqn. (7).
20 P. DELAHAY AND I. TRACHTENBERG, *J. Am. Chem. Soc.*, 79 (1957) 2355.
21 P. DELAHAY AND C. T. FIKE, *J. Am. Chem. Soc.*, 80 (1958) 2628.

THE DETERMINATION OF TRACES OF BISMUTH IN COBALT BY COLORIMETRY AFTER ELECTROLYTIC SEPARATION AND BY PULSE POLAROGRAPHY

A. LAGROU AND F. VERBEEK
Laboratory for Analytical Chemistry, Ghent University, Ghent (Belgium)
(Received March 22nd, 1965)

The colorimetric determination of lead in cobalt after prior deposition onto a mercury cathode was described in a previous investigation[1]. This paper deals with the determination of traces of bismuth in cobalt using dithizone as the colorimetric reagent. The use of dithizone for the separation of bismuth from lead and copper has already been reported by FISCHER AND LEOPOLDI[2]. The method was established by HUBBARD[3,4] particularly for the determination of bismuth in biological materials but as his procedure is difficult to apply to biological materials high in phosphates, an improved modification has been given by LAUG[5]. Another dithizone procedure for the detection of bismuth in biological materials is described by KLUCHESKY *et al*[6].

However, in the presence of an excess of cobalt an immediate colorimetric determination is impossible, as cobalt is also extracted with dithizone from a basic medium[1,7]; therefore a prior separation of bismuth from cobalt is necessary. Electrolytic deposition at a controlled cathode potential onto a mercury cathode was used for separating bismuth from the solution. After anodic stripping of the amalgam, bismuth was determined colorimetrically. Yield control by a pulse polarograph proved the method to be quantitative. Thus no corrections were needed for overall losses, in contrast with the determination of lead in which radioisotopes were used for yield control. The most favourable conditions for deposition, the influence of several variables and possible interferences of other elements have also been investigated.

APPARATUS AND REAGENTS

The assembly for electrolysis and colorimetric determination was identical to the one described previously[1]. A Southern-Harwell MK II pulse polarograph was used for checking the quantitative character of the determination. Analytical-grade reagents and doubly-distilled water and nitric acid were used. Very pure hydrochloric acid and ammonia were obtained by isopiestic distillation. Dilute solutions were freshly prepared and stored in polyethylene containers.

EXPERIMENTAL

Conditions of electrolysis

Electrodeposition of bismuth onto a mercury cathode has already been mentioned by some authors. LINGANE[8–10] separated bismuth from other metals having reduction potentials differing by less than 0.2 V, using a stirred mercury-pool electrode at −0.35 V *vs.* S.C.E. The electrolysis was carried out in a tartrate buffer for a bismuth concentration range 10–100 mg. The depositional behaviour of bismuth in very dilute solution in nitric acid medium was studied by GHOSH-MAZUMDAR AND HAISSINSKY[11].

In the present investigation, the electrolysis of micro-quantities of bismuth in hydrochloric acid has been examined; the influence of several factors were verified and the ideal conditions of cathode potential, electrolysis time and acid concentration for obtaining a quantitative deposition determined.

All experiments were carried out in a cell volume of 50 ml. The quantity of mercury used as cathode was 1 ml. The mercury was stirred with a glass rod dipped about 2 mm in the mercury. The initial (10^{-5} M Bi) and ultimate bismuth concentrations were controlled by a pulse polarograph. The experiments were performed in hydrochloric acid medium; no sorption[1] on the walls was noticed.

Cathode potential. The electrolysis was performed with rapid stirring (600 rev./min) at different cathode potentials in 1 M HCl during 1 h and the decrease of the bismuth concentration in the cell followed. The per cent deposited bismuth as a function of the cathode potential is given in Fig. 1.

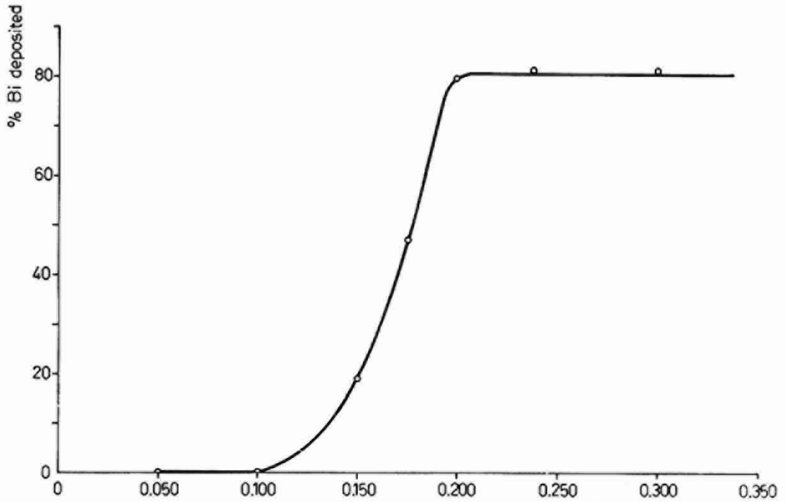

Fig. 1. Percentage of Bi deposited as a function of the cathode potential (V). Bi concn., 10^{-5} M in 1 M HCl; electrolysis time, 1 h.

Electrolysis time. The conditions for electrolysis were identical to those used in previous experiments. The deposition at a well-defined potential (−0.2 V *vs.* mercury pool) was followed as a function of time. The results are shown in Fig. 2.

Acidity of the solution. The electrolysis was carried out in solutions of varying hydrochloric acid concentration. Fig. 3 shows the results after electrolysis for 1 h at a cathode potential of −0.2 V *vs.* mercury pool. In strong acid solution (⩾ 2 *M*) a pronounced decrease in deposition was observed. Between pH 1 and pH 2 bismuth hydrolyses; according to CHARLOT[12] basic salts of the type BiOCl are precipitated. As very dilute solutions easily become colloidal in weakly acidic medium, further experiments were performed in 1 *M* HCl.

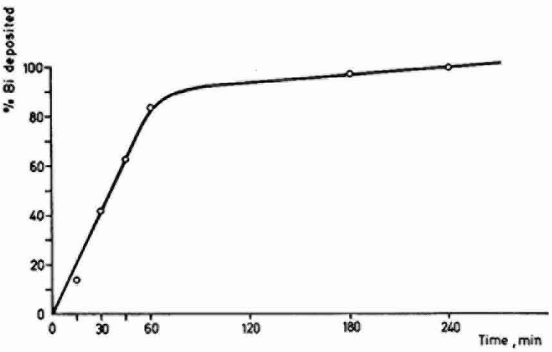

Fig. 2. Percentage of Bi deposited as a function of electrolysis time (h). Bi concn., 10^{-5} *M* in 1 *M* HCl.

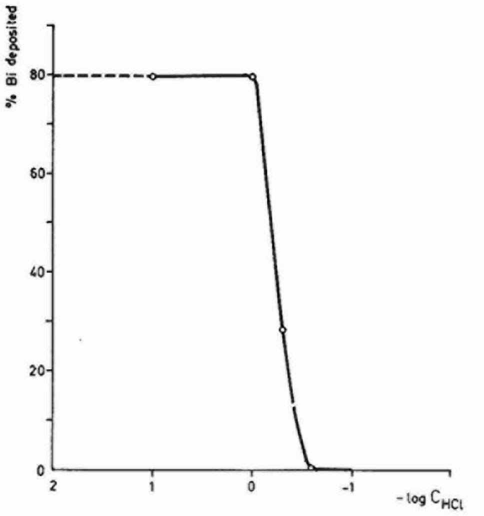

Fig. 3. Percentage of Bi deposited as a function of HCl molarity. Bi concn., 10^{-5} *M*; electrolysis time, 1 h.

Bismuth concentrations. Solutions containing various concentrations of bismuth were electrolysed; the conditions for electrolysis have already been described. The results are given in Fig. 4. Increasing the bismuth concentration lowers the per cent deposited metal, but it is obvious that the yield can be improved by using a larger mercury pool as cathode.

These experiments show that bismuth, in 1 *M* HCl, is almost completely deposited after a 4-h electrolysis at 0.2 V *vs.* mercury pool. All determinations were made under these conditions.

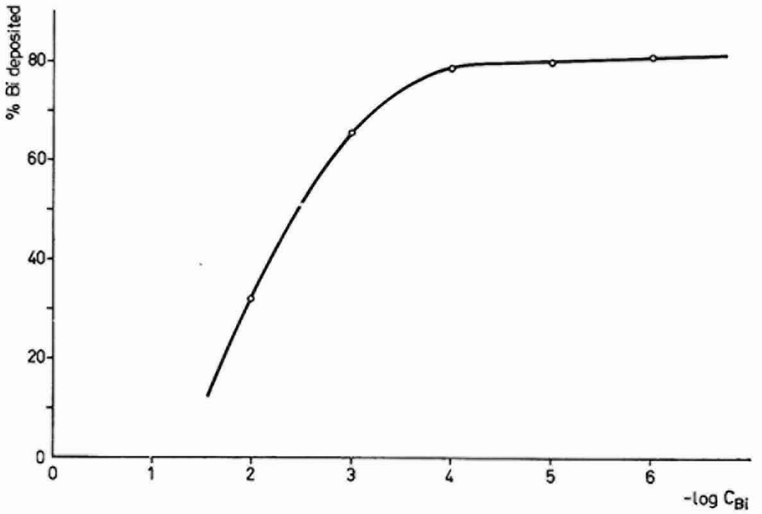

Fig. 4. Effect of Bi concn. on electrodeposition of Bi. Electrolysis time, 1 h; 1 *M* HCl.

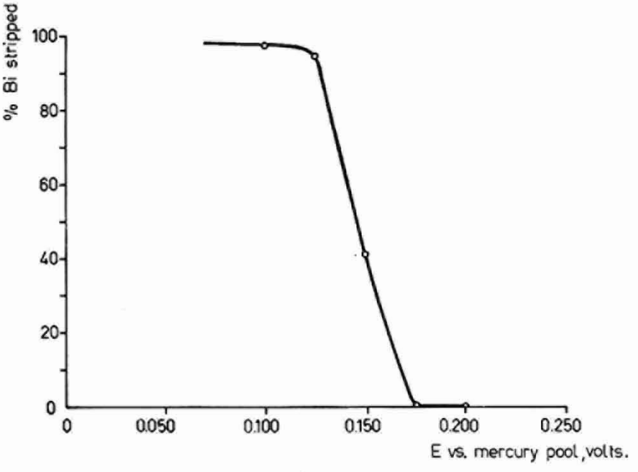

Fig. 5. Percentage of Bi anodically stripped as a function of the anode potential (V). Time, 1 h; 1 *M* HCl.

Decomposition of the amalgam

To separate the bismuth amalgam from cobalt in the solution a system of continuous washing was applied as previously described[1].

The complete removal of bismuth from the mercury may be carried out by (i) treating the amalgam with an oxidising agent; (ii) distilling the mercury or (iii) stripping it at a controlled potential or a controlled current[13].

Distillation of the amalgam[1,14] gave a bismuth yield of 85–90%. By working under standardised conditions it is possible to apply this technique; however, KOZLOVSKII AND TSȲB[15–16] prefer to determine bismuth by anodic oxidation of the amalgam after previous reduction onto a mercury cathode. The metal was quantitatively stripped before the anode potential had reached the value necessary for the oxidation of the mercury. The last method was applied for recovering the bismuth from the amalgam. Fig. 5 shows the per cent bismuth anodically stripped into the acid electrolyte after 1 h at different anode potentials. After 5 min at -0.1 V *vs.* mercury pool nearly all the bismuth had returned into the solution. The same result was obtained by stirring the bismuth amalgam in 1 *M* HCl without current flow; the remaining solution then was evaporated to dryness, redissolved in 1:100 HNO_3 and analysed colorimetrically[17].

PROCEDURE

Add to the electrolysis cell 50 ml of a $CoCl_2$–1 *M* HCl solution. Electrolyse during 4 h at a cathode potential of -0.2 V *vs.* mercury pool. After continuous washing apply to the working electrode a potential of -0.1 V, and keep this constant for 15 min. Without interrupting the current, transfer the solution from the cell into a beaker. Rinse the electrolysis cell and the remaining mercury a few times with 1 *M* HCl. Combine the washings and the original solution and evaporate to dryness. Redissolve in 50 ml of 1:100 HNO_3 and determine the bismuth colorimetrically after extraction with dithizone[17].

INTERFERENCES

Lead, indium, thallium(I) and tin(II) also react with dithizone in basic cyanide medium. Because tin does not react in the stannic state and thallium can be separated from bismuth more easily than lead, the latter is likely to be the only metal giving difficulties. For this reason an electrolysis was carried out on a mixture of $5 \cdot 10^{-6}$ *M* Bi and $5 \cdot 10^{-6}$ *M* Pb in 1 *M* HCl at -0.2 V *vs.* mercury pool. Fig. 6 curve a, gives a pulse polarogram of the initial solution and curve b, after 1-h electrolysis. More than 85% bismuth appears to be deposited onto the mercury, and the lead remains completely in solution. As the other potentially interfering elements are much more electronegative than lead, they would not be expected to interfere.

The effect of increasing quantities of cobalt was also investigated. Fig. 7 shows the extinction at a wavelength of 505 mμ of 50 ml of a solution containing 10 μg of bismuth and amounts of cobalt between 10^{-4} and 10^{-1} *M*, extracted with 15 ml of dithizone–chloroform solution. Above 10^{-2} *M* cobalt, a systematic error occurs in the colorimetric determination. As the electrolysis is performed at -0.2 V *vs.* mercury pool, deposition of cobalt is impossible[1] and cobalt will not, therefore, interfere in the colorimetric determination of bismuth.

As mercury also reacts with dithizone, a blank determination of 50 ml 1 *M* HCl was put through the procedure; it was established that mercury eventually stripped from the cathode did not interfere.

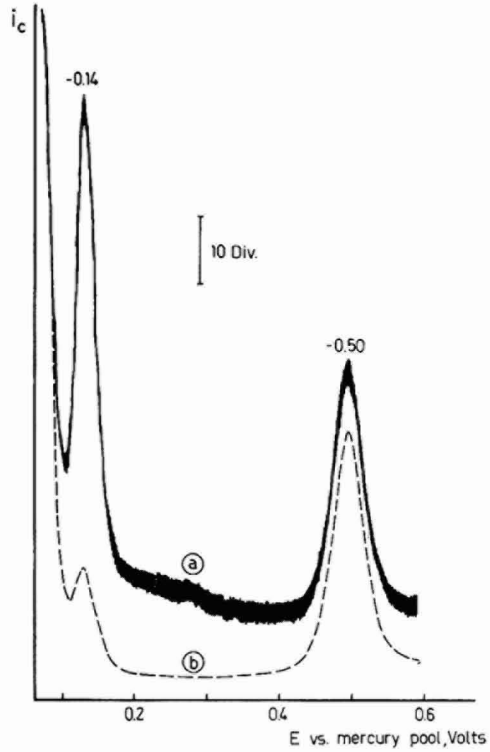

Fig. 6. Pulse polarogram of $5 \cdot 10^{-6}$ *M* Bi and $5 \cdot 10^{-6}$ *M* Pb in 1 *M* HCl (7 mV; 15 min; 3 int.; S.1/10). Curve a, initial solution; curve b, after 1-h electrolysis at −0.2 V *vs.* mercury pool.

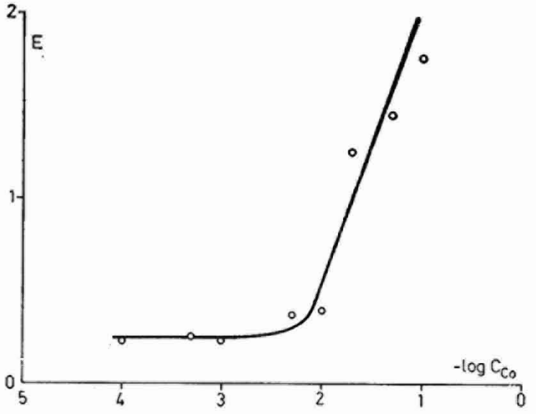

Fig. 7. Effect of Co concn. on the colorimetric determination of Bi (10 μg in 15 ml) with dithizone.

RESULTS

A number of analyses were performed on synthetic samples prepared by adding a known quantity of a standard bismuth solution to a cobalt solution freed from bismuth by electrolysis at a mercury cathode in a Melaven cell. The results are summarised in Table 1, column 3. The determination of 2–20 μg bismuth in 50 ml was possible with an average error of ±5%. For lower bismuth concentrations ($\leqslant 1$ μg/50 ml) much higher deviations (25% and more) were noticed, due to the fact that the sensitivity limit of the colorimetric technique was approached. The method allows the determination of as little as $3 \cdot 10^{-5}\%$ of bismuth in cobalt when electrolysing 50 ml of a 2 *M* cobalt solution.

TABLE 1

DETERMINATION OF BISMUTH IN COBALT

Bi added to 50 ml 2 M Co soln. (μg)	*Bi in Co (p.p.m.)*	*Bi found color. (μg)*	*Bi found polar. 1 M HCl (μg)*	*Bi found polar. acetate buffer (μg)*
20.68	3.51	20.03 21.17	20.87	—
10.34	1.75	10.00 10.44 10.77 10.02 10.96	10.25	—
5.17	0.88	5.43 5.91	5.55	5.38
2.58	0.44	2.93 2.69	—	2.74
1.03	0.18	(1.64)	—	0.94

Since the $E_{\frac{1}{2}}$ values of bismuth and cobalt are, respectively, -0.13 V and -1.24 V *vs.* S.C.E. in 1 *M* HCl[18], the direct polarographic determination of traces of bismuth in cobalt without any separation is feasible. Therefore a number of analogous analyses was performed with the very sensitive Southern-Harwell pulse polarograph[19], using the standard-addition method. The results are given in Table 1, column 4.

Since the $E_{\frac{1}{2}}$ value of bismuth in 1 *M* HCl approaches the oxidation potential of mercury, the peak current of low bismuth concentrations is situated in the slope of the descending base line. This limits the sensitivity of the method to about 10^{-7} *M*. For lower concentrations it is more satisfactory to use HAc–NH_4Ac as base electrolyte, as the $E_{\frac{1}{2}}$ value of bismuth is -0.24 V *vs.* S.C.E.[18] in this medium. To avoid interference of high chloride concentration, the cobalt to be analysed was dissolved in twice-distilled nitric acid, the solution evaporated to dryness and redissolved in the buffer, 2 *M* HAc–2 *M* NH_4Ac. The results of a number of analyses are shown in Table 1, column 5. Although the method for bismuth is only one-third as sensitive in this medium as in hydrochloric acid, about $3 \cdot 10^{-8}$ *M* can be determined[20], corresponding to $6 \cdot 10^{-6}\%$ when using a 2 *M* cobalt solution.

It can be concluded that the colorimetric method described (after preliminary separation of bismuth onto a mercury cathode) and the polarographic method (without any separation) can also be used for the determination of traces of bismuth in other more electronegative elements such as cadmium, indium, nickel, zinc, manganese and others. Thiourea[21] and iodide[21] can also be used as colorimetric reagents. Pulse polarography is less time consuming and also more sensitive than colorimetry, but it is possible to lower the detection limit of the colorimetric method by using larger cobalt samples.

ACKNOWLEDGEMENTS

The authors thank Prof. Dr. J. **Hoste** for his kind interest in this work and Mrs. F. **Van den Abeele** for technical assistance.

SUMMARY

Traces of bismuth (down to $3 \cdot 10^{-5}\%$) in cobalt were determined colorimetrically with dithizone after a prior separation of the bismuth onto a mercury cathode using controlled potential analysis and subsequent anodic stripping of the amalgam. The quantitative character of the method was controlled by pulse polarography. The conditions, (*i.e.*, cathode potential, electrolysis time, acidity, bismuth concentration) for electrodeposition of micro-quantities were investigated. Interferences from cobalt, mercury, tin(II), thallium(I), indium and lead are discussed. Analogous analyses of traces of bismuth in cobalt without preliminary separation (down to $6 \cdot 10^{-6}\%$) were performed with a pulse polarograph using the standard-addition method.

REFERENCES

1 A. Lagrou and F. Verbeek, *J. Electroanal. Chem.*, 9 (1965) 184.
2 H. Fischer and G. Leopoldi, *Angew. Chem.*, 47 (1934) 685.
3 D. M. Hubbard, *Anal. Chem.*, 20 (1948) 363.
4 D. M. Hubbard, *Ind. Eng. Chem., Anal. Ed.*, 11 (1939) 344.
5 E. P. Laug, *Anal. Chem.*, 21 (1949) 188.
6 E. F. Kluchesky, B. J. Longley and F. L. Kozelka, *J. Pharmacol. Exp. Therap.*, 74 (1942) 395.
7 E. B. Sandell, *Colorimetric Determination of Traces of Metals*, Interscience Publishing Co., New York, 3rd ed., 1959, p. 410.
8 J. J. Lingane, *Ind. Eng. Chem., Anal. Ed.*, 16 (1944) 147.
9 J. J. Lingane, *J. Am. Chem. Soc.*, 67 (1945) 1916.
10 J. J. Lingane, *Anal. Chim. Acta*, 2 (1948) 584.
11 A. S. Ghosh-Mazumdar and M. J. Haissinsky, *J. Chim. Phys.*, 51 (1954) 296.
12 G. Charlot, *Nouvelle Méthode d'Analyse Qualitative*, Masson & Cie, Paris, 1942, p. 153.
13 J. A. Page, J. A. Maxwell and R. P. Graham, *Analytical Applications of the Mercury Electrode*, a review, *The Analyst*, 87 (1962) 245.
14 C. J. Rodden, Editor, *Analytical Chemistry of the Manhattan Project*, Division VIII, Vol. I, National Nuclear Energy Series, McGraw-Hill Book Co. Inc., New York, 1950, pp. 513 and 520–521.
15 M. T. Kozlovskii and P. P. Tsȳb, *J. Appl. Chem., USSR*, 23 (1950) 1285.
16 M. T. Kozlovskii, P. P. Tsȳb and E. F. Speranskaya, *Tr. Komis. Analit. Khim., Akad. Nauk, SSSR., Otd. Khim. Nauk*, 4 (1952) 255; *C. A.*, 48 (1954) 1878.
17 E. B. Sandell, *Colorimetric Determination of Traces of Metals*, Interscience Publishers Inc., New York, 3rd ed., 1959, p. 348.
18 M. Brezina and P. Zuman, *Polarography in Medicine, Biochemistry and Pharmacy*, Interscience Publishers Inc., New York, 1958, p. 735.
19 G. C. Barker and A. W. Gardner, *Z. Anal. Chem.*, 173 (1960) 79.
20 E. Temmerman and F. Verbeek, unpublished data.
21 E. B. Sandell, *Colorimetric Determination of Traces of Metals*, Interscience Publishers Inc., New York, 3rd ed., 1959, p. 332.

VOLTAMMETRIC STUDIES OF Eu(III) IN FORMATE BUFFER

THE FORMAL POTENTIAL OF THE Eu(III)-Eu(II) SYSTEM

DANIEL J. MACERO, LARRY B. ANDERSON* AND PAUL MALACHESKY**
Department of Chemistry, Syracuse University, Syracuse 10, N.Y. (U.S.A.)
(Received March 23rd, 1965)

The formal reduction potential of the Eu(III)-Eu(II) system was determined by McCoy[7] in a potentiometric study of the cell:

$$\mathrm{Pt|Eu(HCOO)_3 + Eu(HCOO)_2 + HCOOH} + N\ \mathrm{KCl|N.C.E.}$$

The value obtained was −0.43 V *vs.* N.H.E. at 25°.

Europium(III) is known to form complexes with acetate ion in aqueous solution[3,6]. The existence of these acetate complexes suggests that the formate ion could also enter into preferential complex formation with Eu(III) ion. If this is the case, the value of the formal electrode potential of the Eu system as determined by McCoy would be in error. Evidence supporting this was obtained by Anderson and Macero[1] who determined, from chronopotentiometric measurements, the value of −0.35 V *vs.* N.H.E. for the formal reduction potential of the Eu(III)-Eu(II) system in the non-complexing medium 1 M $NaClO_4$-$HClO_4$.

Polarographic and chronopotentiometric studies were carried out to establish conclusively the existence of formate complexes and to ascertain their effect on the formal potential of the Eu couple.

Ionic strength and pH were held constant while the formate ion concentration was varied from 10^{-2} M to 1 M. The concentration of Eu was kept constant at 1.60×10^{-4} M. The formate ion concentration was, therefore, always at least 60 times greater than the Eu concentration. This fact, combined with the buffering effect of formate ion and formic acid at pH 4.3, eliminated the possibility of any significant changes in the concentration of formate or hydrogen ions at the electrode surface during a run.

EXPERIMENTAL

Apparatus

The chronopotentiometric system and cell has already been described[5]. The polarographic measurements were made on an automatic recording instrument assembled from a Minneapolis-Honeywell Recorder (Model Y153X17) with 2-sec pen speed and a Model 7669 Leeds and Northrup polarizing unit.

---

* Present address: Department of Chemistry, University of North Carolina, Chapel Hill, North Carolina (U.S.A.).

** Participant in the N.S.F. Undergraduate Research Program, held at Syracuse University, summer 1962.

A saturated NaCl, Ag–AgCl electrode served as the reference electrode in both the polarographic and chronopotentiometric runs.

Reagents

All chemicals with the exception of Eu were of analytical-reagent grade. Stock Eu solutions were prepared by dissolving 99.9% pure Eu_2O_3 (Lindsay Chemical Division, American Potash and Chemical Corp.) in a small quantity of concentrated perchloric acid and diluting to volume. For each determination, amounts of sodium formate and formic acid sufficient to buffer the solution between pH 4.0 and 4.5 and yield the desired formate concentration were added to an aliquot of the stock Eu solution. Enough sodium perchlorate was then added to maintain a final ionic strength of 1 when the mixture was diluted to volume. The final pH was determined with a Beckman Zeromatic Expanded Scale pH meter.

The temperature was kept constant at $25° \pm 0.1°$.

RESULTS AND DISCUSSION

In formate medium, the polarographic reduction of Eu(III) at the dropping mercury electrode is irreversible. This was inferred from the fact that the value of n derived from plots of E *vs.* $\ln i/(i_d - i)$ is about 0.5.

The chronopotentiometric reduction of Eu(III) in the same medium at a mercury cathode is reversible. This is deduced from the agreement, to within a few millivolts, of the quarter-wave potential for the reduction of Eu(III) and that for the re-oxidation of Eu(II)[4]. In addition, a value of 0.9 is calculated for n from E *vs.* $\ln (\tau^{\frac{1}{2}} - t^{\frac{1}{2}})/(t^{\frac{1}{2}})$ plots; the current density was of the same order of magnitude in both the polarographic and chronopotentiometric runs.

This apparent difference in the reversibility of the electrode reaction in the two methods is striking and as yet no simple explanation has been established. It is possible, however, that the electrode process, $\mathrm{Eu(III)} + e \rightleftharpoons \mathrm{Eu(II)}$, is facilitated by the adsorption of formic acid on to the electrode surface. In this event the chronopotentiometric method might be expected to result in more reversible behavior because of the longer time of contact between the electrode and solution.

Polarographic results

The polarographic data are summarized in the first three columns of Table 1.

TABLE 1

SHIFT OF $E_{\frac{1}{2}}$ WITH FORMATE ION CONCENTRATION AND VALUES OF $F_n(X)$ FOR POLAROGRAPHIC DATA

$[HCOO^-]$ *(M)*	*pH*	$E_{\frac{1}{2}}$ *(V vs. Ag/AgCl/NaCl sat.)*	$F_0(X)$	$F_1(X)$	$F_2(X)$
0.010	4.25	−0.682	1.00		
0.032	4.05	−0.681	1.097	3.070	
0.100	4.35	−0.689	1.700	7.00	
0.178	4.15	−0.729	10.97	56.01	224
0.316	4.30	−0.750	19.02	57.03	129
0.562	4.45	−0.783	71.38	125.2	194
1.00	4.55	−0.809	207.0	206.0	190

It can be seen that the half-wave potential shifts regularly to more negative potentials as the concentration of formate ion is increased, indicating that there is complex formation between Eu and formate ion. From these data, the nature and stability constants of the Eu formate complexes were determined by use of the Deford and Hume technique[2].

The application of the Deford and Hume method to irreversible systems has been discussed by VLČEK[8]. He has shown that although this method was derived for reversible systems, it may be applied to irreversible cases if α, the transfer coefficient, remains constant over the ligand concentration range studied. The value of αn calculated from the E vs. ln $i/(i_d - i)$ plots in the present study was constant at 0.48 ± 0.06 and the Deford and Hume method could therefore be used.

In this treatment it was assumed that the formation of any Eu(II) formate complexes was negligible since the Eu(II) ion is larger than the Eu(III) ion (ionic radius 1.14 Å vs. 1.05 Å) and has one less formal positive charge.

The values of $F_n(X)$ which characterize the dependence of potential on ligand concentration are tabulated in Table 1. The results have also been plotted in Fig. 1.

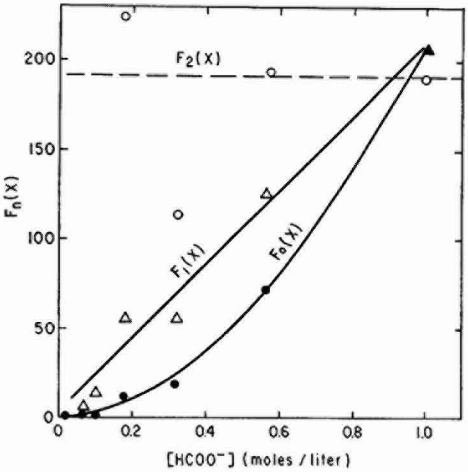

Fig. 1. Plot of $F_n(X)$ vs. formate ion concn. for polarographic data.

A least-squares plot of $F_1(X)$ vs. formate concentration yields a value of 16.3 for the intercept, K_1. The slope of this line is 197, which is in good agreement with the average value of 192 for K_2 derived from $F_2(X)$. Since $F_2(X)$ has zero slope it is evident that $Eu(HCOO)_2^+$, $Eu(HCOO)^{2+}$ and Eu^{3+} are the major species present in solution.

Chronopotentiometric results

The current reversal chronopotentiometric data for both reduction of Eu(III) and re-oxidation of the electrogenerated Eu(II) are listed in Table 2. The quarter-wave potentials are seen to shift systematically in the negative direction on increasing the concentration of formate ions, thus corroborating the corresponding polarographic evidence for complex formation of Eu(III) with formate.

The determination of the stability constants, K_1 and K_2, from the chronopotentiometric data is identical to the Deford and Hume polarographic method with the exception that $F_0(X)$ is calculated using observed $E_{\frac{1}{4}}$ values rather than $E_{\frac{1}{2}}$ values, *i.e.*,

$$F_0(X) = \text{antilog}\left\{\frac{0.43\, nF}{RT}[(E_{\frac{1}{4}})_s - (E_{\frac{1}{4}})_c]\right\} \tag{1}$$

where $(E_{\frac{1}{4}})_s$ is the quarter-wave potential of the aquo-complexed Eu(III) ion and $(E_{\frac{1}{4}})_c$ the quarter-wave potential of the formate complex. Values of $F_n(X)$ calculated from eqn. (1) are presented in the last three columns of Table 2.

TABLE 2

SHIFT OF $E_{\frac{1}{4}}$ WITH FORMATE ION CONCENTRATION AND VALUES OF $F_n(X)$ FOR CHRONOPOTENTIOMETRIC DATA

[HCOO⁻] *(M)*	$E_{\frac{1}{4}}$ *(V vs. Ag/AgCl/NaCl sat.)*	$F_0(X)$	$F_1(X)$	$F_2(X)$
FORWARD				
0.00	−0.535	1.00		
0.010	−0.539	1.17	17.0	
0.0316	−0.556	2.27	40.2	
0.100	−0.557	2.36	13.6	
0.178	−0.577	5.15	23.3	
0.316	−0.605	15.4	45.5	71.8
0.562	−0.613	21.0	35.6	22.9
1.00	−0.642	65.2	64.2	41.4 $K_2=45.4$
REVERSE				
0.00	−0.535	1.00		
0.010	−0.532	1.00		
0.0316	−0.538	1.13	3.96	
0.100	−0.567	3.49	24.9	
0.178	−0.594	10.0	50.6	106
0.316	−0.624	32.3	98.9	238
0.562	−0.627	36.3	62.8	71.3
1.00	−0.655	117	116	93.2 $K_2=127.0$

The uncertainty in the measured quarter-wave potentials is about ±5 mV with a consequent scattering of the calculated points, particularly at the lower formate ion concentrations. By analogy with the corresponding polarographic results $F_1(X)$ was assumed to be linear. A least-squares best straight line gave a value of 23 for K_1 and a value of 68 for K_2. The chronopotentiometric $F_2(X)$ values showed so much scatter that no correlation was attempted.

A careful consideration of the polarographic and chronopotentiometric results indicates that formate complexes with Eu(III) are formed; the polarographic results are more reliable than the chronopotentiometric results despite the reversible character of the system when run under chronopotentiometric conditions. Finally the stability constants of the two complexes were estimated to be:

$$Eu^{3+} + HCOO^- \rightleftarrows Eu(HCOO)^{2+};\quad K_2 = 20$$

$$Eu(HCOO)^{2+} + HCOO^- \rightleftarrows Eu(HCOO)_2^{+};\quad K_2 = 120.5$$

The distribution of Eu(III) among the various complexes as a function of formate ion concentration is shown in Fig. 2.

The formal reduction potential of the Eu(III)–Eu(II) system

It is of interest to investigate the effect that formate complexes of the stability indicated above would have on McCoy's original determination of the formal potential of the Eu(III)–Eu(II) system. McCoy in his study employed[7] "... approximately 0.1 M Eu formate containing a small excess of formic acid... [The amount of formic acid] being sufficient only to prevent precipitation of the base by reason of oxidation by air during the [potentiometric] measurements." This leaves the value of the pH of these solutions as a matter of conjecture. However, it is not unreasonable to assume that the pH of his solution was on the higher end of the formate–formic acid buffer region. Consequently, in the discussion to follow, a pH of 4 will be assumed as a reasonable value.

Figure 2 shows that, at a formate concentration of from 0.1 to 0.3 M, the principal species present in solution is $Eu(HCOO)_2^+$. It can thus be easily shown that

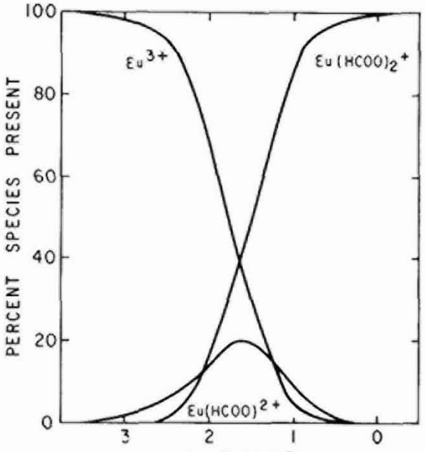

Fig. 2. Distribution of Eu(III) among various complexes at different concns. of formate ion.

the difference between the formal reduction potential of the europium formate complex, $E_c°$, and that of the aquo-complex, $E_s°$, is:

$$E_c^{\circ\prime} - E_s^{\circ\prime} = -0.0591 \log K_1K_2 - 2(0.0591) \log [\mathrm{HCOO^-}] \qquad (2)$$

The necessary equilibrium concentration of uncomplexed formate ion may be estimated from the equilibria:

$$K_1K_2 = \frac{[\mathrm{Eu(HCOO)_2^+}]}{[\mathrm{Eu^{3+}}][\mathrm{HCOO^-}]^2}$$

$$K_a = \frac{[\mathrm{H^+}][\mathrm{HCOO^-}]}{[\mathrm{HCOOH}]}$$

That is, assuming the pH to be 4 and with the original concentration of Eu(III) and formate ion equal to 0.1 *M* and 0.3 *M*, respectively, we have

$$2400 = \frac{x}{(0.1-x)\,(0.3-2x-y)^2}$$

$$1.74 \times 10^{-4} = \frac{(1 \times 10^{-4})\,(0.3-2x-y)}{y}$$

where $x = [\mathrm{Eu(HCOO)_2^+}]$ and $y = [\mathrm{HCOOH}]$.
The solution of these equations yields the value 0.073 *M* for the concentration of uncomplexed formate ion, and the use of this value in eqn.(2) gives

$$E_c^{\circ\prime} - E_s^{\circ\prime} = -0.067 \text{ V}.$$

This approximate calculation indicates that McCoy's observed value of −0.43 V *vs.* N.H.E., which is $E_c^{\circ\prime}$, is about 70 mV more negative than the value of the uncomplexed system, $E_s^{\circ\prime}$, *i.e.* −0.36 V *vs.* N.H.E. This prediction is in excellent agreement with the experimental value of −0.35 V reported by ANDERSON AND MACERO[1].

SUMMARY

Polarographic and chronopotentiometric evidence for the formation of the Eu formate complexes, $\mathrm{Eu(HCOO)^{2+}}$ and $\mathrm{Eu(HCOO)_2^+}$, is given. Values for the corresponding step stability constants were estimated to be 20 and 120, respectively.

The effect of such formate complexes on the original determination of the formal potential of the Eu(III)–Eu(II) couple by McCoy (1963) is discussed. The conclusion is that McCoy's result is in error by approximately 70 mV and that the value of −0.35 V *vs.* N.H.E. is more realistic for the non-complexed system.

REFERENCES

1 L. B. ANDERSON AND D. J. MACERO, *J. Phys. Chem.*, 67 (1963) 1942.
2 D. D. DEFORD AND D. N. HUME, *J. Am. Chem. Soc.*, 73 (1951) 5321.
3 R. S. KOLAT AND J. E. POWEL, *Inorg. Chem.*, 1 (1962) 293.
4 R. LEVINE AND D. J. MACERO, Paper No. 2, 149th Meeting A.C.S., Division of Analytical Chemistry, Detroit, Michigan, 1965.
5 D. J. MACERO AND L. B. ANDERSON, *J. Electroanal. Chem.*, 6 (1963) 221.
6 D. J. MACERO, H. B. HERMAN AND A. J. DUKAT, *Anal. Chem.*, in press.
7 H. N. McCOY, *J. Am. Chem. Soc.*, 58 (1936) 1577.
8 A. A. VLČEK, *Progress in Inorganic Chemistry*, Vol. 5, edited by F. A. COTTON, Interscience, New York, 1963, p. 240.

SHORT COMMUNICATION

Anion effects on the reduction of In(III) in acidic solution

During an investigation of the effect of halides on the anodic dissolution of indium amalgams in perchloric acid, the polarography of In(III) in the same medium was investigated[1]. It was observed, in agreement with earlier investigations, that a minimum does exist in the polarographic wave for In(III). Such minima, regions of apparent negative resistance, have been observed previously in solutions of high[2] and low[3–5] ligand concentration. AIKENS[5] has recently attributed these effects to reduction through adsorbed halide. It was felt that useful diagnostic information could be obtained and, in addition, some correlation found between the results at low- and high-ligand concentration by carrying out experiments at constant current using a dropping mercury electrode, *i.e.*, constant-current polarography[6]. For systems in which the potential is a multi-valued function of the current, by using a growing electrode and choosing an appropriate time during drop life to apply the current pulse, each region of voltage becomes accessible. Galvanostatic experiments have been described several times in the literature for In(III) in solutions of several acids or salts[7,8], but such a bi-stable condition has not been mentioned.

The data reported here are for millimolar In(III) in 0.70 M $HClO_4$ at 20° with additions of NaSCN. Systems with added HCl, NaBr, or NaI behave in a similar manner. A conventional dropping electrode, high-impedance voltage follower, Sargent XV polarograph, and operational-amplifier constant-current source were employed. Voltage–time transients were recorded on a Sargent MR recorder.

Figure I shows a typical polarogram. For a solution $1.0 \cdot 10^{-3} M$ in In(III), a diffusion-limited current of 5.3 μA is expected. For SCN^- concentrations less than $3 \cdot 10^{-3}$ M, the peak current is dependent on the SCN^- concentration. At the lower SCN^- concentrations, neither the current at the peak nor that at the minimum is proportional to the square root of the mercury column height but is almost independent of the height. The current at potentials more cathodic than the minimum, -0.90 V *vs.* S.C.E., is due to both hydrogen evolution and aquo-indic ion reduction.

Four typical constant-current transients for individual drops are shown in Fig. 2. For curve A, a low current was imposed from the birth of the drop; for curve B, a high current was imposed from the birth of the drop; for curve C, a high current was imposed relatively late in drop life; while for curve D, a high current was imposed early in drop life.

For the newly-born drops shown in curves A and B, the current density is initially high and the electrode evolves hydrogen, but as the area grows the current density drops. For the case of curve A, the current density eventually reaches the current density of the minimum in Fig. 1, 0.54 mA/cm² at -0.90 V. At this point, a discontinuous jump in potential occurs to a potential less cathodic than the peak at -0.60 V. The current density of the transition for 1 μA applied current occurs at 0.60 mA/cm², while for 2 μA applied the current density of the transition is at 0.57 mA/cm². If a high current is imposed from the birth of the drop (curve B), the current density at any time during drop life never falls to the value of the minimum and no abrupt potential shift is observed.

If the current is imposed several seconds after the drop is born so that the current density is of the order of the peak, 1.67 mA/cm², the potential during drop growth always remains cathodic to the peak (curve C). On the other hand, if the current is imposed early in drop life, and because of the small area, the current density exceeds that of the peak, the initial potential is anodic to the peak but a potential transition to more negative values quickly occurs. The potential of the transition is identical to that of the peak, but the current density at the time of the transition exceeds the current density of the peak in the polarogram usually by a factor of 2. The potential–time transient resembles a chronopotentiogram in many respects, except that, because the area of the electrode is increasing with time, the current density is decreasing.

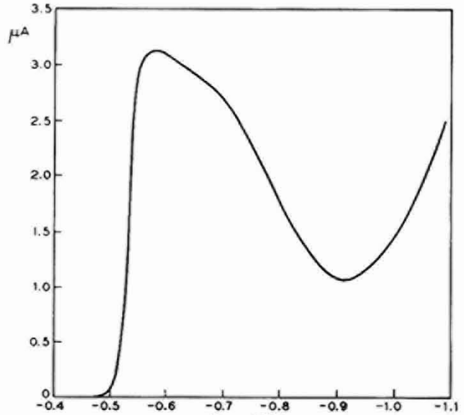

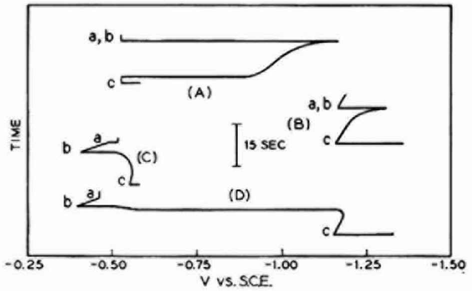

Fig. 1. Polarogram of $1.0 \cdot 10^{-3}$ *M* In(III) in 0.70 *M* $HClO_4$ at 20° with $3 \cdot 10^{-3}$ *M* NaSCN added. Hg-column height, 25 cm; *m*, 0.618 mg/sec; *τ*, 14.7 sec at −0.60 V *vs.* S.C.E.

Fig. 2. Potential–time curves for single drops where the drop is born at "a", the current imposed at "b", and the drop falls at "c". Curves A, B, C and D were run at 2, 4, 6 and 8 μA, respectively, at the same Hg height as in Fig. 1.

The above experiment was performed at several different SCN^- concentrations. The set of constant-current polarograms obtained were consistent with the conventionally recorded polarogram at each SCN^- concentration employed.

It appears that there is a region of negative resistance in the reduction of In(III) in acidic solution of the halides or pseudo-halides. The minima appear to be intimately associated with the anion concentration and the degree of specific adsorption of anion, *i.e.*, $I^- > SCN^- > Br^- > Cl^-$. The concentration of I^- necessary to reach the diffusion-limited current is less than that for SCN^- which is less than that for Br^- which in turn is less than that for Cl^-. The minima observed at both low- and high-halide concentrations appear to be a manifestation of the same process, anion adsorption.

Recently, AIKENS[5] has attributed the peak in the polarograms of acidic solutions of In(III) with added halide to catalysis by an adsorbed halide. Since the standard potential for the In(III)/In(O) couple is near the point of zero charge on mercury, In(III) reduction in dilute halide solution carried out at potentials more negative than the point of zero charge is occurring on an electrode with a lower surface excess of halide than at the standard potential. Since these workers have postulated that the rate step involves adsorbed halide, the experimentally-observed decrease in current with increasing polarization is consistent with this mechanism. The constant-current experiments described here are also consistent with adsorbed halide participating in the rate-determining step. A detailed description of these and other experiments to elucidate the role of adsorbed halide will be described elsewhere[9].

NOTE ADDED IN PROOF: The author has recently become aware of an AC impedance study of the In(III) system with SCN^- additions[10]. These workers also concluded that the region of negative resistance results from a reduction through an adsorbed anion.

Bell Telephone Laboratories, Inc.,
Murray Hill, New Jersey (U.S.A.)

ROBERT E. VISCO

REFERENCES

1 R. E. VISCO, Paper No. 166, 125th Meeting of the Electrochemical Society, Toronto, Canada, 1964. Submitted to *J. Electrochem. Soc.*
2 E. D. MOORHEAD AND W. M. MACNEVIN, *Anal. Chem.*, 34 (1962) 269.
3 D. COZZI AND S. VIVARELLI, *Z. Elektrochem.*, 57 (1953) 408.
4 H. IMAI, *J. Sci. Hiroshima Univ.*, 22 (1958) 291.
5 A. J. ENGEL, J. LAWSON AND D. A. AIKENS, *Anal. Chem.*, 37 (1965) 203.
6 I. M. KOLTHOFF AND Y. OKINAKA, *J. Am. Chem. Soc.*, 80 (1958) 4452.
7 B. LOVRECEK AND V. MARKOVAC, *J. Electrochem. Soc.*, 109 (1962) 727.
8 V. V. LOSEV AND A. I. MOLODOV, *Electrochim. Acta*, 6 (1962) 81.
9 R. E. VISCO AND T. B. REDDY, to be published.
10 N. TANAKA, T. TEKEUCHI AND R. TAMAMUSHI, *Bull. Chem. Soc. Japan*, 37 (1964) 1435.

Received March 17th, 1965.

GENERAL INFORMATION

Papers and communications should be concerned with the chemistry, metallurgy, or inter-related aspects of the less-common metals.

Types of contributions

- original research work not already published
- reviews of specialized topics within the scope of the Journal
- short communications
- letters to the editors
- book reviews

Suggestions for review articles will be welcomed, and prospective authors should obtain preliminary approval from the Editors before preparing such an article.

Languages

Papers will be published in English, French or German.

Submission of papers

Papers should be sent to one of the Editors:

Metallurgy
Professor J. W. CUTHBERTSON: *Department of Metallurgy, The University, University Park, Nottingham, England.*

Chemistry
Professor F. FAIRBROTHER: *8 Athol Road, Bramhall, Cheshire, England.*

Reprints

Twenty-five reprints will be supplied free of charge to the author(s). Additional reprints can be ordered at prices shown on the reprint order form which will accompany the galley proofs.

Frequency

The Journal is a monthly publication: six isues per volume, two volumes per year.

Subscriptions

Subscription price: £ 5.7.6 or $ 15.00 or Dfl. 54.— per volume (post free). Additional cost for copies by airmail available on request.

For advertising rates apply to the publishers.

A specimen copy will be sent on request.

Subscription orders should be sent to:

ELSEVIER PUBLISHING COMPANY, P.O. Box 211, Amsterdam, The Netherlands.

INSTRUCTIONS TO AUTHORS

Manuscripts

Two copies should be submitted to the Editors, in double-spaced typing on pages of uniform size with a wide margin at the left. Each table should be typed on a separate page. Legends to illustrations should be typed in sequence on a separate page or pages. All tables and illustrations should bear a title or legend.

A *summary* of 50–200 words should be included at the beginning of the paper. Authors of papers in French or German should supply in addition a translation in English of the Résumé or Zusammenfassung. No summary is required for a "Short Communication".

References should be numbered consecutively throughout the text and collected together in a reference list at the end of the paper. Footnotes should not include bibliographic material, and reference lists should not include material that could more appropriately appear as a footnote. Numerals for references should be given as superscripts. The following system of giving references is required:

Journals:
G. H. BANNISTER, R. C. BURNETT AND J. R. MURRAY, *J. Nucl. Mater.*, *2* (1960) 51.

Books:
L. S. DARKEN AND R. W. GURRY, *Physical Chemistry of Metals*, McGraw-Hill, New York, 1955, p. 445.

Abbreviations of journal titles should conform to those adopted by *Chemical Abstracts List of Periodicals*, 1961 edition and supplements.

Illustrations

Line drawings should be in a form suitable for reproduction, drawn in Indian ink on drawing or tracing paper, with lettering etc. in thin pencil.

Photographs should be black and white glossy prints and as rich in contrast as possible.

Proofs

Authors will receive galley proofs, which they are requested to correct and return as soon as possible. No new material may be inserted in the text at the time of proof-reading. A "note added in proof" will be accepted only if permission from the editors has been obtained; this will bear the date of receipt.
All joint communications must indicate the name and full postal address of the author to whom proofs should be sent.

SOME TYPICAL PAPERS PUBLISHED IN THE JOURNAL

Quelques sulphures et séléniures complexes
by A. E. van Arkel and C. Crevecoeur (Leiden)

Oxidation of the platinum-group metals
by C. A. Krier and R. I. Jaffee (Columbus, Ohio)

Effect of nitriding on the elevated temperature tensile properties of some molybdenum-base alloys
by A. K. Mukherjee and J. W. Martin (Oxford)

Tungsten-rich region of the system tungsten–carbon
by H. J. Goldschmidt and J. A. Brand (Birmingham)

Pressure dependence of the linear oxidation of niobium in the temperature range 450°–1050°C
by C. H. McLintock and J. Stringer (Liverpool)

Equilibrium diagram of the system molybdenum–cobalt
by T. J. Quinn and W. Hume-Rothery (Oxford)

Über den Aufbau des Systems Uran–Niob–Chrom
by G. Petzow and A. Junker (Stuttgart)

Electrodépostion en bain de sels fondus de poudres d'alliages zirconium–niobium
by C. Decroly and R. Winand (Brussels)

Relations between the structures and phases in the system platinum–molybdenum
by H. P. Rooksby and B. Lewis (Wembley)

Tensile properties of some extruded chromium alloys between 800° and 1000°C
by G. R. Wilms (Maribyrnong, Victoria)

Structure of niobium–hydride alloys
by C. Wainwright, A. J. Cook and B. E. Hopkins (Teddington, Middx.)

The zirconium–tungsten–tantalum system
by L. F. Pease and J. H. Brophy (Cambridge, Mass.)

A note on the intermetallic chemistry of the later transition elements
by W. Hume-Rothery (Oxford)

Carbides of formula T_2MC
by W. Jeitschko, H. Nowotny and F. Benesovsky (Reutte/Tirol)

Carbidnitride des Vanadiums
by G. Brauer and W.-D. Schnell (Freiburg im Breisgau)

Strain-aging effects of nitrogen in vanadium
by R. W. Thompson and O. N. Carlson (Ames, Iowa)

Constitution of yttrium–cerium and yttrium–lanthanum alloys, with special reference to lattice spacings
by I. R. Harris and G. V. Raynor (Birmingham)

Constitution diagram of the niobium–hafnium system
by A. Taylor and N. J. Doyle (Pittsburgh, Pa.)

Preparation and phase studies of titanium phosphides
by M. Knausenberger, G. Brauer and K. A. Gingerich (Freiburg i.B. and University Park, Penn.)

Electrical properties of some compounds having the pyrite or marcasite structure
by W. D. Johnston, R. C. Miller and D. H. Damon (Pittsburgh, Pa.)

Thermal expansion of $LaRu_2$, $CeRu_2$ and $PrRu_2$ from 20° to 900°C
by K. A. Gschneidner, Jr., R. O. Elliott and D. T. Cromer (Los Alamos, N.M.)

Creep properties of the Nb–1% Zr alloy
by H. E. McCoy (Oak Ridge, Tenn.)

Beiträge zur Chemie der Elemente Niob und Tantal
XLV. Ta_4J_{14} – Darstellung, Eigenschaften, Struktur
by D. Bauer, H. G. Schnering and H. Schäfer (Münster/Westfalen)

VOL. 10 NO. 1 JOURNAL OF ELECTROANALYTICAL CHEMISTRY JULY 1965

CONTENTS

Short Communication

PRINTED IN THE NETHERLANDS

MECHANISMS OF SOLID FRICTION

edited by P. J. Bryant and M. Lavik, Midwest Research Institute, Kansas, Missouri, and G. Salomon, Central Laboratory T.N.O., Delft

A conference was held on the Fundamental Mechanisms of Solid Friction at the Midwest Research Institute during September 1963. Its objective was to provide for formal presentations of current research and to encourage informal discussions among the active scientists in the field. The conference dealt with the topics of surface energy and temperature considerations, ionic solids, lamellar solids, metallic friction and metallic wear. The full proceedings were published as the first two issues of the journal WEAR, volume 7, 1964. It was suggested that a bound volume of the Proceedings would be welcomed, and the publishers hope that this compact volume will be a useful guide for workers in the growing field of wear, friction and lubrication research.

viii + 224 pages, 38 tables, 128 illustrations, 278 lit. references, 1964, 50s.

ADHESION AND COHESION

edited by Philip Weiss, Head, Polymers Department, Research Laboratories, General Motors Corporation, Warren, Michigan

This volume on "Adhesion and Cohesion" contains the proceedings of the fifth of a series of annual symposia sponsored by the General Motors Research Laboratories. The purpose of this symposium was to discuss and interpret fundamental knowledge and to interrelate it with the complex phenomena of adhesion and cohesion.

This exchange of ideas made it clear that an adequate theory must include many concepts, e.g. intermolecular forces, imperfections, stress concentrations, surface topography, wetting, and chemical constitution.

The papers presented at the symposium, as well as the informal discussions, are included in this book and the sequence is that of the symposium program.

viii + 272 pages, 47 tables, 121 illustrations, 292 lit. references, 1962, 60s.

ELSEVIER PUBLISHING COMPANY
AMSTERDAM LONDON NEW YORK

389E